WASHINGTON UNIVERSITY

SEVER INSTITUTE OF TECHNOLOGY

LIQUID-PHASE MIXING IN CHURN-TURBULENT BUBBLE COLUMNS

by

Kevin J. Myers

Prepared under the direction of Dr. M. P. Dudukovic

A research proposal presented to the Sever Institute of Washington University in partial fulfillment of the requirements for the degree of

DOCTOR OF SCIENCE

September, 1984

Saint Louis, Missouri

WASHINGTON UNIVERSITY
SEVER INSTITUTE OF TECHNOLOGY

ABSTRACT

LIQUID-PHASE MIXING IN CHURN-TURBULENT BUBBLE COLUMNS

by Kevin J. Myers

ADVISOR: Professor M. P. Duduković

September, 1984

Saint Louis, Missouri

A physically realistic description of liquid mixing is necessary for the proper design and scale-up of bubble columns. Currently, liquid-phase mixing is almost exclusively described by the one-dimensional axial dispersion model in spite of its numerous drawbacks. A new model of liquid-phase backmixing in churn-turbulent bubble columns has been developed. This model divides the column into two regions. The first region consists of the large, fast-rising bubbles which are characteristic of churn-turbulent operation and the liquid that they entrain. The second region consists of the remaining liquid and the small gas bubbles that are violently agitated by the passage of the large gas bubbles. An experimental program has been proposed to characterize the new model and to demonstrate that this model is a more appropriate representation of the physical situation than the axial dispersion model. The main experimental technique involves the determination of the liquid-phase response at different locations to various injections of ionic tracers that can be detected by electrical conductivity probes.

TABLE OF CONTENTS

TABLE OF CONTENTS
(continued)

LIST OF TABLES

LIST OF FIGURES

LIST OF FIGURES
(continued)

LIQUID-PHASE MIXING IN CHURN-TURBULENT BUBBLE COLUMNS

1. INTRODUCTION

Multiphase processes such as evaporation, crystallization, extraction, combustion, pneumatic conveying, and catalytic reaction have long been important to the chemical engineer. Gas-liquid processes are of particular importance in power generation, both conventional and nuclear, chemical processing, biotechnology, and related industries. Bubble columns have become increasingly popular as gas-liquid contactors and are used in the chemical processing industries as absorbers, strippers, and reactors. Bubble columns have been extensively used for chemical processing because of their small floor space requirements, lack of moving parts, low operating costs, and general simplicity of operation. Because of the ease with which the liquid residence time can be varied, bubble columns have been used as reactors for oxidation, hydrogenation, carbonylation, hydroformylation, alkylation, Fischer-Tropsch synthesis, and a number of other reactions (1).

The terminology bubble column is not well-defined. For the purpose of this study a bubble column will be considered to be a cylindrical vertical tower with a length to diameter ratio greater than five. A

bubble column will typically have a diameter greater than 10 cm (4 in) to distinguish it from a tube or pipe. Under normal operating conditions, the superficial gas velocity will be an order of magnitude greater than the superficial liquid velocity (the superficial velocity being defined as the volumetric flowrate divided by the column cross-sectional area). This distinguishes bubble column operation from gas-lift operation where the superficial gas and liquid velocities are of the same magnitude. Typical ranges of superficial velocities for bubble column operation are 1 to 30 cm/s (0.4 to 12 in/s) for the gas phase and 0 to 2 cm/s (0 to 0.8 in/s) for the liquid phase.

A bubble column may be operated in either a cocurrent, countercurrent, or semibatch (batch liquid phase) manner. Coils or other internals may be inserted into a bubble column to promote heat transfer as may be baskets containing a catalyst to promote chemical reaction. If the catalyst is suspended in the liquid phase by the action of the rising gas bubbles, the column is termed a bubble column slurry reactor. A bubble column may also be sectionalized by a baffle system or perforated plates to inhibit liquid-phase backmixing (2) and bubble coalescence (3). In a typical bubble column operation, the faster moving gas phase is sparged into the slower moving liquid phase in the form of discrete bubbles. Therefore, the gas phase is the dispersed phase while the liquid phase is the continuous phase in a bubble column operation. This study will be concerned with cocurrent or semibatch operation of a bubble column that contains no internals or suspended solids.

Because of the extensive use of bubble columns for large-scale chemical processing, the accurate scale-up of laboratory studies to plant scale is necessary. Typical studies of bubble column operation are

concerned with the collection and correlation of data concerning gas hold-up, gas and liquid backmixing, and mass transfer over a range of operating conditions. Often this data is collected indiscriminately without any consideration being given to the prevailing flow regime encountered during the study. Because of the complex nature of the gas-liquid hydrodynamics encountered in bubble column operations and the effects of hydrodynamics on system performance, the scale-up and design of bubble columns is often uncertain.

Three flow patterns, also termed flow regimes, have been observed in bubble columns. These flow patterns are characterized by the appearance of the gas-liquid interface and are most commonly termed the bubble, slug, and churn-turbulent flow regimes. The characteristics of each of these flow regimes will be discussed later. Shah et al. (1) have noted that the prevailing flow regime in a bubble column operation will strongly affect the hydrodynamics and transport and mixing properties such as pressure drop, holdup of the various phases, interfacial area, and the interphase heat and mass transfer coefficients of the system. Because of the effect of flow regime on bubble column performance, it would be expected that care would be taken to delineate between the various flow regimes encountered during an experimental study. However, a review of the pertinent literature indicates that this is not the case and experimental data is generally collected without regard to flow regime. In this study, the emphasis will be placed on studying the churn-turbulent regime of bubble column operation.

The following section of this report discusses the characteristics of the flow regimes encountered in cocurrent gas-liquid upflow and some of the flow regime maps used for the a priori delination of flow regimes.

After this introduction, special attention will be given to bubble column operation particularly those studies that attempt to characterize churn-turbulent bubble column operation.

Very few models have been used to describe the behavior of bubble columns under reacting conditions. The simplest model assumes that the gas phase is in plug flow and the liquid phase is completely backmixed. The next level of sophistication is to consider one or both of the phases to be partially backmixed. Very little work has been performed concerning gas-phase backmixing, partly because of experimental difficulties encountered when studying the gas phase and partly because of the theoretical difficulties encountered when trying to describe the behavior of a dispersed phase that can coalesce and redisperse. Partial backmixing of the liquid phase is exclusively described by the one-dimensional axial dispersion model. Extensive efforts, both empirical and theoretical, have been directed towards prediction of the liquid-phase axial disperison coefficient given the operating conditions of a bubble column. Previous efforts concerning the modeling of liquid-phase backmixing in bubble columns will be discussed in the fourth section of this report.

Very little effort has been spent on developing alternatives to the axial dispersion model for describing liquid-phase backmixing in bubble columns. In the fifth section of this report, a mathematical model will be developed, based upon a sound physical model, to describe liquid-phase backmixing in bubble columns operating in the churn-turbulent regime. This model is based upon division of the column into two regions. The first region is a fast-rising region of high gas holdup which appears at a fairly constant frequency and is the characteristic feature of churn-turbulent operation. The second region is a stationary region of high

turbulence, the turbulence being caused by the fast-rising high gas holdup region. Methods of approximating the model parameters or determining them experimentally are also discussed. The main experimental technique employed is a liquid-phase residence time distribution (RTD) study which allows model parameters to be determined by matching experimental residence time distributions to those predicted by the proposed model. To determine the usefulness of the model for reacting systems without the complicating factors of interphase mass transfer and gas-phase mixing that occur in typical bubble column operations, it is recommended that the proposed model be compared to other models either experimentally or numerically when considering the prediction of the conversion of a homogeneous liquid-phase reaction.

A lab-scale bubble column facility has been constructed and it is described as well as modifications that must be made for completing the experimental portion of this research. Some preliminary results are also presented and they are discussed in relation to the proposed backmixing model. The results are also discussed in relation to the flow pattern transitions that occur in bubble columns and as to the directions they indicate which may lead to a clearer understanding of these flow regime transitions.

2. FLOW REGIMES IN COCURRENT GAS-LIQUID UPFLOW

2.1 GENERAL DESCRIPTION

The following discussion is aimed at describing the various flow patterns encountered in cocurrent gas-liquid upflow over the entire range of flowrates encountered. Special attention will be given to the flow patterns encountered under the lower flowrates typical of bubble column operation in a later discussion. The characterization of gas-liquid flows is difficult because of the large number of flow regimes encountered and the problem is further complicated by discrepancies in the terminology used by various researchers. For the following discussion, only four flow regimes are recognized-bubble, slug, churn, and annular flows, which are generally accepted as the major gas-liquid flow patterns and the terminology used is that most widely encountered in the literature. The flow regimes discussed here are illustrated schematically in Figure 2.1.

Bubble flow is characterized by the gas phase being dispersed in the form of bubbles of an almost uniform size that are uniformly distributed throughout the continuous liquid phase. Larger bubbles caused by coalescence of smaller bubbles may also be present in bubble flow. The gas holdup is sufficiently low so that the gas bubbles rise without much interaction. Because of the action of surface tension effects, the gas bubbles are of a near spherical shape with deformation occurring in the larger bubbles. Bubble flow is intrinsically unstable due to bubble coalescence which causes the individual bubbles to lose their identity. However, in short conduits, bubble flow may be stable because of the short residence time of the bubbles which hinders bubble coalescence. Bubble coalescence may also be hindered by a high level of turbulence in the

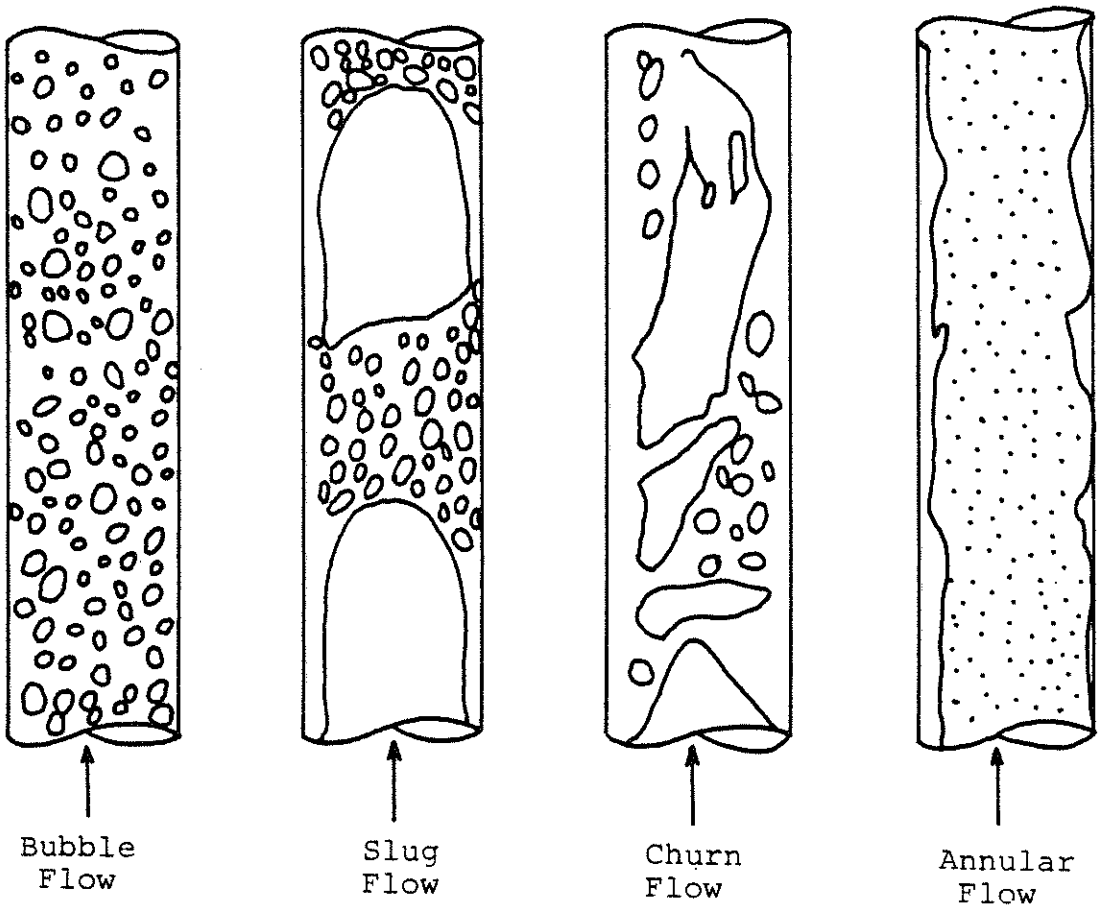

Figure 2.1 Flow Regimes of Cocurrent Gas-Liquid Vertical Upflow (after Taitel et al. (4))

liquid phase or by the addition of surface active agents to the system. Bubble flow is commonly found in evaporation, condensation, nucleate boiling and other nucleation phenomena, and gas-lift operations. A particularly important application of bubble flow is in bubble column operations where the large interfacial area of the gas-liquid dispersion is necessary to achieve adequate interphase mass transfer rates.

Slug flow generally occurs at higher gas holdups than bubble flow and is characterized by the presence of bullet-shaped bubbles of a diameter near that of the conduit. These large bubbles are termed Taylor bubbles and are the result of bubble coalescence. A thin liquid film flows downwards between the Taylor bubbles and the conduit wall and a liquid bridge flows between successive Taylor bubbles. This liquid bridge may or may not contain small, dispersed gas bubbles. Slug flow may also be interchangeably termed plug or piston flow. Names such as quiet slug, dispersed slug, and frothy slug have also been used (5) to help characterize the appearance of the gas-liquid interface at the trailing edge of the Taylor bubble. Slug flow is generally only stable in conduits of smaller diameter and can be found in evaporator tubes and in gas-liquid transport applications. Slug flow must be avoided in mass transfer operations because of the severely decreased interfacial area of the Taylor bubbles.

Churn flow is probably the most poorly characterized gas-liquid flow pattern. Churn flow has an unstable and chaotic appearance and the most commonly noted characteristic of churn flow is an oscillatory or rising and falling motion of the liquid phase. Large gas bubbles are present in churn flow; however, these bubbles are not large enough to fill the entire conduit cross section as in the case of the Taylor bubbles of slug flow.

A variety of opinions exist as to the proper classification of churn flow. Wallis (6) feels that churn flow is simply the transition regime between bubble and slug flow in which bubble coalescence occurs. Based on the ability of gas holdup correlations for the slug flow regime to estimate experimentally determined gas holdups in churn flow in large diameter conduits, Hills (7) proposed that churn flow is slug flow in conduits too large for stable slugs to exist. Hewitt (8) proposed that churn flow is due to a breakdown of the Taylor bubbles of slug flow caused by an increasing gas flow which will lead to annular flow. Taitel et al. (4) believe that churn flow is an entry region phenomenon during which a stable liquid bridge accumulates between successive Taylor bubbles which leads to slug flow. Each of these explanations seems plausible. If more than one of these explanations are correct, this leads to the conclusion that churn flow is actually a poorly defined flow regime that describes the characteristics of a number of flows. The term froth flow has been used to characterize churn flow at higher gas and liquid flows where the system is more finely dispersed. Churn flow can be found in many of the same chemical processing applications as bubble flow where increased throughputs are necessary.

At very high gas velocities, annular flow will occur. Annular flow is characterized by the gas phase flowing as a core at the center of the conduit with the liquid phase flowing as an annulus at the conduit wall. The gas core may contain entrained droplets of liquid that have been sheared from the wavy gas-liquid interface. If the liquid entrained in the gas core is in the form of lumps or wisps, the flow pattern may be termed wispy-annular. At the highest gas velocities, the entire liquid film may be sheared from the conduit wall and flow entirely as small

droplets suspended in the gas. This flow pattern is usually termed mist flow. Annular flow is the predominant flow pattern in evaporator tubes. Annular flow is not suitable for mass transfer because of the reduced interfacial area which in some cases can be compensated by the liquid droplets flowing in the gas core.

Although the transitions between flow regimes are not sharp, they do provide a starting point for the analysis of gas-liquid flows. The majority of experimental flow pattern determinations have been visual; however, a few experimental techniques have been devised to rid the experiments of the subjectivity of visual observation by attempting to detect some quantity characteristic of a given flow pattern. The principles of a few of these experimental techniques and the practical difficulties that arise in their application have been outlined by Hewitt (9) and Jones (10).

2.2 FLOW REGIME MAPS

To model the pressure drop, holdup, and mass transfer characteristics of any gas-liquid process, a clear physical picture of the process is necessary. As indicated in the preceding discussion, the gross properties of the various gas-liquid flow regimes are vastly different. Knowledge of the prevailing flow regime in a gas-liquid process would provide a clear physical picture of the process which would then be the cornerstone of modeling efforts. With this in mind, numerous attempts to provide a flow regime map (or simply flow map) that allows prediction of the prevailing flow regime in a given process have been made.

Two basic approaches have been taken when attempting to develop flow regime maps. The first approach is empirical correlation of the

flow regimes observed in experimental systems over a range of operating conditions. The experimental systems typically studied are air-water or steam-water in conduits of small diameter (1 inch being common). For a specific system, the phase flowrates may be used to correlate the flow regimes. However, extension of these results to arbitrary systems has not been successful. Attempts have been made to extend the empirical flow maps to arbitrary systems by employing dimensionless coordinates or physical property groups for correlation. Oshinowo and Charles (5), Govier et al. (11), Cichy et al. (12), and Griffith and Wallis (13) have each developed gas-liquid flow maps on an empirical basis.

The second approach to developing flow regime maps is mechanistic in nature. In this approach it is attempted to develop a general set of criteria for the existence of the different flow regimes. The earliest attempt at this approach was made by Quandt (14) who recognized three flow regimes on the basis of the physical force dominating the system. The flow regimes considered were defined according to whether pressure gradient, gravitational attraction, or inertial forces dominate the remaining two forces. Although this approach is important because of its theoretical basis, the method of correlation proved to be unwieldy and difficult to use. More recently, Taitel et al. (4) developed generalized criteria for flow pattern delineation based upon proposed physical mechanisms of the flow regime transitions. The final transition criteria are not specific to any size conduit or any specific gas-liquid pair; rather, these criteria have been presented in a generalized form which can be applied to any system. This is probably the best method currently available for predicting flow regimes in cocurrent gas-liquid upflow.

3. BUBBLE COLUMN FLOW REGIMES

3.1 GENERAL DESCRIPTION

As was noted earlier, typical gas and liquid velocities in bubble column operations are on the lower end of the spectrum of gas-liquid flow systems. It is common to recognize only three flow regimes in bubble column operations. These flow regimes are termed bubble flow, churn-turbulent flow, and slug flow.

Bubble flow is similar to the description given earlier. However, in bubble column operations, larger, faster-rising bubbles are not present in bubble flow as they may be in bubble flow as it is defined when considering the entire spectrum of gas-liquid flows. In a bubble column operation, the presence of larger, faster-rising bubbles indicates the onset of the churn-turbulent regime. The presence of larger, faster-rising bubbles in general gas-liquid flows simply indicates the upper range of bubble flow, not a different flow regime as in bubble column operations.

The presence of larger, faster-rising bubbles is the defining characteristic of churn-turbulent flow. The terminology churn-turbulent appears to be limited to the bubble column literature. When compared to the previously discussed flow regimes, churn-turbulent flow would appear to be the upper range of bubble flow and the lower range of churn flow. Because bubble columns are concerned with a narrow range of operating conditions, attention is given to more subtle changes in behavior such as the bubble to churn-turbulent transition. When films of bubble columns operating in the churn-turbulent regime are viewed in slow motion, they indicate that the larger, faster-rising

bubbles appear at an almost constant frequency which is determined by the operating conditions. These films also indicate that the larger bubbles are of an irregular shape and may actually be clumps of smaller bubbles rising together rather than a single large bubble. The hydrodynamics of churn-turbulent flow appear to be governed by the behavior of the larger bubbles. The smaller bubbles are dispersed in the liquid phase and this dispersion appears to behave as a pseudohomogeneous emulsion. The terminology churn-turbulent can be traced back to the work of Zuber and Findlay (15) which was not concerned with bubble column operation but rather with the correlation of gas holdup in various gas-liquid flow systems.

Slug flow in bubble columns is the same as was described earlier. Because of the typically large diameters of bubble columns, slug flow is rarely observed in bubble column operations.

3.2 BUBBLE COLUMN FLOW REGIME MAPS

Because of the effect of flow regime on bubble column performance (1,16), it is important to be able to predict the prevailing flow regime for the proper design of a bubble column system and the proper interpretation of bubble column experiments. It would be expected that the general flow maps discussed earlier (Section 2.2) may not be directly applicable to bubble column operations because of the basic differences between bubble columns and the systems for which these flow maps were developed. The main differences are the large diameters, limited length to diameter ratios, and the small range of operating conditions of bubble columns compared to other gas-liquid flow systems.

Miller (17) performed experimental studies in a 23 cm (9.1 in) diameter bubble column with fluids of varying physical properties ($35 \leq \sigma \leq$ dyne/cm, $1.00 \leq \rho_L \leq 1.28$ g/cm^3, $0.9 \leq \mu_L \leq 49$ cp) over a wide range of operating conditions (superficial liquid velocities of 0.0508, 0.508, and 4.95 cm/s and superficial gas velocities of 0.711, 3.711, 7.67, and 23.4 cm/s). The empirical flow map of Cichy et al. (12) predicted that the majority of the experimental points would be in bubble flow with some points bordering on slug flow. The empirical flow map of Oshinowo and Charles (5), on the other hand, predicted that all of the experimental points would be in slug flow. Because of the large diameter of the column studied, slug flow was never observed. Rather, churn-turbulent flow was observed, but neither flow map considers such a flow regime. In fact, both flow maps had to be extrapolated to accommodate all of the data of Miller (17) and the extrapolication can be seen to be invalid.

Even if the application of empirical flow maps to bubble column operations is invalid, it would be hoped that the mechanistic flow regime transition criteria of Taitel et al. (4) could accurately predict bubble column flow regimes. However, Kirkpatrick (18) photographically studied air-water flow in a bubble column of 18 cm (7.0 in) diameter and although a good number of points were clearly in churn-turbulent flow, the criteria of Taitel et al. (4) predicted that the majority of the points studied were in bubble flow with a few points bordering on churn flow. The failure of both the empirical and mechanistic flow regime maps points to the need for flow maps specific to bubble column operations.

Shulman and Molstad (19), Braulick et al. (20), and Fair (21) developed qualitative guidelines that could be used for bubble column design. A typical example being that bubble flow exists for superficial gas velocities below 5 cm/s (2 in/s) and churn-turbulent flow exists for superficial gas velocities greater than 10 cm/s (4 in/s). Yoshitome and Shirai (22) studied bubble column hydrodynamics and classified the flow regimes according to the behavior of the pressure drop across the gas distributor. At low gas flows the pressure drop across the gas distributor was found to be constant and the flow was termed laminar. At high gas flows the pressure drop across the gas distributor was found to be equal to that for gas flow through a dry perforated plate and the flow was termed turbulent. The region at intermediate gas flows was simply termed a transition zone. It is unlikely that the pressure drop across the gas distributor will control the hydrodynamics of the entire column.

More recently, Kawagoe et al. (23) proposed a method of flow regime delineation in bubble columns based upon the relationship between the superficial gas velocity and the gas holdup. In the bubble flow regime the bubbles all behave in a similar manner and do not interact significantly. In this regime, Kawagoe et al. (23) proposed that the superficial gas velocity and the gas holdup should be linearly related. In the churn-turbulent regime the large, fast-rising bubbles determine the behavior of the system and in this regime Kawagoe et al. (23) proposed that the inverse of the superficial gas velocity and the inverse of the gas holdup should be linearly related. After examining numerous data, Kawagoe et al. (23) found that bubble flow existed for superficial gas velocities below about 3.5 cm/s (1.4 in/s) and

churn-turbulent flow existed for superficial gas velocities greater than about 10 cm/s (4 in/s) which agree well with the qualitative design guidelines discussed earlier (19,20,21). The flow regime delineation criteria of Kawagoe et al. (23) may be the best currently available for bubble columns since they are general in nature and can be applied to any system. Also, these criteria concentrate on the changes that occur in gas holdup behavior which should have a significant effect on bubble column performance. It should also be noted that other bubble column researchers (24,25) have employed changes in gas holdup behavior based upon drift-flux theory to delineate between flow regimes. These researchers have defined a relationship between the relative velocity between the phases and the gas holdup (6,26,27) for the bubble flow regime. When deviations from this relationship occur, the system is no longer considered to be in bubble flow.

Noting the difficulties encountered in the design and scale-up of bubble columns due to their complex hydrodynamics, Shah et al. (1) and Deckwer et al. (28) presented the flow map illustrated in Figure 3.1 to aid in the prediction of the prevailing flow pattern in a bubble column operation. The source of this flow map was not stated explicitly and no theoretical or mechanistic justification was cited with its presentation. Two possible sources may explain the origins of this flow map. The first is that the map may simply be the result of surveying the observations of numerous investigators. The second, and more probable, source of this flow map is the following guidelines that may be found in the bubble column literature. Fair (21) noted that bubble flow will occur for superficial gas velocities below about

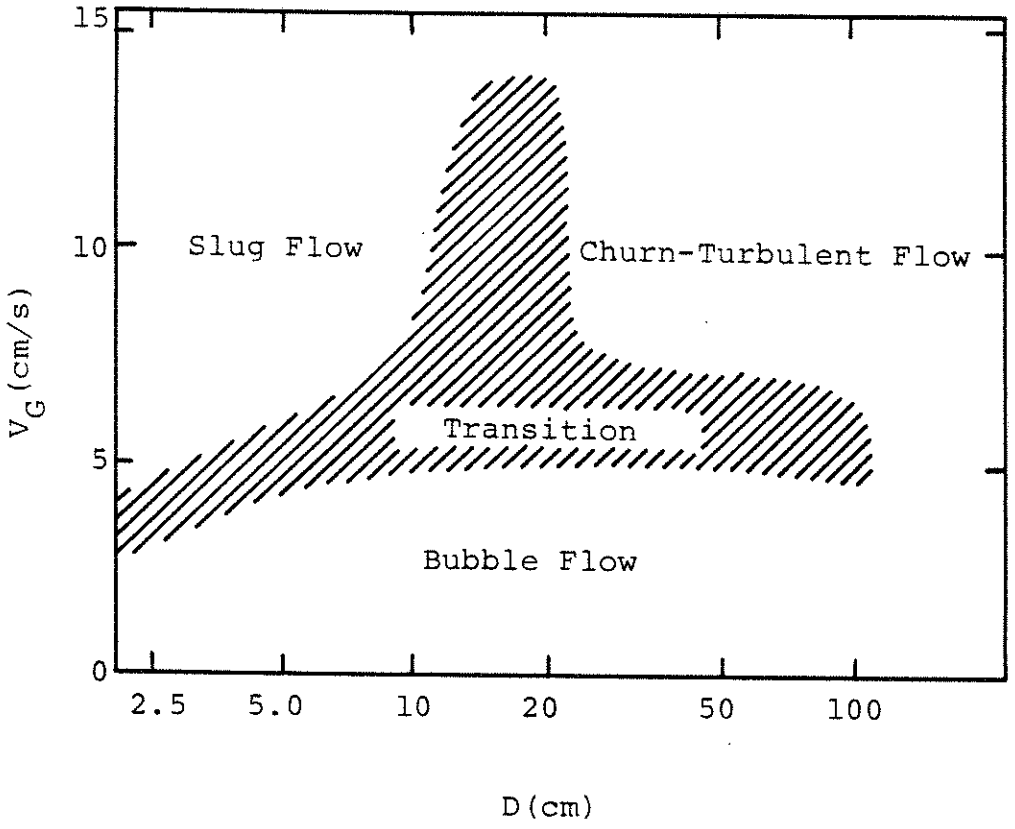

Figure 3.1 Flow Regime Map of Deckwer et al. (28) and Shah et al. (1)

5 cm/s (2 in/s) and Hills (7) and Miller (17) noted that slug flow can only occur in columns with diameters less than 15 cm (5.9 in). Examination of the flow map indicates that these guidelines do correspond well to the flow pattern transitions of the map with a transition range superimposed on the approximate guidelines. Note that this transition region is likely to be spanned in any experimental attempt to determine the effect of column diameter or superficial gas velocity on bubble column behavior thus making the experimental results difficult to interpret.

Shah et al. (1) note that this flow map is generally valid for water and dilute aqueous solutions. The coordinates of the flow map, the column diameter and the superficial gas velocity, are the parameters that are believed to exert a controlling influence on bubble column behavior. The more subtle effects of the gas sparger design, liquid physico-chemical properties, and liquid velocity are not accounted for in this map. The flow regimes used in this map, bubble, slug, and churn-turbulent, are those commonly used in bubble column studies. This flow map is a step in the right direction in that it is specifically intended for bubble column operations, but without any justification or means of extending the map to a general system, its usefulness is questionable.

The preceding discussion indicates that only minimal work has been performed concerning the flow regime transitions that occur in bubble columns. Only the criteria of Kawagoe et al. (23) appear to have any basis in the physical processes that occur during transition and enough generality to be applied to any system. However, these studies

will provide a basis for delineating between experiments performed in the bubble and churn-turbulent regimes.

3.3 CHURN-TURBULENT FLOW IN BUBBLE COLUMNS

The following discussion outlines a number of studies that have attempted to characterize the churn-turbulent regime of bubble column operation. The findings of these studies will provide the basis for the liquid-phase backmixing model to be developed later.

To help quantify the characteristics of churn-turbulent flow, Ohki and Inoue (29) placed conductance probes in the flow field to detect the passage of large, coalesced bubbles (see Hewitt (9) or Jones (10) for more information concerning this technique). Using this technique they were able to determine the frequency of passage of the large, coalesced bubbles, the rise velocity of these bubbles, and some linear dimension characteristic of the size of the coalesced bubbles. Because of the small size of the columns used in this study, it should be noted that bubble slugs may have formed at higher superficial gas velocities, particularly in the smaller columns. Although the data are not conclusive, the results of Ohki and Inoue (29) indicated that the passage frequency of the coalesced bubbles is fairly constant with superficial gas velocity with values in the range of 1 to 2 per second depending on the column diameter and the gas distributor design. Since the gas holdup does not increase rapidly with the superficial gas velocity in the churn-turbulent regime, the constancy of passage frequency would indicate that the bubble size and/or rise velocity must increase with superficial gas velocity to transport the increased gas volume through the column. The results of Ohki and Inoue (29) reflect this with both

the bubble size and rise velocity increasing in a linear manner with the superficial gas velocity.

Hills (30) measured the radial variation of bubble passage frequency, average (with respect to time) local gas holdup, and average (also with respect to time) liquid velocity in a 13.8 cm (5.43 in) diameter bubble column with an air-water system. The liquid velocity was measured with a modified Pitot tube. The liquid velocity was found to exhibit a profile with a maximum upwards velocity on the column centerline and with negative velocities in the wall region. This type of circulation profile is to be expected in the churn-turbulent regime because the large, coalesced gas bubbles will tend to rise along the column axis where the drag effects of the wall are lowest. These fast-rising coalesced bubbles will both push liquid ahead of their caps and drag liquid behind in their wakes. The negative liquid velocities near the wall are a result of continuity since the liquid velocities at the column centerline are much greater than the liquid superficial velocity. An example of the large liquid velocities encountered on the column centerline is that the liquid velocity exceeds 50 cm/s (20 in/s) at a superficial gas velocity of 16.9 cm/s (6.65 in/s). The centerline liquid velocity was found to follow a power law relation with respect to the gas superficial velocity.

Hills' (30) studies of the radial variations in gas holdup are also enlightening for the characterization of the churn-turbulent flow regime. The local gas holdup was determined using the conductance probe technique with a point probe. These results are illustrated in Figure 3.2 for the case of a gas distributor with 61 holes (1 central,

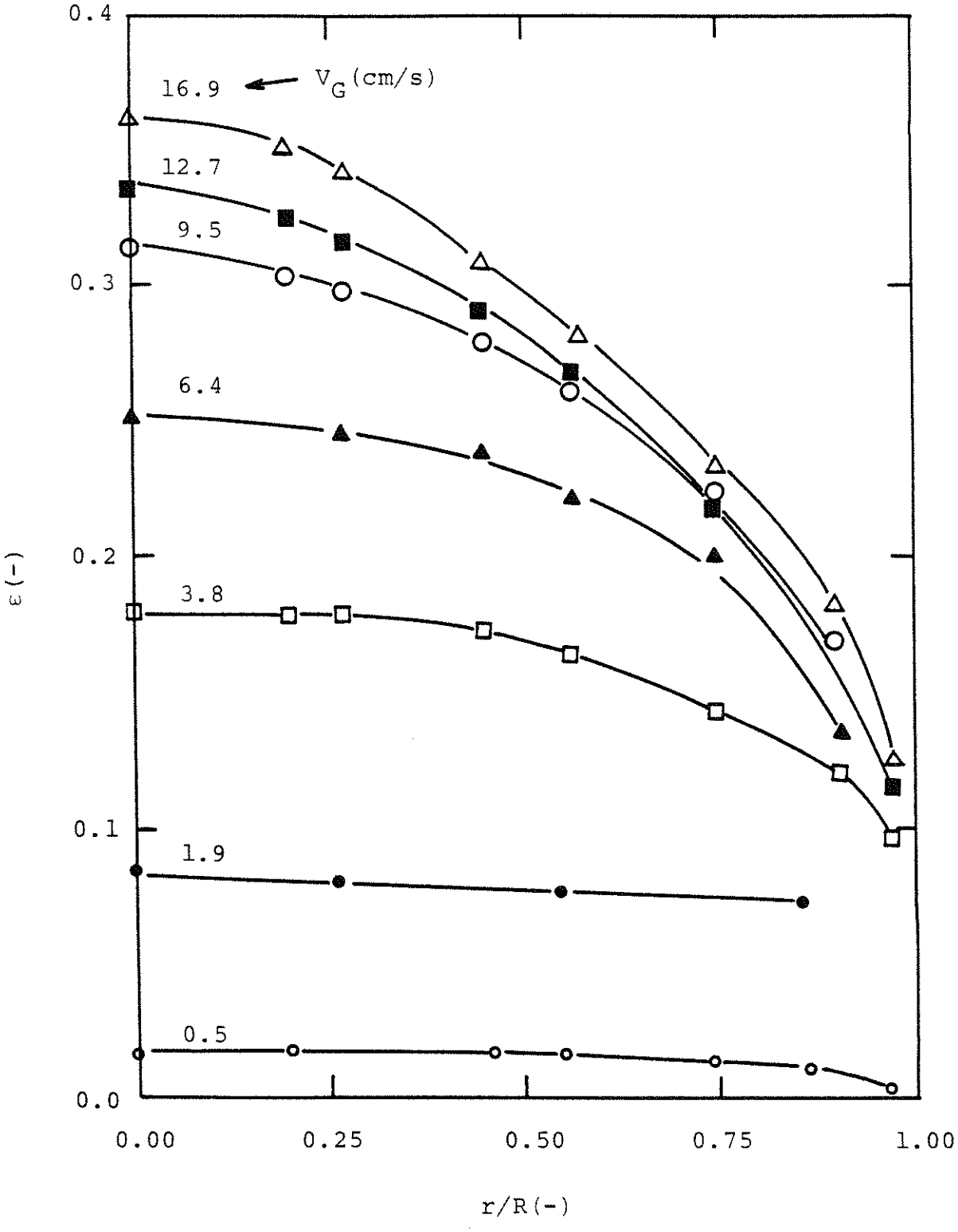

Figure 3.2 Radial Gas Holdup Data as Determined by Hills (30)

the remainder uniformly spaced on three concentric circles) of 0.04 cm (0.016 in) diameter. It should be noted that the results varied somewhat with sparger design. The local gas holdup is fairly uniform over most of the column for a superficial gas velocity as high as 3.8 cm/s (1.5 in/s). As the superficial gas velocity is increased above this value the local gas holdup in the wall region remains constant at about 0.1 while the local gas holdup at the column centerline continually increases. At a superficial gas velocity of 16.9 cm/s (6.65 in/s), the local gas holdup at the column centerline is greater than 0.35 while the average (with respect to the column volume) gas holdup is only about 0.24. The high gas holdup at the column centerline is indicative of the presence of the large, coalesced bubbles characteristic of churn-turbulent flow. These bubbles will tend to rise along the column centerline because of the reduced wall drag. The work of Hills (30) discussed here is very good experimentally; an analysis of his data to determine the characteristics of the large coalesced bubbles would probably be productive.

Kirkpatrick (18) performed a photographic study of an 18 cm (7.0 in) diameter bubble column with an air-water system. The column was photographed at 1/8 real time at a variety of operating conditions. At low superficial gas velocities the flow pattern was definitely bubble flow. Under these conditions, a uniform dispersion of nearly spherical bubbles exists in a liquid phase that shows very little visual agitation. The bubbles appear to exert very little influence on each other under these conditions. As the superficial gas velocity was increased, the transition to churn-turbulent flow occurred. Large,

irregular-shaped bubbles were observed to rise rapidly near the column axis at a somewhat constant frequency of about two per second which agrees well with the observations of Ohki and Inoue (29). From Kirkpatrick's (18) film it is unclear whether the large, fast-rising bubbles are actually one integral bubble or an agglomeration of smaller gas bubbles in an area of high gas holdup. Under these operating conditions, the large bubbles control the hydrodynamics of the column and they violently agitate the liquid phase which contains a dispersion of smaller gas bubbles. If the superficial liquid velocity is increased to near that of the gas, the operation is closer to that of a gas-lift operation and the flow once again appears to be bubble flow although some large bubbles are still present. The films of Kirkpatrick (18) dramatically illustrate the different flow behavior of the bubble and churn-turbulent regimes.

Rice et al. (25) compared the performance of rigid polyethylene and flexible rubber gas distributors with respect to gas holdup and liquid-phase dispersion. The flexible gas distributors exhibited a number of desirable properties when they were compared to the rigid gas distributors that are used in most bubble column operations. Visual comparison of the flexible and rigid gas distributors indicated that the flexible spargers produced a uniform bubble dispersion in the distributor region while gas jetting was observed with the rigid distributors. Gas jetting results in a few large bubbles existing in a region of very low holdup near the gas distributor. Further from the gas distributor these large bubbles break up into a dispersion of smaller bubbles; however, even in regions far from the gas distributor,

the flexible distributor produced a more uniform dispersion than the rigid distributor. These observations are in direct contradiction of the results of Towell et al. (31) which indicated that the gas distributor design had no significant effect on column operation (note that Towell et al. (31) studied only rigid gas distributors).

Rice et al. (25) found that the flexible gas distributors gave a higher gas holdup than the rigid gas distributors. They also noted that the bubbles produced by the flexible distributors were of a more uniform size and were about half the size of the bubbles produced by the rigid distributors. Visual observation indicated that bubble coalescence and the transition from bubble flow to churn-turbulent flow occurred at a gas holdup of about 0.2 for the flexible distributors and about 0.1 for the rigid gas distributors. These gas holdups corresponded to superficial gas velocities of 3.7 and 2.8 cm/s (1.5 and 1.1 in/s), respectively.

Rice et al. (25) also determined the liquid-phase axial dispersion coefficients with both flexible and rigid gas distributors. The dispersion coefficients for the flexible distributors were always somewhat lower than those obtained with the rigid gas distributors. This result would be expected because the flexible distributor produced a more uniform bubble dispersion which should reduce liquid-phase mixing. The liquid-phase axial dispersion coefficient exhibited maxima and minima when plotted as a function of the superficial gas velocity. Rice et al. (25) attributed these maxima and minima to changes in flow regime; however, they have no other data or observations which specifically support this contention.

Rice et al. (25) proposed that the enhanced performance of the flexible gas distributors is due to what they termed the self-regulation properties of the flexible gas distributors. By this they mean that the hole size in the flexible distributors can change to adjust for changes in the gas flowrate and the pressure drop across the distributor. The study of Rice et al. (25) indicates that, contrary to previous studies (31), the initial conditions in the column, meaning the gas distributor performance, can affect the flow characteristics of a bubble column.

Vermeer and Krishna (32) studied the hydrodynamics and mass transfer characteristics of a bubble column operating in the churn-turbulent regime. The column studied was 19 cm (7.5 in) in diameter and nitrogen and turpentine 5 were used as the gas and liquid phases, respectively. Using a batch liquid phase, Vermeer and Krishna (32) noted that at superficial gas velocities above 10 cm/s (4 in/s) coalescence of the gas bubbles occurred in the gas distributor region and these large, coalesced bubbles rose rapidly upwards through the column. These coalesced bubbles did not slug the column, were of an irregular, constantly changing shape, and did not change in size after initial formation as far as visual observation could perceive.

Vermeer and Krishna (32) were able to characterize the gas holdup in the churn-turbulent regime by employing an interesting technique which they termed dynamic gas disengagement. If the liquid phase is batch and the gas flow to the column is stopped instantaneously, the change in the dispersion height with time can be indicative of the column hydrodynamics. Although the decrease in dispersion level as

the gas escapes is not a smooth function of time at higher gas velocities, video recordings of the dispersion level with time allowed for a meaningful interpretation of the experimental data. The dynamic gas disengagement technique and some typical experimental results are presented in Figure 3.3. At a superficial gas velocity of 2.2 cm/s (0.87 in/s) where the flow is bubble flow, the dispersion height falls in a uniform manner with time as the small, uniform gas bubbles which characterize bubble flow disengage from the dispersion. At superficial gas velocities greater than 10 cm/s (4 in/s) where the flow was visually noted to be in the churn-turbulent regime, two distinct regions of the dynamic gas disengagement curve are discernible. The region at small times which has a larger slope corresponds to the disengagement of the large, fast-rising bubbles, while the region at later times which has a smaller slope corresponds to the disengagement of the smaller bubbles that are dispersed as a pseudohomogeneous phase with the liquid in churn-turbulent flow.

The dynamic gas disengagement technique is subject to a simple interpretation. From Figure 3.3 it can be seen that the slope at small times when the large gas bubbles disengage is equal to the superficial gas velocity. This implies that in the churn-turbulent flow regime most, if not all, of the gas fed to the column is transported in the form of large bubbles. The smaller gas bubbles that disengage slowly (at later times) can then be seen to only contribute to the total gas holdup and not to the transport of gas through the column. These small gas bubbles must then be entrained by the liquid circulation in the column as was reported by Hills (30) and was discussed earlier. Vermeer and Krishna (32) were then able to divide the total gas holdup into

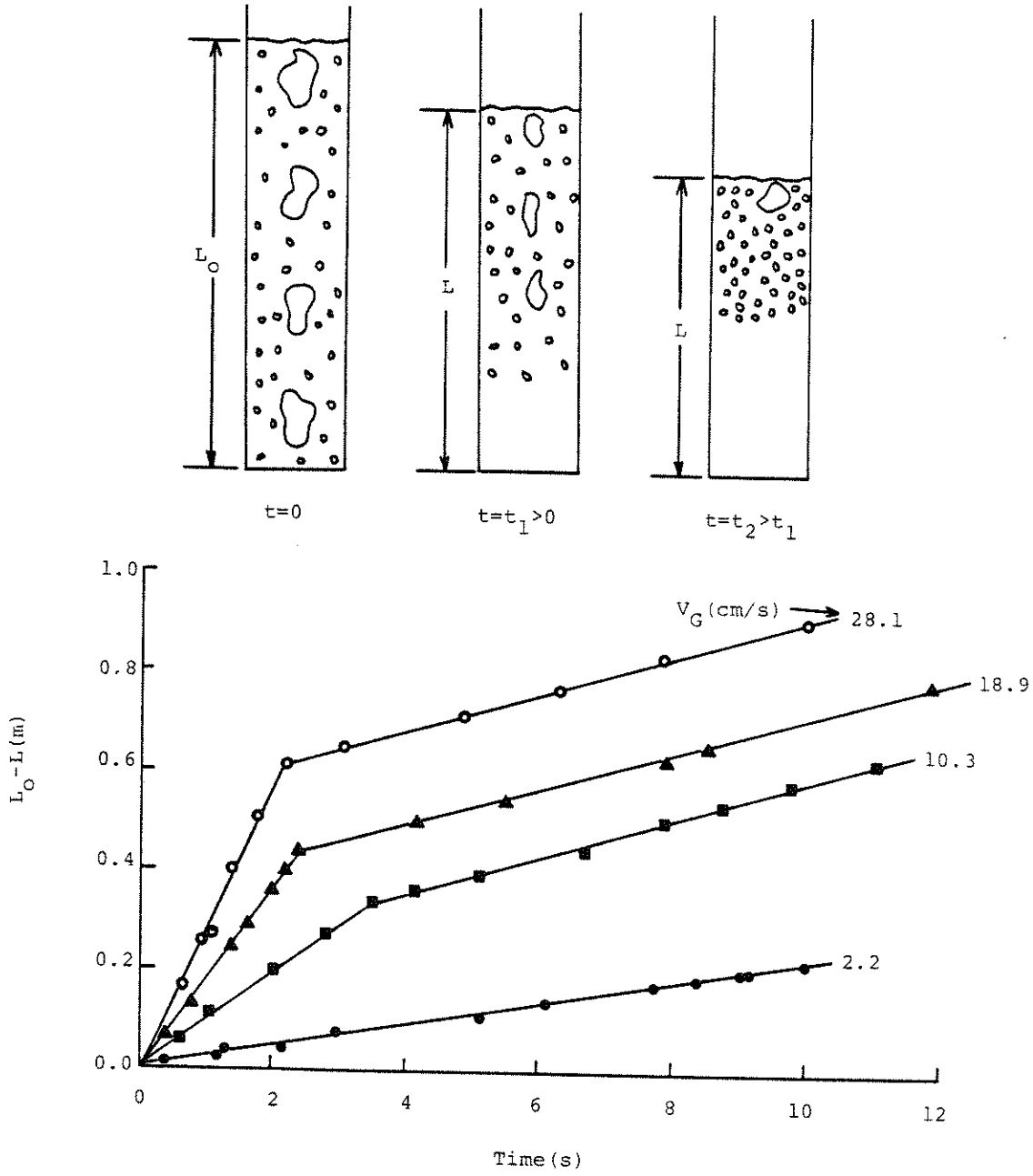

Figure 3.3 The Dynamic Gas Disengagement Technique Illustrated Including Experimental Results of Vermeer and Krishna (32)

two components, the transport and entrained holdups, which correspond to the large, fast-rising bubbles and the small, entrained bubbles, respectively. The total, transport, and entrained gas holdups as determined by Vermeer and Krishna (32) are presented as functions of the superficial gas velocity in Figure 3.4. From this figure it can be seen that for this system (turpentine 5 and nitrogen) both the transport and entrained gas holdups increase with the superficial gas velocity with the transport holdup increasing at a somewhat greater rate than the entrained holdup. It is interesting to note that, at the conditions studied, the entrained holdup is approximately twice that of the transport holdup. The rise velocities of the large bubbles could be determined from the dynamic gas disengagement studies and also from gas-phase residence time distribution studies. These values agreed closely and indicated that the large bubble rise velocity increased continually with the superficial gas velocity which agrees with the results of Ohki and Inoue (29) although the relationship between the large bubble velocity and superficial gas velocity is not a linear one in this case as was reported by Ohki and Inoue (29). At a superficial gas velocity of 10 cm/s (4 in/s), the large bubble rise velocity was about 120 cm/s (50 in/s), while at a superficial gas velocity of 30 cm/s the large bubble rise velocity had increased to 180 cm/s (70 in/s). These rise velocities are considerably larger than those on the order of 100 cm/s (40 in/s) reported by Hills and Darton (33) for an air-water system.

Based on an in depth and insightful interpretation of these hydrodynamic and some mass transfer experiments, Vermeer and Krishna (32) formulated the schematic representation of churn-turbulent hydrodynamics and mass transfer illustrated in Figure 3.5. At the base of the column,

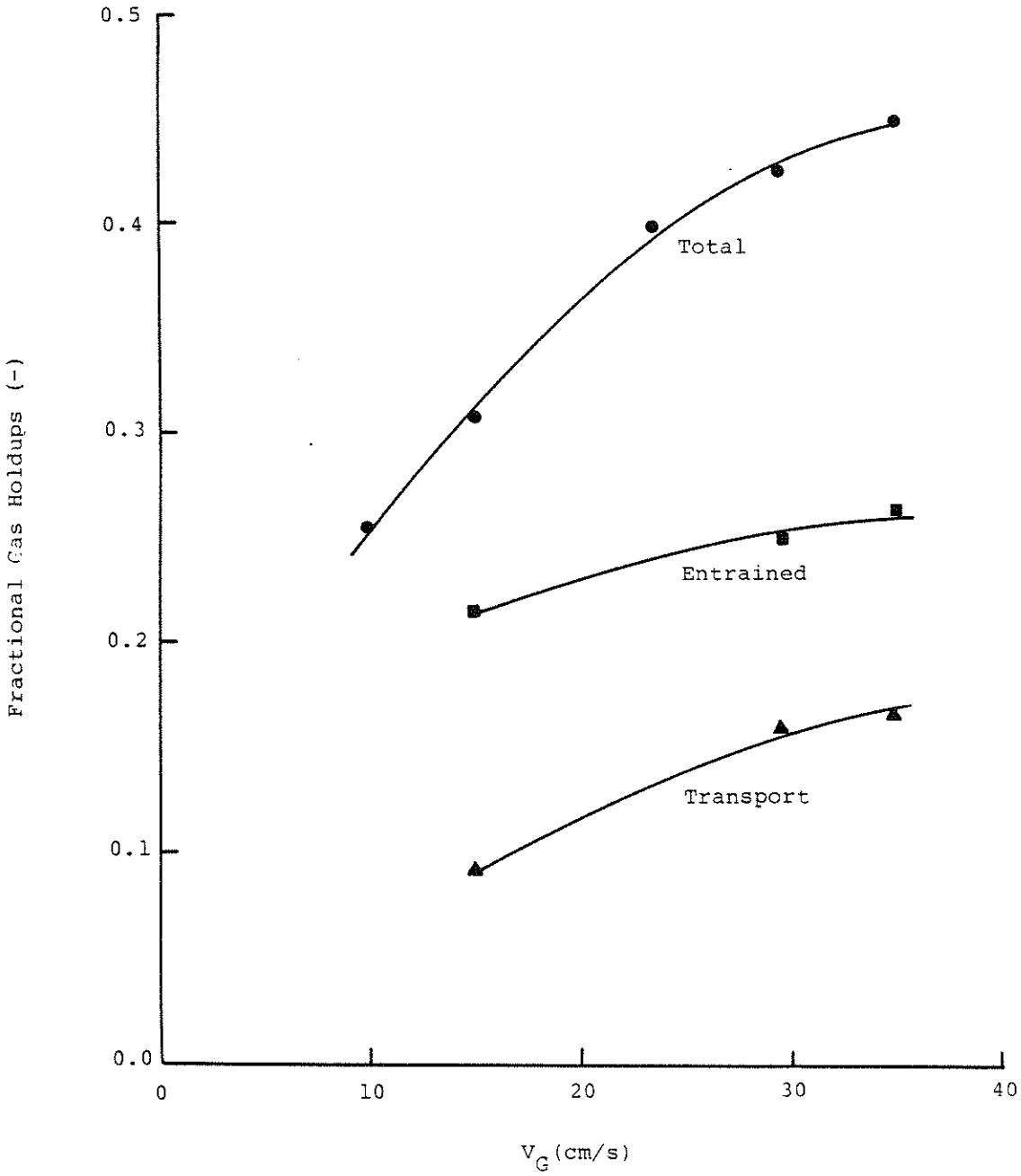

Figure 3.4 Total, Transport, and Entrained Gas Holdups as Determined by Vermeer and Krishna (32)

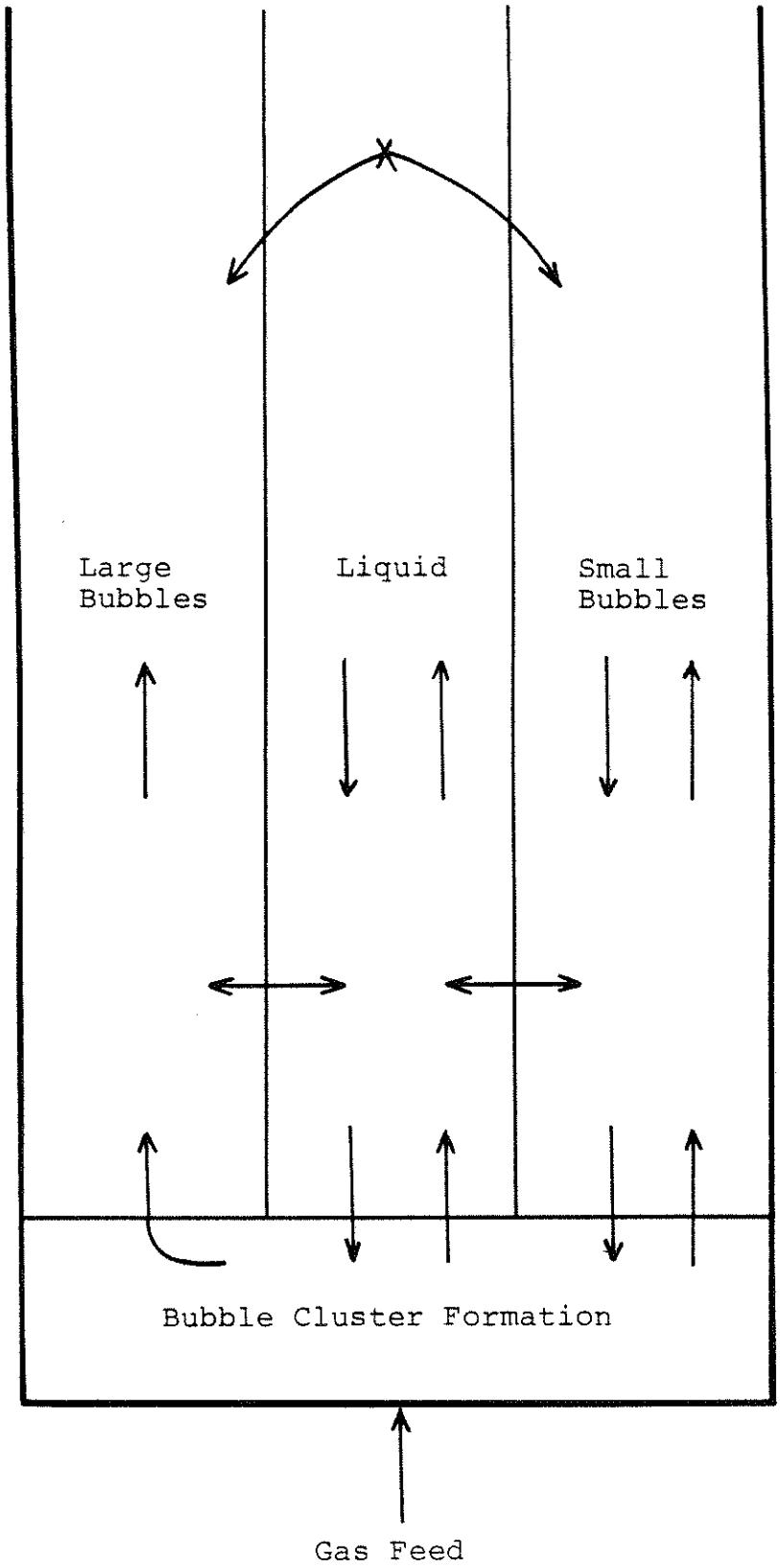

Figure 3.5 Schematic of Churn-Turbulent Bubble Column Behavior as Presented by Vermeer and Krishna (32)

the gas phase is sparged into the liquid phase and is dispersed into small bubbles by the gas distributor. If the superficial gas velocity is sufficient to cause churn-turbulent flow to occur, the small gas bubbles coalesce to form large bubbles that rise in a nearly plug flow manner. These large bubbles do not grow or break up to any appreciable extent and they transport the majority of the gas through the column. Because of the rising of these large, coalesced bubbles, the mixture of small gas bubbles and liquid are agitated violently. Through their work, Vermeer and Krishna (32) did a good job of characterizing the churn-turbulent regime of bubble column operation.

Schumpe et al. (34) noted a marked decrease in the conversion of the gas-phase reactant with an increase in the gas flow in churn-turbulent flow when carbon dioxide is absorbed into and reacted in an aqueous solution of sodium hydroxide. Since this reaction is quite fast, the performance of the column will be determined to a large extent by the mass transfer characteristics of the column. Absorption and reaction in a bubble column is typically modeled by assuming that the gas phase can be represented by a single class of bubbles of an average size. This type of model assumes that all of the gas bubbles behave in the same manner which does not correspond to the observations of Vermeer and Krishna (32) and others. Joseph and Shah (35) attempted to model the behavior of a bubble column operating in the churn-turbulent regime by dividing the gas holdup into two classes. The first bubble class consists of the large, coalesced bubbles that are assumed to travel through the column in a plug flow manner. The second bubble class consists of the small bubbles that are dispersed in the liquid phase and

are assumed to be in a partially or totally backmixed state. Using only the large bubble size as an adjustable parameter, Joseph and Shah (35) were able to correlate the reduced gas-phase conversion in the churn-turbulent regime of bubble column operation. The model of Joseph and Shah (35), combined with the experimental data of Schumpe et al. (34), illustrates the need to treat bubble columns operating in the churn-turbulent regime differently than those operating in the bubble flow regime. In this case, gas bypassing in the large, coalesced bubbles reduces the gas-phase reactant conversion in a manner similar to gas bypassing in a fluidized bed operating at gas velocities above the minimum fluidization velocity.

4. LIQUID-PHASE BACKMIXING IN BUBBLE COLUMNS

4.1 INTRODUCTION

Because of the previously discussed effect of flow regime on column behavior, knowledge of the flow regime in a bubble column operation is helpful in predicting and correlating the parameters that describe the column behavior. To design a bubble column or any other gas-liquid reactor, three factors, two of which may depend on flow regime, that determine the system behavior must be quantified (in the general case; in some special cases not all factors are operative). These factors are the mixing of the gas phase and liquid phase (the residence time distributions, RTDs), interphase mass transfer, and reaction kinetics (not dependent on flow regime). The main focus here is the liquid-phase mixing, particularly in the churn-turbulent regime. The subject of liquid-phase backmixing in bubble columns has received considerable attention. In his review of bubble column design, Mashelkar (36) qualitatively discussed liquid-phase backmixing and its effect on system design while Pavlica and Olson (37) and Mecklenburgh (38) presented generalized methods for the design of partially back-mixed systems. Shah and coworkers (39) presented a complete review of backmixing in all types of gas-liquid reactors and, in a number of recent reviews (1,40,41), have discussed the current status of the hydrodynamic and mixing models of bubble column reactors.

Hartland and Mecklenburgh (42) define backmixing in a strict sense as "the case of non-ideal flow in which a random movement of fluid is superimposed on, and is in the direction of, the main flow" where ideal flow is considered to be plug flow. In this sense,

backmixing does not consider any effects due to transverse mixing, channeling, or large-scale recirculation. However, in any flow system, the different dispersion mechanisms cannot be clearly separated and any model of nonideal flow behavior must consider all modes of dispersion. A number of dispersion mechanisms can be observed in bubble columns, the magnitude of each mechanism depending on the operating conditions of the system. The mechanisms that contribute to liquid-phase backmixing in bubble columns include large-scale liquid circulation due to nonuniform velocity profiles, entrainment in bubble wakes and wake shedding, turbulent eddy transport, and molecular diffusion.

The design of reactor systems is generally based upon simple models. For a bubble column operating in the churn-turbulent regime, the liquid phase will tend to complete backmixing due to the high level of turbulence and vigorous agitation provided by the large, fast-rising bubbles. The assumption of complete backmixing can be made for simplicity. However, Argo and Cova (43) have shown that even small deviations from complete backmixing can have a strong effect on column sizing when high conversion of the liquid-phase reactant is desired. The next level of model sophistication requires consideration of partial backmixing of the liquid phase.

4.2 THE AXIAL DISPERSION MODEL

Mixing of both the gas and liquid phases in bubble columns has been described almost exclusively by the one-dimensional axial dispersion model. Levenspiel (44,45) has discussed the development and application of the axial dispersion model in detail. The axial dispersion model was developed for the case of both laminar and turbulent homogeneous

(single-phase) flow by Taylor (46,47,48) and was later extended by Aris (49). The axial dispersion model was applied to the classical chemical engineering problem of residence time distribution by Levenspiel and Smith (50), van der Laan (51), and Aris (52). Bischoff (53) has verified the applicability of the axial dispersion model in reacting homogeneous systems.

In its original form as applied to homogeneous flow, the axial dispersion model was developed from Taylor's (46) approximate solution to the problem of dispersion by flow and molecular diffusion in tubes. This analysis showed that the combined mechanisms of solute dispersion (velocity gradients causing the majority of axial dispersion with molecular diffusion causing the majority of radial dispersion) may be described by an equivalent one-dimensional dispersion about a front moving with the mean velocity of the fluid. Taylor's (46) analysis is strictly valid only for long times and Gill and coworkers (54,55) have provided an exact analysis of the problem using a generalized dispersion approach. Their analysis indicated that Taylor's (46) approximate analysis could lead to errors for small times that could be significant in systems where fast reactions occur.

The mixing process during flow is due to a repeated redistribution of material by eddy motion and relative velocity between fluid elements. This redistribution can be envisioned to be statistical in nature and has been described mathematically by a gradient transport model that is directly analogous to Fick's law of molecular diffusion.

$$N = - E \frac{\partial C}{\partial z} \tag{4.1}$$

where: N, dispersive flux of a solute species

E, axial dispersion coefficient

C, solute concentration

z, axial coordinate (direction of dispersion)

In this model, all deviations from plug flow are assumed to be described by being lumped into one dispersive flux that can be described by Equation 4.1. The species conservation equation for the axial dispersion model can be developed from a shell balance for a representative fluid element.

$$\frac{\partial C}{\partial t} = E \frac{\partial^2 C}{\partial z^2} - u \frac{\partial C}{\partial z} \qquad (4.2)$$

where: t, time

u, velocity (the constant, mean velocity)

The first term of Equation 4.2 represents the accummulation in the system while the second and third terms represent the net input to the system by dispersion and convection, respectively. The axial dispersion model predicts that any species spreads into a Gaussian (bell-shaped) concentration profile about a front moving with the mean fluid velocity. The simplicity of the axial dispersion model is evident from Equation 4.2 which utilizes only one model parameter. The magnitude of this one model parameter, the axial dispersion coefficient, E, determines the rate at which a solute spreads about the moving front. If the axial dispersion coefficient is zero, the system is in plug flow, while if the axial dispersion coefficient is infinite, the system is completely backmixed. Intermediate values of the axial dispersion coefficient can

be employed to describe intermediate degrees of backmixing. This model may also be expressed in the following dimensionless form.

$$\frac{\partial C'}{\partial t'} = \frac{E}{uL} \frac{\partial^2 C'}{\partial z'^2} - \frac{\partial C'}{\partial z'} \qquad (4.3)$$

where: $C' = \frac{C}{C_o}$, dimensionless concentration

C_o, reference concentration

L, reactor length

$t' = \frac{tu}{L}$, dimensionless time

$z' = \frac{z}{L}$, dimensionless axial coordinate

The dimensionless parameter $\frac{E}{uL}$ is the inverse Peclet number and its magnitude also determines the system behavior.

4.3 CRITIQUE OF THE AXIAL DISPERSION MODEL

The appeal of the axial dispersion model is obvious; it is a one-parameter model that can describe all degrees of backmixing and its one parameter has been well characterized by both theoretical and empirical studies. However, the axial dispersion model has recently received criticism related to its application in multiphase systems. General criticisms include the following. Application of the model leads to a split boundary-value problem that may be difficult to solve. Also, the choice of boundary conditions that are applicable to a given system may not be clear (56) and may significantly influence the solution to the model equations (45). Also related to the mathematical characteristics of the model is its prediction of an instantaneous response at all points in the system to the presence of a tracer or

solute anywhere else in the system; however, this response may be exponentially small. On a more practical basis, the axial dispersion model is incapable of describing any transverse mixing effects, there are difficulties in scaling the model up, and it does not properly describe mixing effects related to reaction kinetics.

More specifically, the axial dispersion model is based upon an extension of Taylor's (46) analysis of homogeneous flow systems. This analysis is based upon the consideration of small deviations from plug flow and the ability of the axial dispersion model to describe large degrees of backmixing such as occurs in the liquid phase of churn-turbulent bubble columns is simply a result of the mathematics of the problem. Among others, Wen and Fan (57) and Rice et al. (25) have cautioned against use of the axial dispersion model for systems that deviate greatly from plug flow.

Another criticism of the axial dispersion model is its basis as a gradient transport model in which the flux of some quantity, mass in this case, is proposed to be proportional to the spatial gradient of its concentration (density). The best known gradient transport models are Newton's law of viscosity, Fourier's law of heat conduction, and Fick's first law of diffusion. Analogous forms of these transport models have been applied to turbulent flow systems to describe the eddy transport mechanisms which are the time averages of a product of two fluctuating parameters that remain after time averaging of the turbulent conservation equations. However, in the case of the axial dispersion model, not only eddy transport is being described by a gradient transport model. Rather, all flow nonidealities are being lumped into the gradient transport form. Also, a major assumption of gradient

transport models is that the scale of the transport mechanism be small compared to the length over which the gradient changes significantly. Corrsin and coworkers (58,59) have noted with surprise the number of gradient transport models that have achieved general acceptance despite not fulfilling this basic assumption. Turbulent eddies on the scale of the column diameter (31) and large-scale liquid circulation (30) have been observed in churn-turbulent bubble columns which would seem to point to the inadequacy of a gradient transport model for describing liquid-phase mixing in bubble columns. Barkelew (60) has alluded to this criticism on the basis of an inconsistency encountered when developing the axial dispersion model for churn-turbulent bubble columns.

Justification for extending the axial dispersion model to multiphase systems has typically been qualitative in nature. Danckwerts (61) has discussed the conditions under which the axial dispersion model can be applied to flow through a bed of packed solids. Recent studies by Carbonell (62) and Sundaresan et al. (63) have shown that this application may be invalid. This led Carbonell (62) to modify the dispersion model for packed bed applications while Sundaresan et al. (63) formulated a new class of packed bed models termed the cross flow models. The most commonly cited justification for applying the axial dispersion model to multiphase systems has been its ability to describe tracer data. Levenspiel and Fitzgerald (64) have warned against this type of justification and cited the one-parameter convective models as a class of flow models that can yield Gaussian residence time distributions like the axial dispersion model. However, convective

models are based upon different fluid elements always having different velocities rather than fluid elements having fluctuating velocities as in the axial dispersion model. Due to this difference, the model parameters are not subject to the same interpretation and the two models do not scale up in the same manner.

There is presently no theoretically satisfying justification for extending the axial dispersion model to the problem of describing liquid-phase backmixing in bubble columns. The mixing of the liquid phase of a bubble column is caused by the action of the rising gas bubbles. The gas bubbles entrain liquid in their wakes and create an intense turbulence field that vigorously agitates the liquid phase. Reith et al. (65) suggest that the eddies generated by the rising gas bubbles are random in nature and are therefore amenable to treatment by an axial dispersion model. In their study, Reith et al. (65) drew upon the findings of Hanratty and coworkers (66) who demonstrated that mixing due to eddy movement can be described by a dispersion coefficient. It should be noted that Hanratty and coworkers (66) were concerned with the turbulence generated by fluidized particles that would be expected to generate a random turbulence field because of their random motion. On the other hand, the gas bubbles in a bubble column rise in a more or less unidirectional manner and may or may not generate a random turbulence field. In fact, Reith et al. (65) found that the magnitude of the turbulence in a bubble column varies between the axial and radial directions.

On a more empirical basis, Kunugita et al. (16) observed the motion of a mutually bouyant particle in the liquid phase of a bubble column.

They noted that the probability density of the particle position was a Gaussian curve centered at the point of particle injection. This led them to accept the validity of the axial dispersion model for describing liquid-phase backmixing in bubble columns. It should be noted that the particle was confined to the system and could not leave the system as a fluid element might. Also, the time period over which the particle was observed was short when compared to the typical mean residence time of the liquid in a bubble column operation. Despite these criticisms, this study is the best experimental attempt to verify the adequacy of the axial dispersion model. To date, few experimental efforts have been made to critically evaluate application of the axial dispersion model to reacting multiphase systems.

The final criticism of the axial dispersion model is related to the work of Hatton and Lightfoot (67) who approached the problem of dispersion, interphase mass transfer, and chemical reaction in multiphase systems by developing a generalized dispersion model. Through a complex analysis it was shown that the one-dimensional, area-averaged axial dispersion model is incapable of describing dispersion in multiphase systems. In particular, the axial dispersion coefficient was found to be time-dependent as well as a function of interphase mass transfer and chemical reaction. Experimental support of these findings has been presented by Linek et al. (68) who found different values of the liquid-phase axial dispersion coefficient in packed absorption columns when gas-liquid mass transfer occurred as opposed to those values obtained in the absence of interphase mass transfer. No such data has been obtained in bubble columns. Hatton and Lightfoot (67) determined the general form of the axial dispersion coefficient in

multiphase systems, but it is too complex to use for reactor modeling. If this criticism and those discussed previously indicate the inadequacy of the one-dimensional axial dispersion model, new models must be generated to describe dispersion.

4.4 CORRELATION OF THE AXIAL DISPERSION COEFFICIENT

Despite the objections of the preceding discussion, the axial dispersion model has been routinely applied to the problem of liquid-phase backmixing in bubble columns and some discussion of the methods employed to correlate the axial dispersion coefficient is in order. The number of studies of axial dispersion in bubble columns and the associated literature is overwhelming. Table 4.1 summarizes a number of correlations for predicting the axial dispersion coefficient.

The early studies, such as those of Argo and Cova (43), Bischoff and Phillips (69), Reith et al. (65), and Deckwer et al. (70), were designed to determine the effect of system parameters and operating conditions on the axial dispersion coefficient. It was generally found that the liquid-phase axial dispersion coefficient was strongly affected by the superficial gas velocity because this determined the intensity of turbulence in the column and also by the column diameter because this determined the scale of the largest turbulent eddies present in the column. The effects of other operating variables were found to be secondary. Chen (71) found that the superficial liquid velocity had little effect on liquid-phase dispersion which was attributed to the typically low liquid velocities employed in bubble columns compared to the rise velocity of the gas bubbles. Aoyama et al. (72) found no effect due to liquid physical properties while Hikita and Kikukawa (73) found that the liquid physical properties had a slight effect on liquid

Table 4.1 Summary of Available Correlations for the Axial Dispersion Coefficient

Source	Correlation	Comments
Deckwer et al. (70)	$E_L = 2.7\ D^{1.4}\ V_G^{0.3}$ (c.g.s. units)	Obtained strictly from the correlation of experimental data.
Ohki and Inoue (29)	$E_L = 0.30\ D^2\ V_G^{1.2} + 170\ d_o$ (c.g.s. units)	Valid for the bubble flow regime; based upon an extension of Taylor's (67) approach for homogeneous flows and matching experimental liquid-phase dispersion data.
Ohki and Inoue (29)	$E_L = \frac{14\ D}{(1-\varepsilon)^2}$ (c.g.s. units)	Valid for the churn-turbulent flow regime; based upon an expansion model of flow in this regime and matching experimental liquid-phase dispersion data.
Baird and Rice (74)	$E_L = 0.35\ D^{4/3}\ (V_G g)^{1/3}$	Based on an isotropic turbulence model and dimensional analysis; the coefficient 0.35 was obtained by matching experimental liquid-phase dispersion data for bubble columns, liquid-liquid spray columns, and fluidized beds.
Mashelkar and Ramachandran (75)	$E_L = \frac{1}{192}\left[\frac{V_C^2\ D^2}{E_m}\right]\left(1 + \frac{5\alpha}{3} + \frac{\alpha^2}{6}\right)$ $V_c = \alpha\ V_L$ $\alpha = \frac{V_G\ \rho_L\ g\ D^2}{8\mu_L\ V_{b\infty}\ V_L}$	Obtained using the liquid-phase velocity profile of Crabtree and Bridgewater (96) for chain bubbling by extending the method of Taylor (67); α determines the intensity of liquid circulation and for $\alpha = 0$ (no gas flow) this reduces to Taylor's (67) result for laminar flow.
Ueyama and Miyauchi (78), Miyauchi et al.	$E_L = 1.35\ V_G^{1/2}\ D^{3/2}$ (c.g.s. units)	Obtained by matching a theoretical velocity profile to liquid-phase axial dispersion data; velocity profile obtained using a liquid-phase momentum balance with the turbulent kinematic viscosity as an adjustable parameter.
Walter and Blanch (80)	$Pe_L = \frac{V_C\ D}{E_L} = 1.65$ $V_C = \left\{\frac{V_G\ g\ L}{4 + \frac{70}{Re_L^{0.25}} \cdot \frac{L}{D}}\right\}^{1/3}$ $Re_L = \frac{D\ V_C\ \rho_L}{\mu_L}$	Obtained by matching a theoretical velocity profile to liquid-phase axial dispersion data; velocity profile obtained using microscopic momentum and macroscopic energy balances with two adjustable parameters; valid for $1{,}000 < Re_L < 70{,}000$, $L/D > 3$, and $\varepsilon > 0.02$.
Joshi and Sharma (82), Joshi and Shah (40)	$Pe_L = \frac{V_C D}{E_L} = 3.2$ $V_C = 1.4\left\{gD\left[V_G + \frac{\varepsilon\ V_L}{1-\varepsilon} - \varepsilon\ V_{b\infty}\right]\right\}^{1/3}$	Obtained by matching a theoretical liquid circulation velocity to axial dispersion data; liquid circulation velocity obtained by solving the inviscid vorticity equations by an energy balance method.
Viswanathan and Rao (89, 90)	$Pe_L = \frac{V_C\ D}{E_L} = 2.6$ $V_C = V_{b\infty}\left(\frac{g\ R\ V_G}{V_{b\infty}^3}\right)^{0.4}$	Obtained by matching a theoretical liquid circulation velocity to axial dispersion data; liquid circulation velocity obtained by solving the inviscid vorticity equations by a force (pressure) balance method.

dispersion although they did not vary the physical properties over a significant range. Earlier studies also noted that gas distributor design only affected column behavior in a limited entry region although more recently Rice et al. (25) have observed that the gas sparger design can affect the quality of the entire gas-liquid dispersion and the mixing characteristics of the liquid phase. Deckwer et al. (70) developed a correlation based upon their own experimental data and that of other investigators. This correlation is typical of the earlier empirical equations and is listed in Table 4.1. The exponents of the empirical correlations have been observed to vary and this has been attributed to the studies being performed in columns operating in different flow regimes.

More recent studies have attempted to find some theoretical basis behind the correlations for the liquid-phase axial dispersion coefficient. Ohki and Inoue (29) were among the first investigators to propose a theoretical model of liquid-phase backmixing in bubble columns. One significant point of their development is that they noted two distinct flow regimes of bubble column operation, bubble flow and churn-turbulent flow, and developed separate correlations for each flow regime based upon the flow characteristics of these regimes. Under the conditions of bubble flow, Ohki and Inoue (29) developed what was termed the velocity distribution model. This model assumes that liquid dispersion is caused by the combined action of the liquid velocity distribution and the motion of the individual bubbles. Following the work of Taylor (46) and Aris (49) and assuming that the column behaves in a homogeneous

manner, Ohki and Inoue (29) proposed the following general form for the liquid-phase axial dispersion coefficient under the conditions of bubble flow.

$$E_L = \frac{D^2 \, u_L^2}{k \, E_B} + E_B \qquad (4.4)$$

where: E_B, a dispersion coefficient caused by bubble motion (analogous to the molecular diffusion coefficient)

u_L, characteristic liquid velocity

k, a constant determined by the velocity distribution

The first term of Equation 4.4 represents the effect of the velocity distribution on dispersion while the second term represents the contribution of the individual rising gas bubbles. Ohki and Inoue (29) related the characteristic liquid velocity, u_L, to the superficial gas velocity, V_G, by literature correlations and determined the value of kE_B from experiment. They found that the contribution of the individual bubbles was generally negligible, but could become significant if the gas sparger holes are large enough. Their final correlation for the bubble flow regime is listed in Table 4.1.

In the churn-turbulent flow regime the column can no longer be considered to be homogeneous and Ohki and Inoue (29) proposed an expansion model based upon the heterogeneity of the column. They assumed that the majority of the gas travels in the form of large, coalesced bubbles which act to agitate and expand the liquid in the column. These large bubbles are assumed to exist uniformly along the column when observed on a time scale typical of the dispersion process.

Ohki and Inoue (29) defined a new dispersion coefficient, E_L^*, that describes the dispersion characteristic of the turbulent motion of the liquid. Experiments indicated that E_L^* was independent of the superficial gas velocity, but was directly proportional to the column diameter.

$$E_L^* = 14\ D \qquad \text{(c.g.s units)} \tag{4.5}$$

Ohki and Inoue (29) then related E_L^* to the actual dispersion coefficient, E_L, and presented the correlation of Table 4.1 for the liquid-phase axial dispersion coefficient in the churn-turbulent flow regime. Ohki and Inoue (29) took the lack of dependence of the axial dispersion coefficient on the superficial gas velocity as an indication that the liquid phase had achieved a maximum turbulence intensity in the churn-turbulent regime.

Baird and Rice (74) developed a dimensionally consistent model based upon the theory of isotropic turbulence. Employing a dimensional analysis of the problem, the following relation between the eddy diffusivity, E_e, a length parameter, ℓ, and the specific energy dissipation rate, P_m, can be developed.

$$E_e = K\ell^{4/3} P_m^{1/3} \tag{4.6}$$

K is a dimensionless constant that should have a universal value if the proper choice of the length parameter and specific energy dissipation rate is made for different systems. To relate the eddy diffusivity relation of Equation 4.6 to the liquid-phase axial dispersion coefficient in bubble columns, an appropriate choice of ℓ and P_m must be made.

Baird and Rice (74) chose the column diameter as the length parameter because the column diameter determines the size of the largest eddies in the system which are responsible for dispersing the liquid. If the superficial liquid velocity is low and the dissipation of energy in the gas phase is neglected, the specific energy dissipation rate is equal to the product of the superficial gas velocity, V_G, and the acceleration of gravity, g. Baird and Rice (74) checked their correlations with the experimental results of other workers and found K to have an approximate value of 0.35 for bubble columns, liquid-liquid spray columns, and fluidized beds. The final form of the liquid-phase axial dispersion coefficient correlation is listed in Table 4.1. Although this model has some interesting points, the model is based on the theories of isotropic turbulence and it should be recalled that Reith et al. (65) observed that the macroscopic turbulence field which is responsible for liquid-phase dispersion in bubble columns is not isotropic.

Previously it was noted that large-scale liquid circulation has been observed in some bubble column operations. Mashelkar and Ramachandran (75) developed a correlation for the liquid-phase axial dispersion coefficient for bubble columns where the effects of liquid circulation are the dominant mechanism of dispersion. Their analysis was based on an approximate solution of the convective-diffusion equation following the classical approach of Taylor (46) for homogeneous systems. To follow this approach it is necessary to know the liquid-phase velocity distribution. Since Mashelkar and Ramachandran (75) were concerned with bubble columns in which large-scale liquid circulation occurs, they used the velocity distribution of Crabtree and Bridgwater (76) derived for

central core of the column while essentially gas-free liquid recirculates in the annular region of the column. The presence of the gas in the central core reduces the density in this region which causes the liquid to recirculate in a manner such that it flows upwards in the core region and downwards in the annular region outside the draft tube. This is a gas-lift operation and as such is not directly applicable to bubble column operation. However, as was noted earlier, Hills (30) found that the gas holdup profile in bubble columns is nearly parabolic with a maximum on the column axis. This gas holdup profile causes density differences that can drive liquid circulations within the column. In fact, this is what Hills (30) observed when he measured the time-averaged liquid velocity profiles in bubble columns; the liquid flowed upwards in the central core of the column and downwards in an annular region near the column wall. This behavior is similar to that studied by de Nevers (77) even though no physical barrier such as a draft tube was present to separate the core and annular regions.

Miyauchi and coworkers (78,79) employed an empirical (radial) gas holdup profile to approximate the density difference driving force in bubble columns under turbulent operating conditions. To determine the velocity profile of the recirculating liquid, this empirical gas holdup profile was employed in writing a momentum balance for the liquid phase. In this momentum balance, an empirical parameter termed the turbulent kinematic viscosity, ν_t, was used to model the shear stress in the liquid. Note that the turbulent kinematic viscosity is not a fluid property, but is a property of the system and the operating conditions. The following liquid velocity profile was obtained.

$$u_L + |u_W| = \frac{1}{32} \frac{g D^2 \varepsilon}{\nu_t} [1 - (\frac{r}{R})^2]^2 \qquad (4.7)$$

In this equation, $|u_W|$ is the absolute value of the liquid velocity at the column wall. In this solution of the liquid-phase momentum balance, the laminar sublayer at the column wall was assumed to be negligibly small so that the universal (turbulent) velocity profile could be used to generate the boundary condition at the column wall rather than using the no-slip condition. $|u_W|$ can be determined using an overall mass balance for the liquid phase.

$$|u_W| = \frac{1}{192} \cdot \frac{g D^2 \varepsilon}{\nu_t} \cdot \frac{2 - 3\varepsilon}{1 - \varepsilon} - \frac{V_L}{1 - \varepsilon} \qquad (4.8)$$

Note that in Equations 4.7 and 4.8, ε refers to the average gas holdup and not to the gas holdup at a specific point in the system. The turbulent kinematic viscosity was determined by a best fit of experimental liquid velocity profiles. It was found to have a strong dependence on the column diameter and a very small dependence on the superficial gas velocity.

$$\nu_t = 0.160 \, V_G^{1/6} \, D^{3/2} \qquad \text{(c.g.s. units)} \qquad (4.9)$$

Note that Equation 4.9 must be used with c.g.s. units. This velocity profile was then used to correlate axial dispersion data in bubble columns and the correlation is listed in Table 4.1.

Walter and Blanch (80) also employed an empirical gas holdup profile to model density difference driven liquid circulation in bubble columns. To determine the average liquid circulation

velocity, a combination of microscopic momentum balances and macroscopic energy balances were employed. Two types of flow were characterized by the proper choice of boundary conditions. These types of flows were termed turbulent flow which is characteristic of systems with high superficial gas velocity or a low viscosity liquid and slow flow which is characteristic of systems with low superficial gas velocity or a high viscosity liquid. Walter and Blanch (80) attempted to correlate liquid-phase axial mixing data in terms of a liquid-phase Peclet number, Pe_L, that incorporated the column diameter, D, as a length scale and the average liquid circulation velocity, V_C, as a velocity scale.

$$Pe_L = \frac{V_C D}{E_L} \tag{4.10}$$

Analysis of data from a number of investigations indicated that the liquid-phase Peclet number defined in Equation 4.10 is constant at a value of 1.65 in turbulent flow ($1{,}000 < Re_L < 100{,}000$; $Re_L = \frac{D\ V_C\ \rho_L}{\mu_L}$). The average liquid circulation velocity for this regime was found to be of the form presented in Table 4.1 using a combination of microscopic momentum balances and macroscopic energy balances.

Whalley and Davidson (81) employed an energy balance method to describe the hydrodynamics of bubble column systems. In the energy balance method, the vorticity equations for an inviscid axisymmetric flow field (such as a bubble column of circular cross section) are solved to yield the liquid-phase velocity flow field. This velocity profile contains the circulation strength (or maximum vorticity) as an unknown which can be determined by an energy balance which equates

the rate of energy input to the system to the rate of energy dissipation in the system. The energy balance as employed by Whalley and Davidson (81) was suitable for shallow bubble columns ($L/D \approx 1$); however, the liquid circulation velocity was found to depend on the column height, L, which has not been found to be the case for bubble columns of larger height to diameter ratios (70).

Joshi and Sharma (82) modified the energy balance method to make it applicable to systems with height to diameter ratios greater than unity. Since Whalley and Davidson (81) were concerned with shallow bubble columns, they found it necessary to consider only one liquid circulation path (or cell) with a height equal to the column height. On the other hand, when studying columns with height to diameter ratios greater than unity, Joshi and Sharma (82) were faced with the possibility of multiple circulation cells in the axial direction. This led to a representation of the liquid-phase velocity profile illustrated in Figure 4.1a. Van den Akker and Rietema (83) objected to this representation because the radial velocities in two (axially) neighboring cells have an opposing sense. Van den Akker and Rietema (83) modified the energy balance method so that it would yield the liquid-phase velocity profile shown in Figure 4.1b. Joshi (84) dismissed this view on the basis of the study of Hills (30) which indicated that the liquid in the central region of a bubble column always flows upwards while that in the wall region always flows downwards which is contrary to the physical representation of van den Akker and Rietema (83). Despite this disagreement, the energy balance of Joshi and Sharma (82) will be presented as it leads to a novel interpretation of liquid-phase axial dispersion in bubble columns.

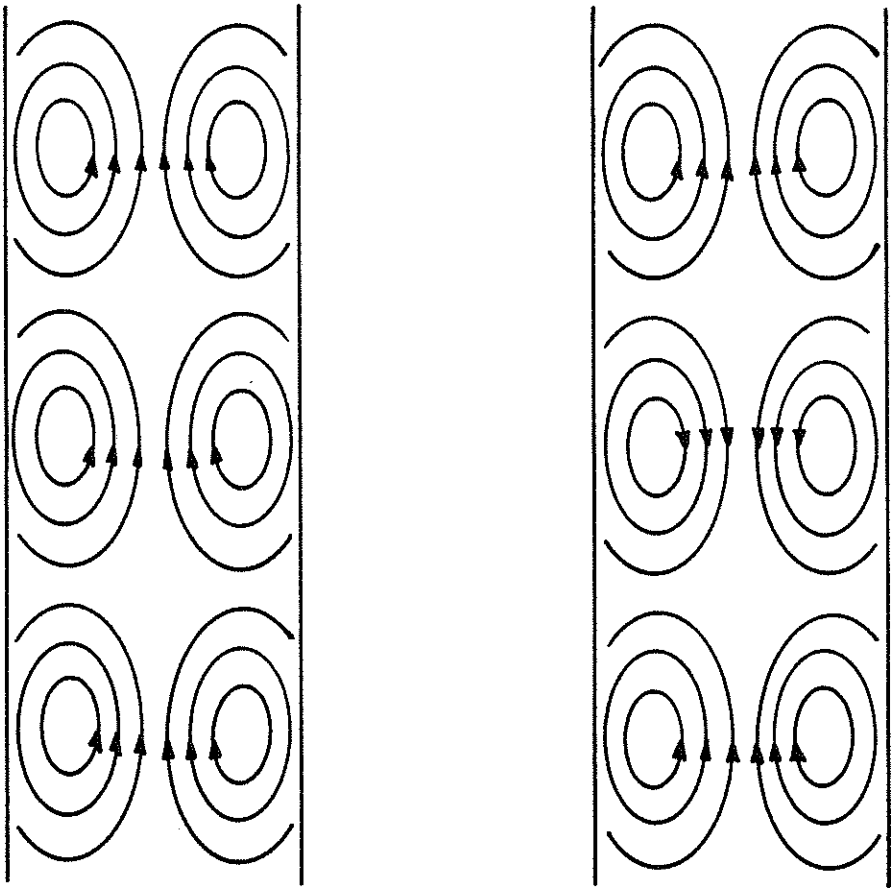

Figure 4.1 Circulation Cells in Bubble Columns

a. According to Joshi and Sharma (82)
b. According to van den Akker and Rietema (83)

As has been discussed by Lehrer (85), Joshi (86), and Field and Davidson (87), the rate of energy input to a bubble column consists of pressure, kinetic, and potential energy contributions from both the gas and liquid phases. However, in most cases the only term of significance is the potential energy of the gas which was the only term included by Joshi and Sharma (82) in their analysis. Energy dissipation was considered to occur by six mechanisms. Energy could be dissipated in the bubble wakes, by the net bubble break-up, in the hydraulic jump at the liquid surface, by turbulent dissipation in the gas distributor region, by viscous dissipation at the column walls, and by loss of kinetic energy without pressure recovery during the downward flow of the liquid (eventually this energy would be lost to viscous dissipation in turbulent eddies). By order of magnitude estimates and physical reasoning, Joshi and Sharma (82) neglected all modes of energy dissipation except for that dissipated in bubble wakes and the liquid kinetic energy lost without pressure recovery during downflow. The rate of energy input to the column and the energy dissipation rate in the bubble wakes are of known form (analytical expression) and their difference is equal to the rate of liquid kinetic energy dissipation without pressure recovery which can be related to the liquid circulation velocity through the inviscid vorticity equations.

To complete their analysis it was necessary for Joshi and Sharma (82) to determine the height of the circulation cells (assuming that there are no multiple circulation cells in the radial direction) pictured in Figure 4.1a. Following the results of Whalley and Davidson (81), it was assumed that the size of the circulation cells adjust so

as to minimize the maximum vorticity in the column. This led to circulation cells with heights equal to the column diameter. The liquid circulation velocity then takes the form listed in Table 4.1 (40). Using this circulation velocity, Joshi and Sharma (82) correlated liquid-phase axial dispersion data in a Peclet number form, also listed in Table 4.1. Recall that Walter and Blanch (80) found the Peclet number to have a value of 1.65 when their expression for the circulation velocity was used. Joshi (88) has further extended the energy balance method to the case where there is communication (exchange) between adjacent circulation cells which is a more physically realistic model.

Viswanathan and Rao (89,90) have also used inviscid flow theory to describe liquid circulation in bubble columns. They followed the same approach as Whalley and Davidson (81) and Joshi and Sharma (82); however, they employed a force balance (similar to the pressure balance of Freedman and Davidson (91) rather than an energy balance to determine the circulation strength (maximum vorticity) which arises from the solution of the vorticity equations for inviscid flow. In this force balance the weight of liquid in a circulation cell is balanced by (equal to) the pressure force that acts upwards on the base of the circulation cell. The pressure force can be divided into a dynamic (flow) component and a stagnation component which allows for the determination of the liquid circulation strength. This force balance leads to the expression of Table 4.1 for the liquid circulation velocity. Correlation of experimental liquid-phase axial dispersion data leads to a corresponding Peclet number correlation.

Some of these analyses of liquid-phase backmixing in bubble columns are very insightful. However, they usually only consider one dispersion mechanism and they all utilize the axial dispersion model to describe the backmixing process. This model has been shown to be inadequate and it is hoped that a more physically realistic model would be more appropriate.

5. PROPOSED RESEARCH

5.1 INTRODUCTION

The following discussion describes a research program that can be followed to develop a better understanding of bubble column hydrodynamics. The research is aimed at building upon previous work which was described in the preceding discussion while attempting to follow some new directions that will add new insights to the modeling of bubble column behavior. The following discussion is broken into four sections. The first is concerned with presenting a model to describe liquid-phase backmixing in bubble columns operating in the churn-turbulent regime and the experiments that would be necessary to determine the model parameters and to attempt to validate the model. The second section describes a lab-scale bubble column system that has been constructed to carry out the experiments. Modifications and additional equipment that will be necessary will also be discussed. The third section reports some preliminary results obtained in the lab-scale bubble column and relates them to the flow transitions that occur in bubble columns and the proposed liquid-phase backmixing model. The final section compares the proposed backmixing model with the axial dispersion model for a number of liquid-phase tracer studies.

5.2 LIQUID-PHASE BACKMIXING MODEL

5.2.1 Insights

Two basic approaches have been followed when attempting to model gas-liquid flows. The first approach stems from a hydrodynamic approach to the modeling problem. This approach, which has been discussed by Rietema (92) and Bouré and Delhaye (93), is based upon writing

conservation equations (mass, momentum, and energy) for the system and solving these equations subject to the appropriate boundary conditions. Modeling in this manner is generally aimed at prediction or correlation of hydrodynamic parameters such as fractional gas holdup, frictional pressure drop, and the mass fluxes of the gas and liquid phases.

A variety of hydrodynamic modeling approaches exist, each with its own level of sophistication and inherent assumptions. One common approach is to consider the conservation equations for the gas and liquid phases which contain interaction terms due to interphase transport. These conservation equations are generally derived by the control volume (shell balance) approach (94) and disagreement exists as to their proper form. Disagreement arises over the proper choice of control volume and the means of averaging quantities over the surface and volume of this element (95,96). Application of these conservation equations is impractical because some terms, particularly the interaction terms, and the initial and boundary conditions of the equations can't be evaluated in a useable form. Rietema (92) has discussed constitutive equations that can be used with these models. Application of these models to bubble column operations would seem particularly difficult because of the complex hydrodynamics in the gas distributor region where a boundary condition must be specified.

Some of the previously discussed attempts to theoretically correlate the liquid-phase axial dispersion coefficient followed this hydrodynamic approach. However, it was assumed that the liquid-phase behavior could be described by the conservation equations of single-phase flow. The interaction terms that arise from the proper formulation of the conservation equations of two-phase flow were never considered. In each

case, the complex hydrodynamics of bubble columns were reduced to a description by the one-dimensional axial dispersion model. This is characteristic of the second approach to modeling gas-liquid flows. This is the approach followed for reactor design in which the hydrodynamics are described approximately by a simplified model. This second approach will be followed here in the development of a model to describe liquid-phase backmixing in churn-turbulent bubble columns.

As was mentioned previously, deviation from ideal plug flow in bubble column reactors is described almost exclusively by the axial dispersion model for both the gas and liquid phases. For the most part it is assumed that the behavior of the gas and liquid can be described independently, meaning that the backmixing in each phase can be described by an axial dispersion coefficient that is independent of the behavior of the other phase. The proposed model will attempt to link the behavior of the gas and liquid phases when considering backmixing of the liquid phase in churn-turbulent flow.

The drawbacks associated with the application of the axial dispersion model to bubble column operations were presented in a previous discussion. Barkelew (60) has given special attention to the requirement that for a gradient transport model such as the axial dispersion model to be applicable in a given system, the characteristic scale of the transport mechanism must be small compared to the distance over which the mean gradient of the transported property changes significantly. Observations of bubble columns operating in the churn-turbulent regime indicate that large bubbles or clumps of bubbles rise rapidly through the pseudo-homogeneous mixture of liquid and small gas bubbles at a somewhat

regular frequency. Immediately following the passage of a large bubble, the mixture of liquid and small gas bubbles at the rear of the bubble circulates rapidly in a vortex pattern. The scale of this organized vortex motion is approximately equal to the column diameter which would appear to violate the assumptions of gradient transport models.

Barkelew (60) has discussed the invalidity of the application of the axial dispersion model to bubble column operations from the perspective of the derivation of the species conservation equation of the model. The general species conservation equation for a parcel of fluid flowing through a system may be stated as follows.

$$\text{Accumulation} = \text{Source} + \text{Net Inward Flux} \tag{5.1}$$

The accumulation in a fluid element following the flow can be written as the substantial time derivative of the species concentration, $\frac{DC}{Dt}$. The source term can include the effects of interphase mass transfer and chemical reaction and can be written as a general volumetric source term, S(C), which is usually a function of the species concentration. The species conservation equation can then be written in the following form.

$$\frac{DC}{Dt} = S(C) + \frac{F}{V} \tag{5.2}$$

F represents the net inward flux to the fluid parcel while V represents the parcel volume. For gradient transport models such as the axial dispersion model, the net inward flux is expressed as the surface integral of the product of a diffusion coefficient and the normal component of the gradient of the species concentration.

$$F = \int_S [\lambda \ (\bar{\nabla} C \cdot \bar{n})] \ dS \tag{5.3}$$

The Gauss-Ostrogradskii theorem (94) can be used to convert the surface integral to a volume integral.

$$F = \int_V [\bar{\nabla} \cdot (\lambda \bar{\nabla} C)] \ dV \tag{5.4}$$

The fluid parcel volume is then shrunk to the infinitesimal according to the Dubois-Reymond lemma (97) and, if the diffusion coefficient, λ, is assumed constant, the species conservation equation takes the familiar form common to the gradient transport models.

$$\frac{DC}{Dt} = S(C) + \bar{\nabla}^2 C \tag{5.5}$$

where: $\bar{\nabla}^2 = \bar{\nabla} \cdot \bar{\nabla}$, Laplacian operator

Barkelew (60) believes that the physics of the system does not allow the volume of the fluid element to be shrunk to the infinitesimal. Because of the organized vortex motion that occurs during churn-turbulent operation, there is a characteristic size below which local properties no longer represent the entire volume. For bubble columns the appropriate fluid element appears to be a cylinder with a height and diameter roughly equal to the column diameter. Barkelew (60) therefore feels that the axial dispersion model is inappropriate for describing liquid-phase backmixing in bubble columns and a more appropriate model would consider the column to be composed of a series of fluid elements of the characteristic size which can exchange mass. The exchange of

mass is caused by entrainment of liquid in bubble wakes and large-scale liquid circulation and exchange of mass can occur between any two fluid elements in the system. The net inward flux to a fluid element centered at position z could then be described in the following manner.

$$F(z) = \sum_{x} K(z,x)C(x) \tag{5.6}$$

K(z,x), the dispersion kernel, represents the average net rate at which material is transported from position x to position z. The summation should be taken over all fluid elements in the system. The species conservation equation can then be expressed in the following form.

$$\frac{DC(z)}{Dt} = S[C(z)] + \sum_{x} K(z,x)C(x) \tag{5.7}$$

Application of this type of species conservation equation rests upon the determination of the form of the dispersion kernel. For bubble column operations a number of forms of the dispersion kernel can be hypothesized. One possible form of the dispersion kernel would be to limit communication (mass exchange) to adjacent fluid elements. This model then represents the system as a series of tanks with backmixing betwen adjacent stages. Another possible form of the dispersion kernel would be to express the communication between fluid elements as a function that decays as the distance separating the elements increases. The following liquid-phase backmixing model departs from the gradient transport form (Equation 5.5) of describing dispersion and adopts the opinion of Barkelew (60) that dispersion is the result of communication between fluid elements of some characteristic size at different points throughout the system.

5.2.2 Physical Model

Before a mathematical model of a process can be developed, a physical model of the process must be developed. The physical model of the process provides a clear understanding of the process upon which mathematical modeling efforts can be based. The physical model should be as close to physical reality as possible to ensure the validity of the mathematical model. In the previous discussion concerning the theories used to develop correlations for the liquid-phase axial dispersion coefficient in bubble columns, each correlation was developed based upon a physical model of bubble column operation. These physical models included an isotropic turbulent flow field, chain bubbling circulation, density difference driven circulation, and circulation cells among others. Each of these physical models has good and bad points. The physical model presented here will attempt to combine some of the good points of these models and some of the insights of Barkelew (60) to develop a new method for describing liquid-phase backmixing in churn-turbulent bubble columns.

It has often been noted that the turbulence level in a churn-turbulent bubble column is very high and that all quantities characteristic of the column operation oscillate around a mean value. For the most part, the physical models discussed above consider the time-averaged behavior of a bubble column operation. Considering only the time-averaged behavior may be suitable for describing the column behavior in the bubble flow regime where the turbulence level is comparatively low. Under the conditions of bubble flow it is probably suitable to describe the liquid-phase behavior with an axial dispersion model because the motion

of the rising gas bubbles will tend to redistribute small parcels of liquid in a random manner which is the behavior described by the axial dispersion model. The behavior of the gas phase could probably best be described by a convective model as suggested by Levenspiel and Fitzgerald (64) because the gas bubbles are relatively noniteracting and will rise at a range of velocities because of their slightly different sizes.

On the other hand, in the churn-turbulent regime the behavior is quite different because of the different behavior of the gas phase. Large gas slugs (not large enough to slug the column though) rise rapidly through the frothy mixture of liquid and small gas bubbles at a more or less regular frequency during churn-turbulent operation. It is the passage of these gas slugs that causes the high level of turbulence in the column and determines the column behavior. No previous physical model of churn-turbulent bubble column behavior has specifically considered the influence of these gas slugs. The physical model to be employed here will attempt to account for the effect of the gas slugs by dividing the column into two regions. The first region consists of the gas slugs themselves and any liquid and small gas bubbles that they entrain. This region will be designated as the slug region. The slug region is taken to be a fast-rising region of high gas holdup which is similar to the pulses investigated by Block and Drinkenburg (98) at high throughputs in cocurrent trickle bed operations. The second region of the column is the remainder of the column which is a dispersion of small gas bubbles in liquid. Observations of bubble columns operating in the churn-turbulent regime indicate that this dispersion of small gas

bubbles in liquid behaves in a pseudohomogeneous manner with its behavior being determined by the passage of the large gas slugs. This second region should be further divided into a number of cells of the characteristic size as suggested by Barkelew (60) since each of these cells represents a region of the column that should be treated individually because they each exhibit their own behavior. The physical model as outlined above is shown schematically in Figure 5.1.

To model the liquid-phase backmixing behavior, the behavior of the slug and cell regions must be postulated. The gas slugs (meaning the large gas bubble and the liquid and small gas bubbles it entrains) rise preferentially along the column axis although they can be observed to meander around the column centerline. This is consistent with the radial gas holdup profiles measured by Hills (30) and shown in Figure 3.2. The highest local gas holdup is at the column centerline where the highest frequency of slug appearance is expected. The centerline holdup increases with the superficial gas velocity which can be taken to indicate an increase in the slug size if the slug frequency is assumed constant (as discussed previously). The local holdup decreases from the maximum at the column axis and the meandering behavior of the gas slugs can be taken to be responsible for the smoothness of the profile. In the wall region, the holdup profile is not a strong function of the superficial gas velocity at the conditions characteristic of churn-turbulent operation (V_G = 9.5, 12.7, and 16.9 cm/s in Figure 3.2) which indicates the absence of gas slugs in the wall region.

Observation of churn-turbulent operation indicates that the gas slugs rise very quickly through the cell regions and the cells are

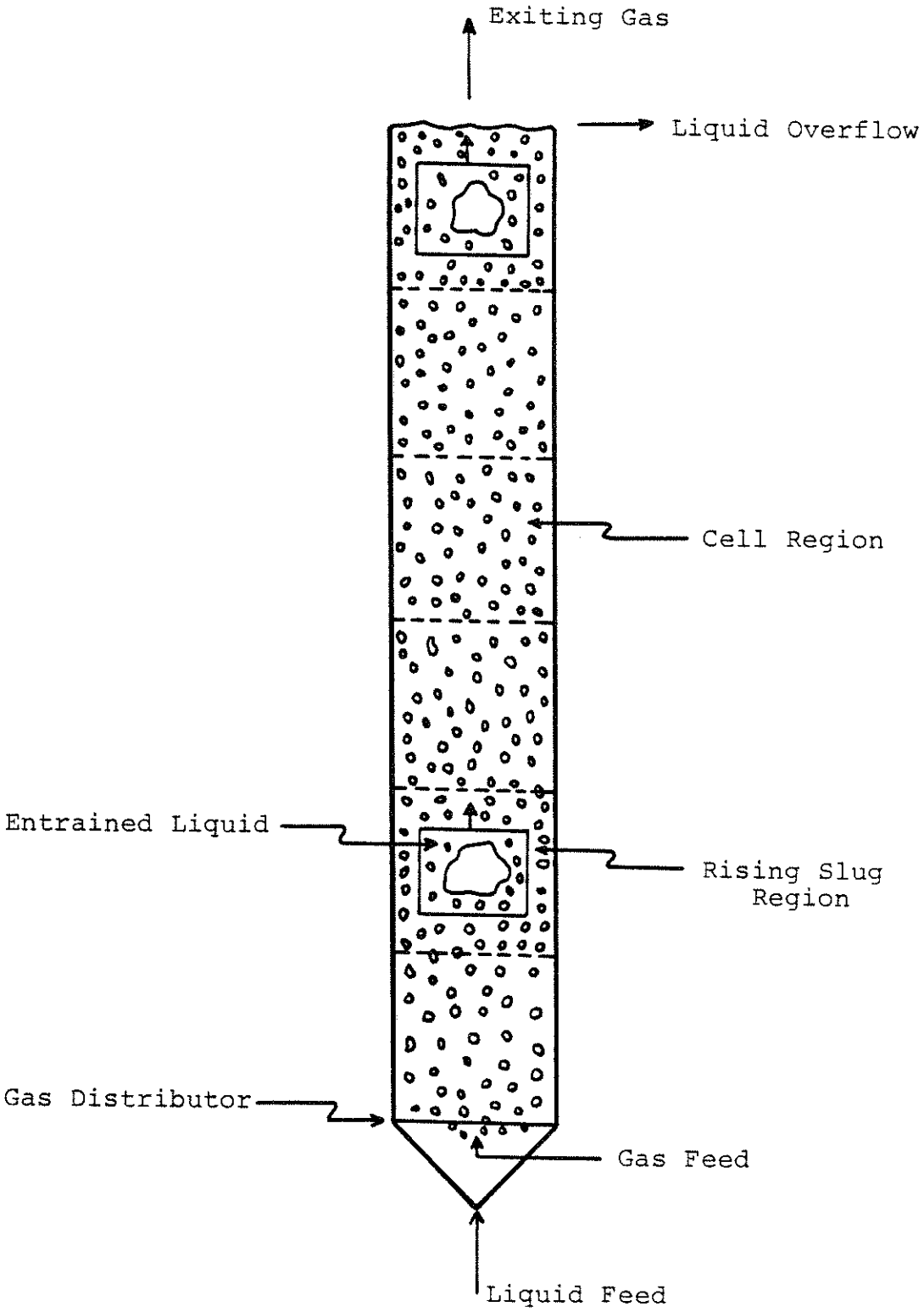

Figure 5.1 Schematic of the Physical Model of Churn-Turbulent Bubble Column Operation

agitated violently by this passage. However, the cells show no consistent upward or downward motion except during slug passage. Vermeer and Krishna (32) noted that all of the gas (or at least the majority of the gas) fed to the column appeared to be transported as slugs in churn-turbulent flow. The same reasoning will be employed here, and because the cell regions appear to show directed motion only during slug passage, it will also be assumed that all the liquid fed to the column is transported by the slugs. This is consistent with experimental liquid velocity profiles which show high upward liquid velocities near the column axis where the majority of slugs rise. These liquid velocities are not as high as the slug velocities; however, they are time-averaged velocities that show a good deal of oscillation. This oscillation could indicate the rapid rise of liquid during slug passage with little or no directed liquid motion at other times. Unfortunately, no one has statistically treated local liquid velocity or gas holdup (as discussed in the preceding paragraph) data to show how it may be correlated with slug passage.

Time-averaged liquid velocity profiles also indicate that the liquid in the wall region is actually flowing downward although the liquid is intended to flow cocurrently with the gas from the bottom to the top of the column. This can easily be explained from the current physical model as illustrated in Figure 5.2. Since all the gas and liquid fed to the column has been assumed to be transported in the slugs, the cell regions will be fixed in space. As a slug passes from one cell to the next, a mass balance at the plane separating the adjacent cells will indicate that the rising slug will displace an

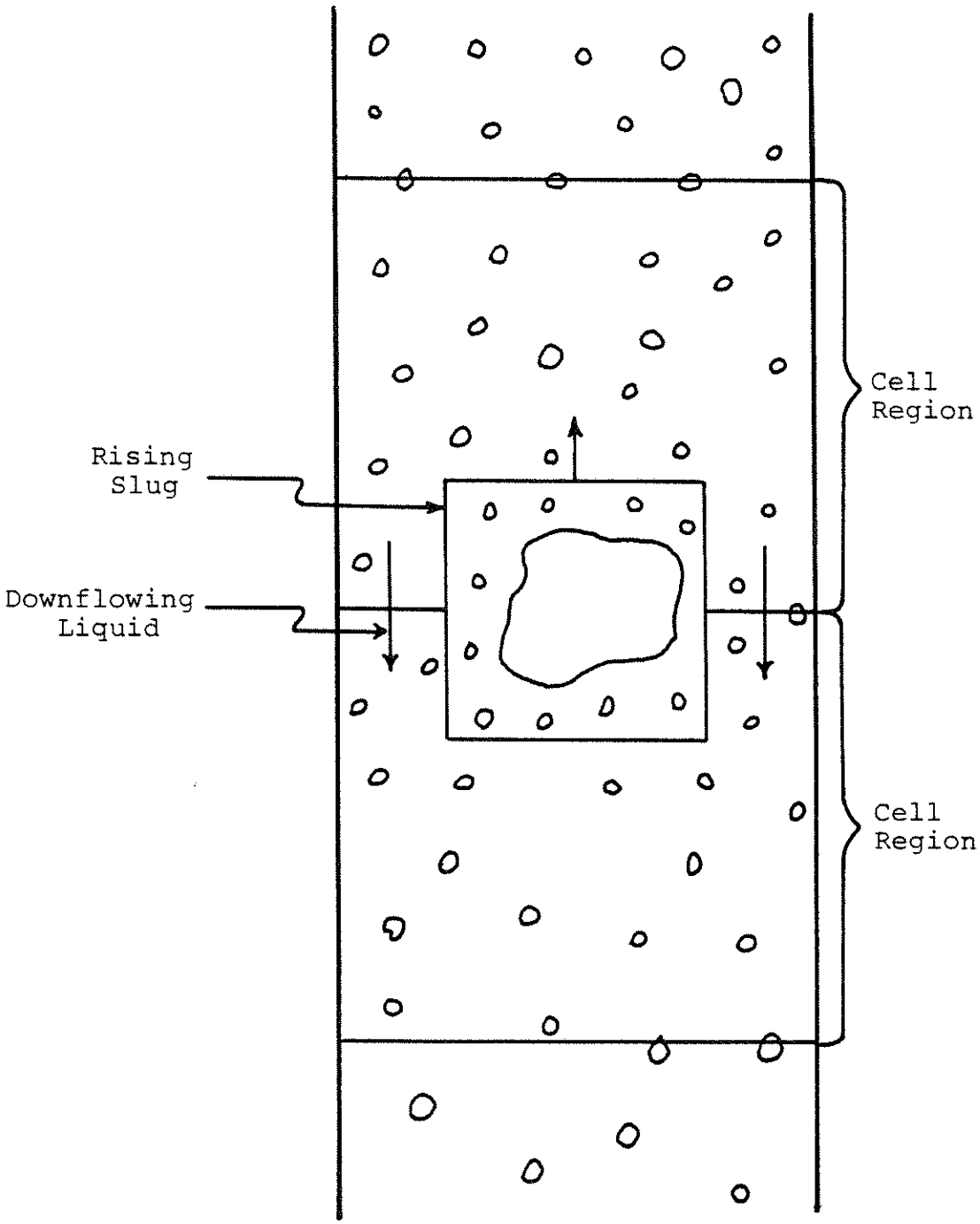

Figure 5.2 Slug Passage from Cell to Cell

equivalent volume of the gas-liquid dispersion from the upper cell which then flows down to the lower cell. Of course, as a gas slug rises into a cell it could be proposed that an equivalent volume is displaced into the next higher cell; however, this seems inconsistent with the experimental liquid velocity profiles which demonstrate downflow in the wall region. Note that this physical picture is similar to that in slug flow in smaller conduits in which a gas slug occupies a majority of the conduit cross section except for a film of liquid which flows downward between the gas slug and the column wall (refer to Section 2.1). Because of the high turbulence level in bubble columns and the large diameters of bubble columns, the gas phase cannot completely slug the column, but a similar process still occurs.

To formulate a liquid-phase species conservation equation, communication in the form of mass exchange between the slug and cells and between cells must be taken into account. Note that it will be assumed that the slugs rise independently and there is no direct communication between slugs. Because of the high level of turbulence in churn-turbulent bubble columns, there will be exchange of liquid between a rising slug and each cell region as the slug consecutively passes through each cell region. Since this mass exchange is a function of the turbulence level in the column, it may be represented simply as the product of a volumetric exchange rate and the time that a gas slug resides in each cell. The exchange rate should be a function of system geometry (most likely the column diameter) and operating conditions (most likely the superficial gas velocity and liquid physical properties). The mass exchange between adjacent cells has already been discussed in the preceding paragraph. This discussion only included mass exchange

between adjacent cells as a slug passes from cell to cell. However, since the exchange is so rapid as the slugs pass and the cells exhibit little directed motion except as the slugs pass, it will be assumed that adjacent cells only communicate as slugs pass.

The preceding discussion can be interpreted in terms of the species conservation balance proposed by Barkelew (60), presented as Equation 5.7, which contains the dispersion kernel, K (z,x), which describes communication between the various points in the column. In the proposed physical model, adjacent cells can communicate directly as the slugs pass and cells that are not adjacent cannot communicate directly. All cells can, however, communicate indirectly with all other cells. Cells can communicate indirectly in the forward sense (up the column) by first exchanging mass with a slug which will then exchange mass with each cell that it comes in contact with as it moves through the system. The time lag for exchange in this manner is equal to the distance separating the cells divided by the rise velocity of the slugs. Cells can communicate indirectly in the reverse sense (down the column) by exchanging mass with the adjacent lower stage as a slug passes. The lower stage will then exchange some of this mass with the next lower cell when the next slug passes. The time lag for exchange in this manner is equal to the number of stages separating the cells in question divided by the slug passage frequency.

The mixing that occurs in each slug and cell must be known so that the concentration of any species in the exchanged mass can be characterized. Because of the high turbulence level in a churn-turbulent bubble column, both the slug volume and the cell volume will be assumed

to be completely mixed on a time scale equal to the inverse of the slug passage frequency. Note that this means that each slug and each cell will be completely mixed individually, meaning that each slug and each cell will have its own characteristic concentration. This does not mean that all slugs have the same concentration and all cells have the same concentration or that the slug concentration is the same as the concentration of the cell in which it resides.

This completes the development of the physical model which will be summarized here for clarity. A bubble column is assumed to consist of two regions, the slug and cell regions. The slug region refers to the large gas bubbles and any liquid and small gas bubbles that they may entrain. These slugs tend to rise preferentially along the column axis at a fairly constant frequency. The cell region is the pseudo-homogeneous mixture of liquid and small gas bubbles that fills the remainder of the column. A number of cells exist along the length of the column. Previous studies would indicate that the height of one cell is equal to the column diameter. All of the gas and liquid fed to the column is assumed to be transported in the slugs so that the cells remain at a fixed point in the column. Mass may be exchanged from a slug to a cell as the slug passes through the cell. Adjacent cells also exchange mass directly as a slug crosses the plane separating the cells. The cells are assumed to be isolated except when a slug passes. Each individual slug and each individual cell is assumed to be completely mixed when considering species conservation. It is believed that this physical model more accurately describes the liquid-phase behavior and more accurately accounts for the various mechanisms that cause liquid-phase dispersion in churn-turbulent bubble columns. As was mentioned

earlier, the gas and liquid behaviors have been considered together in this physical model. In fact, a corresponding gas-phase backmixing model can be developed simply by considering the behavior of the gas dispersed in the cells and the communication between the gas in the cells and slugs.

Questions concerning the physical model that should be addressed during the research program include the following. Is all of the gas and liquid that is fed to the column transported by the slugs? Can the cells be assumed to communicate only as a slug passes? Should the cells be assumed to have a height equal to the column diameter or is some other scale more appropriate? As a slug passes from one cell to the next higher cell, can all of the downflowing liquid be assumed to be mixed into the first cell or does the liquid actually flow to a number of lower cells? Can the individual slugs and individual cells be assumed to be completely mixed on the time scale required for slug passage?

5.2.3 Mathematical Model

Now that a physical model of churn-turbulent bubble column operation has been developed, a mathematical model can be developed to describe bubble column behavior. Simple steady-state mass balances can be written around the entire column for both the gas and liquid assuming that there is no significant interphase mass transfer. If the phase densities are assumed constant, the mass balances can be written as volume balances.

The overall balance for the gas phase around the entire column can be written as follows.

$$\left(\begin{array}{l}\text{Volumetric Rate of Gas}\\ \text{Fed to Column}\end{array}\right) = \left(\begin{array}{l}\text{Volumetric Rate of Gas}\\ \text{Leaving Column}\end{array}\right) \quad (5.8)$$

$$\dot{Q}_{G,In} = \dot{Q}_{G,Out} \quad (5.9)$$

The volumetric rate of gas fed to the column can be expressed as the product of the superficial gas velocity and the column cross sectional area (assuming a cylindrical conduit of constant cross section).

$$\dot{Q}_{G,In} = V_G \cdot \frac{\pi D^2}{4} \quad (5.10)$$

Since all the gas has been assumed to be transported through the column by the slugs, the volumetric rate of gas leaving the column can be expressed as follows.

$$\dot{Q}_{G,out} = f_s \, (Vol)_s \, \varepsilon_s \quad (5.11)$$

where: f_s, frequency of slug passage

$(Vol)_s$, slug volume

ε_s, fractional gas holdup in slug (gas volume in slug/total slug volume)

Note that this assumes that as the slug leaves the column, none of the gas is recirculated and all of the gas in the slug leaves the system. These equations can be combined to yield the final form of the overall gas balance.

$$V_G \cdot \frac{\pi D^2}{4} = f_s \, (Vol)_s \, \varepsilon_s \tag{5.12}$$

The overall balance for the liquid phase around the entire column can be written in the same form as the overall gas balance.

$$\begin{pmatrix}\text{Volumetric Rate of Liquid} \\ \text{Fed to Column}\end{pmatrix} = \begin{pmatrix}\text{Volumetric Rate of Liquid} \\ \text{Leaving Column}\end{pmatrix} \tag{5.13}$$

$$\dot{Q}_{L,In} = \dot{Q}_{L,Out} \tag{5.14}$$

The volumetric rate of liquid fed to the column can be expressed as the product of the superficial liquid velocity and the column cross sectional area.

$$\dot{Q}_{L,In} = V_L \cdot \frac{\pi D^2}{4} = \dot{Q}_{L,Out} \tag{5.15}$$

Because the liquid in the column circulates with a much higher velocity than the superficial liquid velocity, it cannot be assumed that all of the liquid entrained in a slug leaves the column to complete the overall liquid balance. Rather, the behavior as a slug enters the top cell of the column must be considered. This is illustrated in Figure 5.3.

$$\begin{pmatrix}\text{Volumetric Rate of} \\ \text{Liquid Carried} \\ \text{into Cell by Slug}\end{pmatrix} = \begin{pmatrix}\text{Volumetric Rate} \\ \text{of Liquid} \\ \text{Downflow}\end{pmatrix} + \begin{pmatrix}\text{Volumetric Rate} \\ \text{of Liquid} \\ \text{Leaving Column}\end{pmatrix} \tag{5.16}$$

The volumetric rate of liquid carried into the cell can be expressed in the following form.

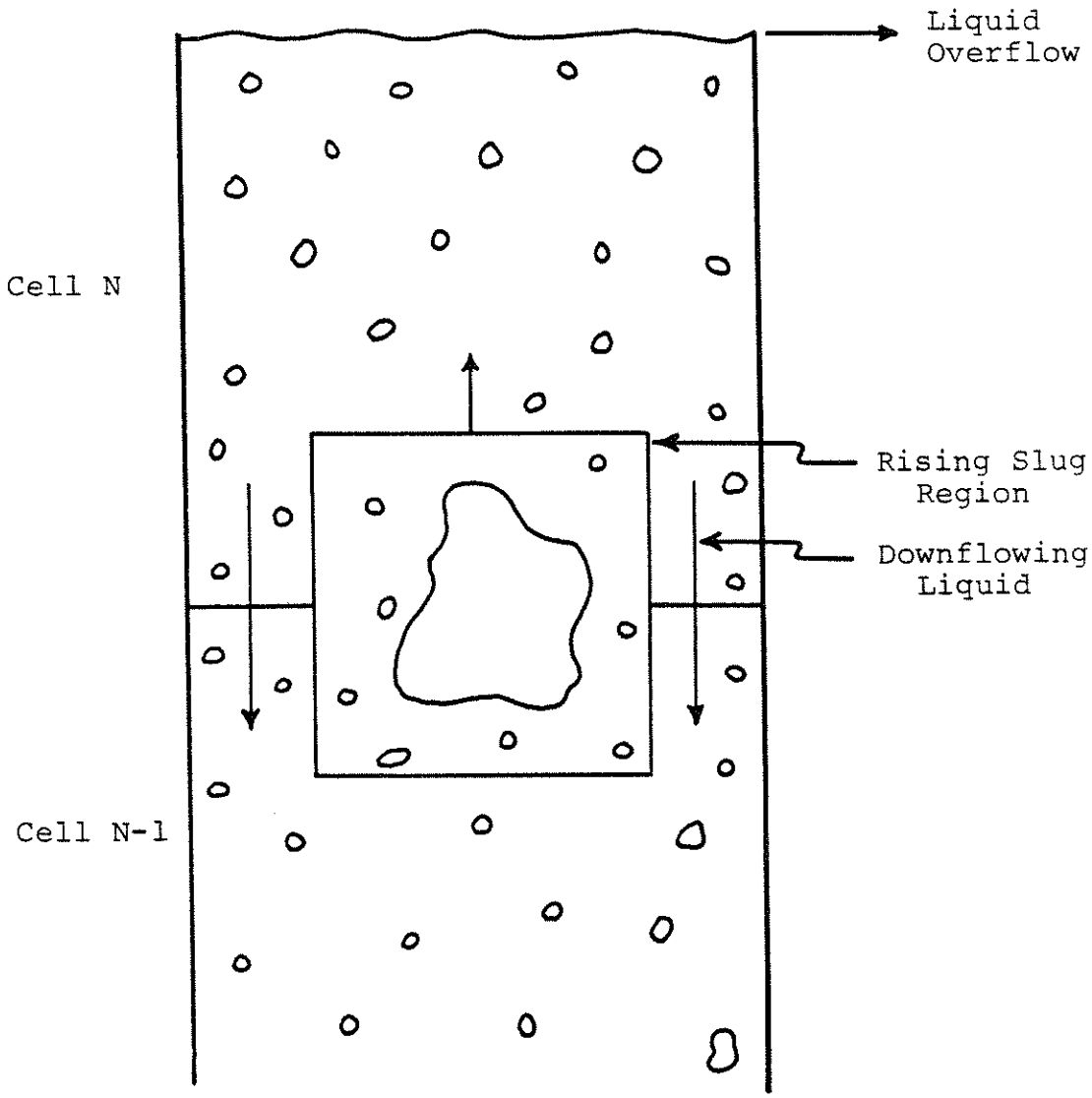

Figure 5.3 Slug Entering Cell N

$$\begin{pmatrix}\text{Volumetric Rate of Liquid} \\ \text{Carried into Cell by Slug}\end{pmatrix} = f_s\,(\text{Vol})_s\,(1 - \varepsilon_s) \tag{5.17}$$

The volumetric rate of liquid leaving the column can be taken from Equation 5.15 and the liquid balance around the top cell of the column may be written as follows.

$$f_s\,(\text{Vol})_s\,(1 - \varepsilon_s) = f_s\,Q_{L,DF} + V_L \cdot \frac{\pi D^2}{4} \tag{5.18}$$

$Q_{L,DF}$ represents the quantity of liquid that flows downward as a slug enters the cell. The product $f_s\,(\text{Vol})_s$ can be obtained from the overall gas balance of Equation 5.12 and Equation 5.18 can be arranged into the following form.

$$\frac{1 - \varepsilon_s}{\varepsilon_s} = \frac{V_L}{V_G} + \frac{4}{\pi D^2} \cdot \frac{f_s\,Q_{L,DF}}{V_G} \tag{5.19}$$

To complete the mathematical model of liquid-phase backmixing in churn-turbulent bubble columns, species conservation equations for a nonreactive system must be derived for the liquid phase. This can be accomplished by numbering the cells from 1 to N beginning at the bottom of the column. The processes that occur as a slug rises through a cell are demonstrated by the sketches in Figure 5.4. As a slug enters a cell, liquid flows down into the next lower cell. As a slug passes through a cell, liquid can be exchanged at a volumetric rate that can be described by a volumetric exchange coefficient, k_E. As a slug leaves a cell, liquid flows down into the cell from the next higher cell.

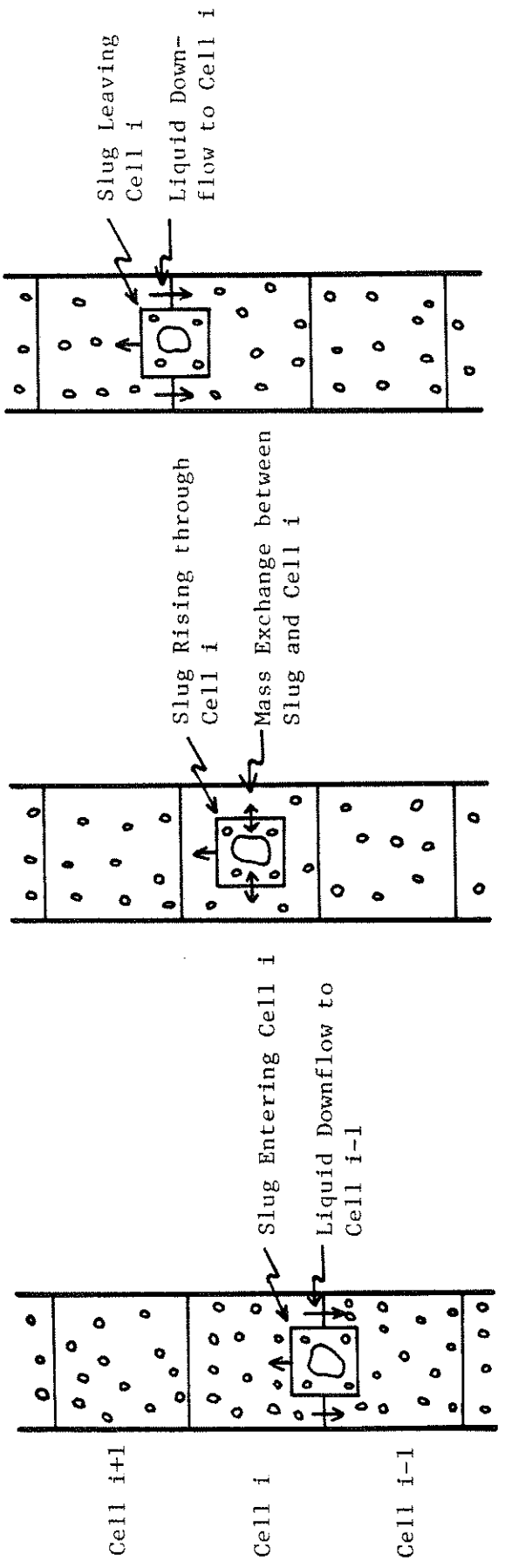

Figure 5.4 Slug Passage through a Cell

Now consider a liquid species balance for a slug as it passes through an arbitrary cell designated as cell i ($i \neq 1$). Denote the concentration of some liquid species in the slug liquid as it enters cell i as $C_{s(i-1)}$ (the concentration in the slug as it leaves cell i-1) and the concentration in the slug liquid as it leaves cell i as C_{si}. As the slug passes through cell i, it exchanges a volume of liquid that is equal to the product of a volumetric exchange coefficient, k_E, and the contact time between the slug and the cell, t_c. Since the slug and cell are assumed to be completely mixed, the concentration of the slug liquid as it leaves cell i, C_{si}, can be expressed as an average (volumetric) of the concentration of the unexchanged volume (the liquid carried out of cell i-1) and the concentration of the exchanged volume from cell i (with a concentration of C_{ci}).

$$C_{si} = \frac{C_{s(i-1)} \left[(1-\varepsilon_s)\ (Vol)_s - k_E t_c\right] + C_{ci}\ (k_E t_c)}{(1-\varepsilon_s)\ (Vol)_s} \tag{5.20}$$

If the following substitution is made,

$$X = \frac{k_E t_c}{(1-\varepsilon_s)\ (Vol)_s} \tag{5.21}$$

Equation 5.20 can be written in the following succint form.

$$C_{si} = C_{s(i-1)}\ (1-X) + C_{ci} \cdot X \tag{5.22}$$

Since the slugs are formed near the gas distributor (which corresponds to cell 1), it can be assumed that the initial concentration of the slug liquid is equal to the concentration of the liquid in cell 1.

$$C_{s1} = C_{c1} \tag{5.23}$$

Combining Equations 5.22 and 5.23, species conservation balances can be written from cell 1 where the slug is formed through cell N where the slug exits the column.

$$C_{sN} = C_{c1}\,(1-X)^{N-1} + C_{c2}\,(1-X)^{N-2}\cdot X + \ldots$$

$$+ C_{c(N-1)}\,(1-X)\cdot X + C_{cN}\cdot X \tag{5.24}$$

The expression for the concentration of a species in a slug as it leaves the column is of a simple form and has been expressed completely in terms of the cell concentrations. Since all of the liquid fed to the column is assumed to be transported in the slugs, the concentration given by Equation 5.24 is the concentration of a species in the liquid overflow of the column. Note that the cell concentrations employed in Equation 5.24 must be the cell concentrations that exist just prior to the slug entering the cell. Since the cells are assumed not to communicate except when a slug passes, the concentrations in the cells that are encountered by a slug were established when the previous slug passed through the column.

Referring to Figure 5.4 it can be seen that a cell gains liquid from the next higher cell, loses liquid to the next lower cell, and exchanges liquid with the slug as it passes. The concentration in a cell after the slug passage, C'_{ci}, can be obtained as an average (volumetric) of the concentration in the cell before the slug passed, C_{ci}, and the concentrations of the liquid flowing into the cell as the slug passes.

$$C'_{ci} = \frac{C_{ci}[(1-\varepsilon_c)(Vol)_c-(k_E t_c)-Q_{L,DF}] + C_{s(i-1)}(k_E t_c) + C_{c(i+1)}(Q_{L,DF})}{(1-\varepsilon_c)\ (Vol)_c} \tag{5.25}$$

If the following substitutions are made,

$$Y = \frac{k_E t_c}{(1 - \varepsilon_c)\ (Vol)_c} \tag{5.26}$$

$$Z = \frac{Q_{L,DF}}{(1 - \varepsilon_c)\ (Vol)_c} \tag{5.27}$$

Equation 5.25 can be written in the following manner.

$$C'_{ci} = C_{ci}\ (1-Y-Z) + C_{s(i-1)} \cdot Y + C_{c(i+1)} \cdot Z \tag{5.28}$$

The cells at the top and bottom of the column must be treated somewhat differently since they have only one adjacent cell apiece. The situation for these cells is illustrated in Figure 5.5. First, consider cell N. As a slug enters cell N, liquid flows down to cell N-1 and, as the slug passes through cell N, mass is exchanged between the slug and cell. Both of these processes are identical to what occurs in other cells; however, as the slug leaves cell N, only a fraction of the slug liquid overflows and the remainder recirculates into cell N. The quantity of liquid that overflows is equal to the volumetric liquid flowrate fed to the column divided by the slug frequency.

$$Q_{L,Out} = \frac{V_L \cdot \frac{\pi D^2}{4}}{f_s} \tag{5.29}$$

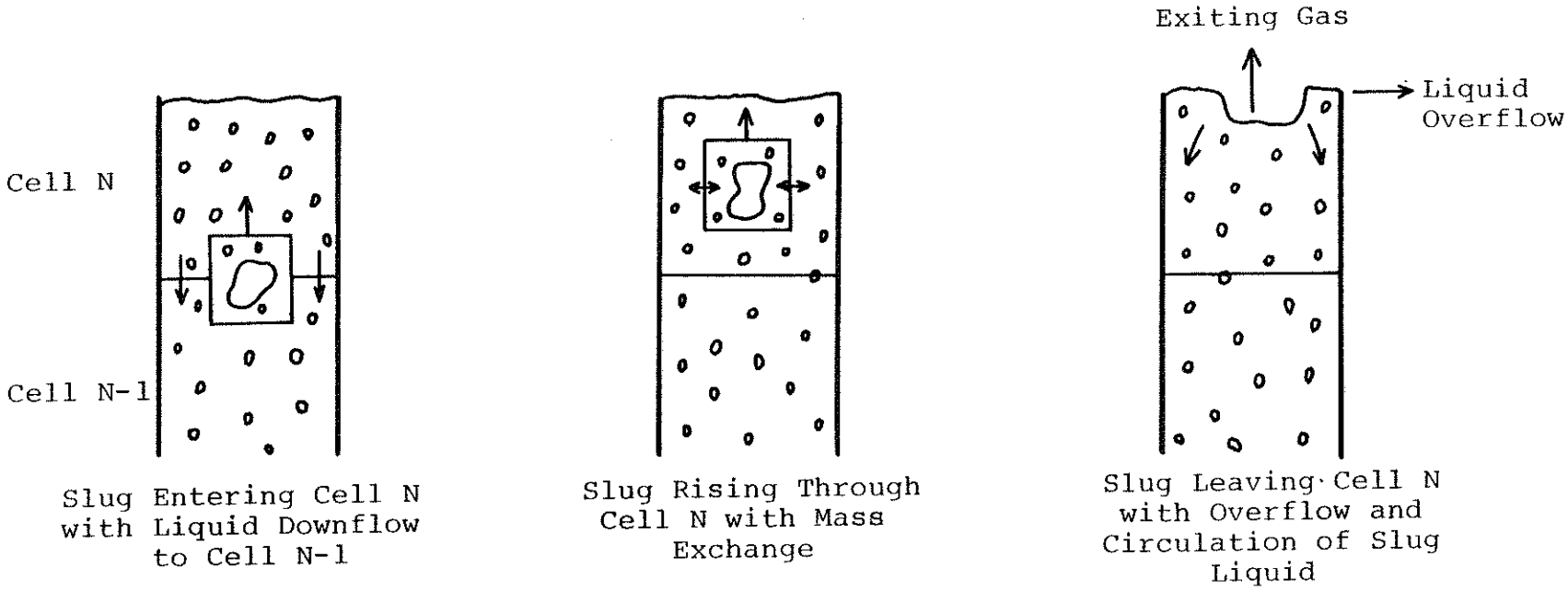

Figure 5.5 Slug Formation and Exit from Column

a. Slug Exit from Cell N

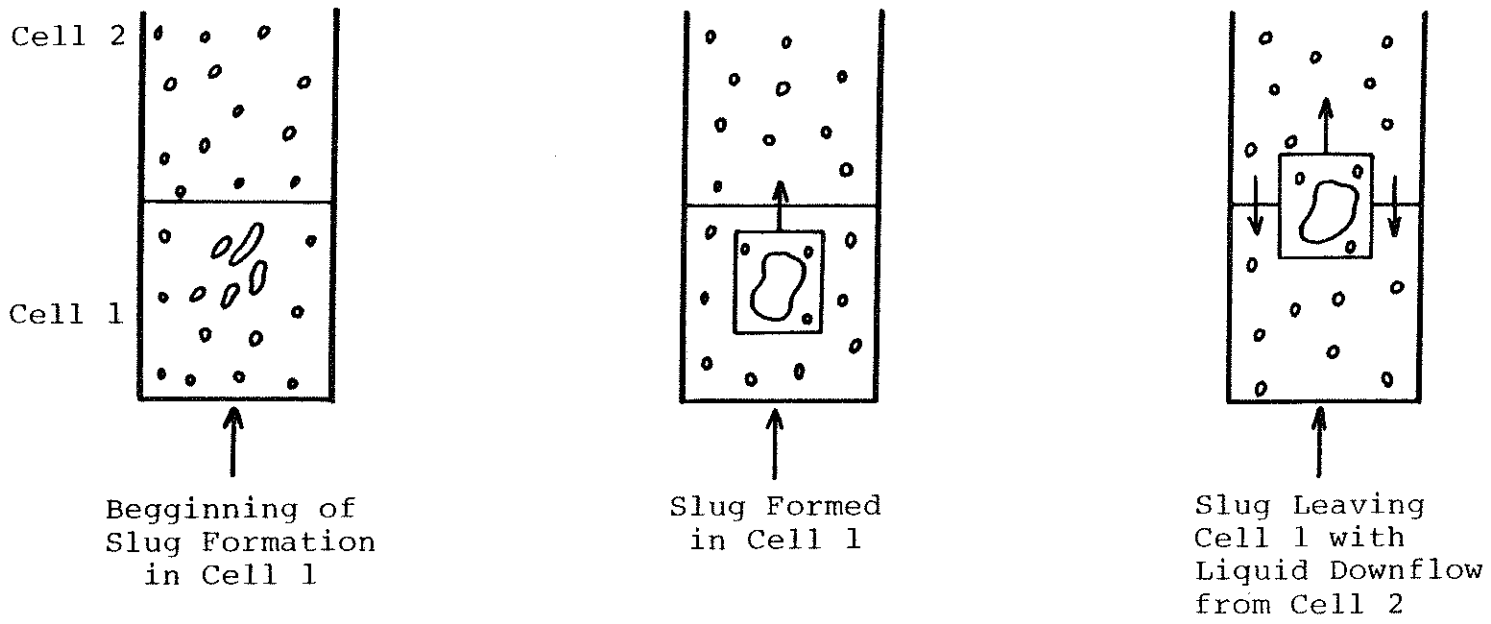

Figure 5.5 Slug Formation and Exit from Column

b. Slug Formation in Cell 1

The concentration in cell N after slug passage can be found from an average (volumetric) of the concentration before the slug passed and the concentration of the liquid flowing into cell N.

$$C'_{cN} = \frac{C_{cN}[(1-\varepsilon_c)(Vol)_c-(k_E t_c)-Q_{L,DF}]+C_{s(N-1)}(k_E t_c)+C_{sN}[(1-\varepsilon_s)(Vol)_s-\frac{V_L \frac{\pi D^2}{4}}{f_s}]}{(1-\varepsilon_c)\ (Vol)_c} \tag{5.30}$$

The volume of liquid recirculated from the slug as it leaves cell N can be obtained from Equation 5.18 and can be substituted into Equation 5.30.

$$C'_{cN} = \frac{C_{cN}\ [(1-\varepsilon_c)(Vol)_c-(k_E t_c)-Q_{L,DF}] + C_{s(N-1)}(k_E t_c)+C_{sN}(Q_{L,DF})}{(1-\varepsilon_c)\ (Vol)_c} \tag{5.31}$$

If the definitions of Equations 5.26 and 5.27 are recalled, Equation 5.31 can be written in the following form.

$$C'_{cN} = C_{cN}\ (1 - Y - Z) + C_{s(N-1)} \cdot Y + C_{sN} \cdot Z \tag{5.32}$$

Again referring to Figure 5.5, a liquid species conservation equation for cell 1 as a slug passes can be developed. When the slug leaves cell 1, it carries out liquid and liquid from cell 2 flows down into cell 1. Also during this time, liquid is fed into the column at a rate of $V_L \cdot \frac{\pi D^2}{4}$. The concentration in cell 1 after a slug passes can be obtained as an average (volumetric) of the cell concentration before slug passage and the concentrations of the liquid entering the cell.

$$C'_{c1} = \frac{C_{c1}[(1-\varepsilon_c)(Vol)_c-(1-\varepsilon_s)(Vol)_s] + C_{c2}(Q_{L,DF}) + C_o\left(\frac{V_L \cdot \frac{\pi D^2}{4}}{f_s}\right)}{(1-\varepsilon_c)\ (Vol)_c} \quad (5.33)$$

C_o represents the concentration in the liquid fed to the column. If the definitions of Equations 5.21, 5.26, and 5.27 and the balance of Equation 5.18 are recalled, Equation 5.33 can be written in the following manner.

$$C'_{c1} = C_{c1}\left(1 - \frac{Y}{X}\right) + C_{c2} \cdot Z + C_o\left(\frac{Y}{X} - Z\right) \quad (5.34)$$

When the conservation equation is written in this last form, it can easily be seen that the volume of liquid leaving cell 1 as the slug passes is equal to the volume of liquid entering cell 1 as the slug passes as required by continuity. Note that this is true of all of the equations developed here.

This completes the development of the mathematical model which has been summarized in Table 5.1. A comparmental model of the back-mixing model is illustrated in Figure 5.6. This illustrates the upward plug flow motion of the liquid in the slugs, the downward motion of the liquid through the series of well-mixed cells, and the communication between the slug and cell regions.

5.2.4 Model Parameters

A number of parameters were introduced in the development of the mathematical model for liquid-phase backmixing in churn-turbulent bubble columns (note that all of the model parameters can be reduced to the three dimensionless parameters X, Y, and Z). These parameters can be classified as system parameters, operating parameters, and model

Table 5.1 Summary of Model Equations

Number	Source	Equation
5.12	Overall Gas Balance	$V_G \cdot \frac{\pi D^2}{4} = f_s (Vol)_s \varepsilon_s$
5.18	Overall Liquid Balance around Top Cell	$f_s (Vol)_s (1-\varepsilon_s) = f_s Q_{L,DF} + V_L \cdot \frac{\pi D^2}{4}$
5.19	Combination of Equations 5.12 and 5.18	$\frac{1-\varepsilon_s}{\varepsilon_s} = \frac{V_L}{V_G} + \frac{4}{\pi D^2} \cdot \frac{f_s Q_{L,DF}}{V_G}$
5.22	Species Conservation in Slugs	$C_{si} = C_{s(i-1)} (1-X) + C_{ci} \cdot X$
5.24	Concentration in Exiting Slug	$C_{sN} = C_{c1}(1-X)^{N-1} + C_{c2}(1-X)^{N-2} \cdot X + \cdots + C_{c(N-1)}(1-X) \cdot X + C_{cN} \cdot X$
5.28	Species Conservation in Cells	$C'_{ci} = C_{ci}(1-Y-Z) + C_{s(i-1)} \cdot Y + C_{c(i+1)} \cdot Z$
5.32	Species Conservation in Top Cell	$C'_{cN} = C_{cN}(1-Y-Z) + C_{s(N-1)} \cdot Y + C_{sN} \cdot Z$
5.34	Species Conservation in Bottom Cell	$C'_{c1} = C_{c1}(1-\frac{Y}{X}) + C_{c2} \cdot Z + C_o(\frac{Y}{X} - Z)$

$$X = \frac{k_E t_c}{(1-\varepsilon_s)(Vol)_s} \qquad Y = \frac{k_E t_c}{(1-\varepsilon_c)(Vol)_c} \qquad Z = \frac{Q_{L,DF}}{(1-\varepsilon_c)(Vol)_c}$$

Note - Only two equations of Equations 5.12, 5.18, and 5.19 are independent.

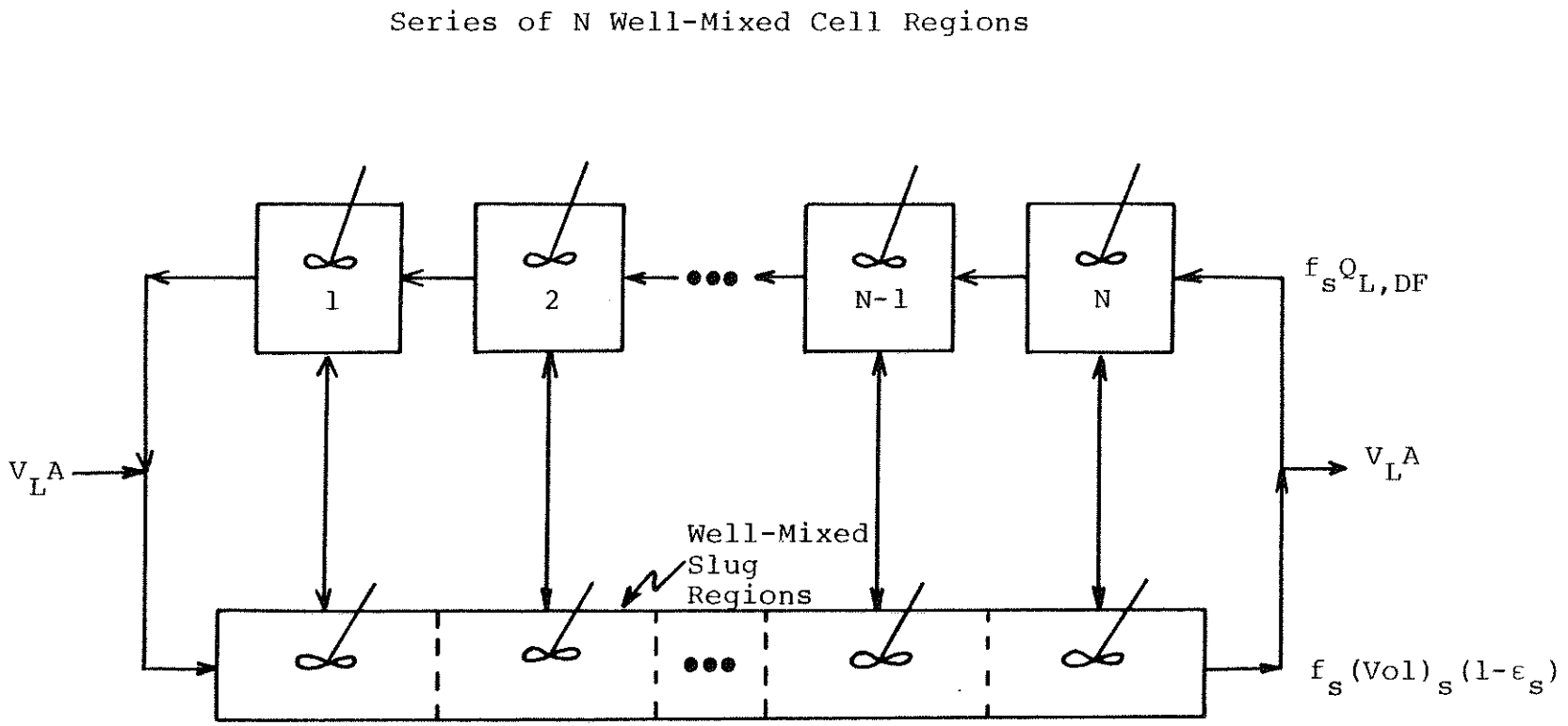

Figure 5.6 Compartmental Equivalent of Proposed Model

parameters and they are listed in Table 5.2. The system parameters are related to the geometry of the system and only the column diameter, D, was introduced in the development of the mathematical model (the column length or height, L, will be introduced in the following discussion). The operating parameters may include the gas and liquid physical properties and the phase flowrates and only the superficial gas and liquid velocities, V_G and V_L, were introduced in the development of the mathematical model. Both the system and operating parameters are known parameters. The model parameters, on the other hand, are not known parameters and must be evaluated from theory, physical reasoning, or experiment. The following discussion is aimed at expressing the model parameters in terms of system or operating parameters or other terms that can be determined experimentally.

The contact time between a slug and a cell, t_c, is equal to the height of the cell divided by the rise velocity of the slugs, V_s. Barkelew (60), among others, has noted that the length of one cell region is approximately equal to the column diameter based upon the visual appearance of the vortices that occur in churn-turbulent bubble columns. Also, Joshi and Sharma (82) found that the height of a circulation cell in a bubble column is equal to the column diameter based upon the criterion of minimizing the circulation strength. In the development of the physical model, it was assumed that all of the gas fed to the column is transported as slugs. Previously, the dynamic gas disengagement technique of Vermeer and Krishna (32) was discussed as a method of determining the transport and entrained gas holdups, ε_T and ε_E, respectively. The slug velocity is then equal to the superficial

Table 5.2 - Classification of Parameters

Parameter Type	Parameter
System	D, L
Operating	V_G, V_L
Model	f_s, $(Vol)_s$, ε_s, $(Vol)_c$, ε_c, k_E, t_c, $Q_{L,DF}$

gas velocity divided by the transport holdup. If the transport holdup can be determined from dynamic gas disengagement experiments and the length of the cells is set equal to the column diameter, the contact time between a slug and cell may be expressed as follows.

$$t_c = \frac{D\varepsilon_T}{V_G} \tag{5.35}$$

Some results concerning the transport and entrained gas holdup and the slug velocity will be presented in a later discussion.

The volume of a cell, $(Vol)_c$, can be determined simply from geometric considerations if the length of a cell is considered to be equal to the column diameter as was discussed in the preceding paragraph.

$$(Vol)_c = \frac{\pi D^3}{4} \tag{5.36}$$

The entrained gas holdup, ε_E, determined from dynamic gas disengagement experiments, is the difference between the total gas holdup, ε, and the transport holdup, ε_T. The entrained gas holdup corresponds to the cell holdup, ε_c, in the proposed model; however, the entrained holdup is based upon the entire column volume while the cell holdup is based upon only the cell volume (the total column volume minus the slug volume). The slug volume in the column is equal to the volume of one slug, $(Vol)_s$, multiplied by the (time-averaged) number of slugs in the column, $(Num)_s$. The number of slugs in the column is equal to the product of the residence time of the slugs in the system, L/V_s, and the slug frequency, f_s.

$$(\text{Num})_s = \frac{L}{V_s} \cdot f_s = \frac{L f_s \varepsilon_T}{V_G} \tag{5.37}$$

This last form of Equation 5.37 makes use of the relation between the slug velocity, V_s, the superficial gas velocity, V_G, and the transport holdup. The relation between the entrained gas holdup and the cell gas holdup is as follows.

$$\varepsilon_E \left(\frac{\pi D^2 L}{4}\right) = \varepsilon_c \left[\frac{\pi D^2 L}{4} - (\text{Vol})_s (\text{Num})_s\right] \tag{5.38}$$

Using the information of Equation 5.37, this relation may be arranged to give the cell holdup as a function of the entrained holdup and the model parameters $(\text{Vol})_s$ and f_s.

$$\varepsilon_c = \frac{\varepsilon_E}{1 - (\text{Vol})_s \left(\frac{f_s \varepsilon_T}{V_G}\right) \left(\frac{4}{\pi D^2}\right)} \tag{5.39}$$

The frequency of slug appearance, f_s, was found to be in the range of one to two per second by Ohki and Inoue (29). This appears to agree well with the slow motion photographs of a churn-turbulent bubble column taken by Kirkpatrick (18). This value can be used as an approximation or a better value can be obtained by visual observation of an operating bubble column or from some suitable probe that can detect slug passage. The quantity of liquid that flows downward as a slug moves into a cell can most easily be approximated by integrating empirical velocity profiles such as those of Hills (30) or theoretical

(with an empirical parameter) velocity profiles such as those of Miyauchi and coworkers (78,79) over the region of downflow.

Out of the original eight model parameters listed in Table 5.2, five have been discussed and only three remain to be treated. The three model parameters remaining are the gas holdup in the slugs, ε_s, the slug volume, $(Vol)_s$, and the exchange coefficient, k_E. If the first five model parameters discussed previously can be approximated or determined experimentally, the gas holdup in the slug and the slug volume can be determined by solving any two of Equations 5.12, 5.18, and 5.19. The only remaining model parameter to be evaluated is the exchange coefficient, k_E. The exchange coefficient should be a function of the turbulence level in the column and, as such, should be a function of the superficial gas velocity, the column diameter and, to a lesser extent, the liquid physical properties and the superficial liquid velocity. The exchange coefficient enters into the proposed model only when liquid species conservation is considered so that the exchange coefficient can be determined from residence time distribution (RTD) studies (recalling the caveat discussed earlier that parameters determined in nonreactive systems may not apply to reactive systems, particularly for the axial dispersion model). Equations 5.24, 5.28, 5.32, and 5.34 listed in Table 5.1 describe the conservation of a nonvolatile tracer species injected into the liquid-phase of a churn-turbulent bubble column. The value of the exchange coefficient can be determined by matching experimentally determined RTD data with model predictions according to some error minimization criterion such as the least squares error criterion. The previous discussion indicates the approximate nature of the proposed model. However, the model is more

physically realistic than the axial dispersion model. This model should be capable of describing the behavior that the axial dispersion model describes plus this model is capable of describing liquid bypassing which has been noted by Kirkpatrick (18). The experimental program presented here should be capable of discerning the usefulness of the proposed model. If the model appears promising, further research concerning this model can be pursued. This further research could reduce the empirical nature of the model. If the model does not appear promising, modeling efforts in other directions should then be pursued.

5.2.5 Experimental Program

As was noted in the preceding discussion, characterization of the proposed liquid mixing model rests upon correlating the exchange coefficient between the slug and cell regions, k_E. The exchange coefficient enters into the proposed model only when considering species conservation and can most easily be determined by nonreactive tracer studies. Levenspiel (44,45) has discussed the use of tracers for determining both the exit age density function, E(t), by employing a (near) perfect pulse input of tracer and the exit age distribution function, F(t), by employing a step change input of tracer. Shah et al. (39) have discussed the use of tracer studies in gas-liquid (- solid) systems.

The ideal tracer would be nonvolatile, nonreactive, and would imitate the behavior of the liquid as closely as possible without modifying the behavior of the system. A wide variety of liquid-phase tracers have been employed in gas-liquid systems. These tracers include heat which can be detected by thermocouples, ionic species that can be detected by conductivity meters, dyes that can be detected

by spectrophotometers, and flourescent dyes that can be detected by flourimeters.

Electrical conductivity has been chosen for the proposed experiments for a number of reasons. The primary reason is the ease with which ionic species can be prepared, handled, and detected. Numerous inorganic salts have been used for electrical conductivity studies with potassium chloride being the accepted standard for which accurately determined values of the electrical conductivity at different concentrations and temperatures in aqueous solution are available. Typically, electrical conductivity is employed with very dilute solutions of tracer for greatest sensitivity. This is an advantage in that ionic species have been observed to affect the behavior of bubble columns by producing a finer dispersion of small gas bubbles than that observed in pure liquids. Low tracer concentrations should limit this effect. Before proceeding with the proposed tracer studies, a series of studies to determine the gas holdup structure in dilute solutions of tracer should be performed and compared to the results obtained for pure water (see Section 5.4). One possible disadvantage of employing dilute tracer solutions is the problem of obtaining a steady baseline determined by the conductivity of the water used in the experiments. This will be particularly critical in determining the 'tail' portion of a pulse response where the final portions of tracer are being washed from the column.

The electrical conductivity of an aqueous solution is typically determined by measuring the resistance presented by a portion of the solution contained between electrodes of fixed separation and area (a fixed 'cell constant'). For the purpose of the present study it is

believed that two large electrodes or a combination of a number of smaller electrodes can be used to directly determine the cross-sectional average tracer concentration. This concentration is equivalent to the cell concentration in the proposed mixing model and also to the concentration specified by the axial dispersion model (recall that the axial dispersion model assumes complete radial mixing). Probes determining the area-averaged concentration are superior to point probes that are more susceptible to erratic responses caused by the random oscillations that occur in bubble columns. It will probably be necessary to calibrate the probes with solutions of known tracer concentration both for accuracy and to determine the range of tracer concentration where the probes exhibit the greatest sensitivity. Ideally, the studies should be performed in a region where the probe response is linear with respect to tracer concentration so that the raw data can be used directly for data analysis.

Electrical conductivity measurements offer the advantage of being well suited for automated data acquisition. If the resistance of the solution is measured with a Wheatstone bridge arrangement, the voltage output can be converted to a digital signal and logged on a computer. The digital record of tracer concentration is then amenable to numerical manipulation. Use of an automated data acquisition system allows exploitation of the analog to digital converter and Apple II plus computer currently available in the Chemical Reaction Engineering Laboratory. This system is capable of gathering data at each probe at a rate that allows a close monitoring of the tracer movement without generating an overabundance of data (approximately one reading every second at each

probe should be an adequate sampling rate). The raw data can then be transferred to a mainframe computer for data treatment. The combined response time of the measuring system will be sufficiently short (on the order of microseconds) when compared to the liquid mean residence time (on the order of minutes) so as to introduce no appreciable time lag.

The initial tracer tests will rely on pulse injections because of the simplicity and rapidity of these tests. It has been reported (18) that the repeatability of these tests is not good so it may be necessary to consider alternate tracer methods. Standard tracer tests generally involve the determination of a steady-state tracer concentration profile throughout the column (such as the tests of Argo and Cova (43) discussed in Section 5.5) or the determination of the time record of the tracer concentration at a specific point within the system (usually the mixing cup concentration in the column overflow is monitored). Steady-state tracer methods will not be employed in this study because they actually only measure the magnitude of the mixing within the column and give no indication as to the mechanism of mixing. Rather than employ a single-point unsteady tracer test, it is proposed that a series (probably three) probes be placed at different axial locations in the column. This not only facilitates a more stringent test of the proposed mixing model, but also provides a test of the applicability of the axial dispersion model. The axial dispersion model predicts that the spread of tracer as it passes through the system (measured as the variance of the pulse response) is proportional to the distance from the point of injection (64). It is believed that no previous tests have employed the method of multiple probes as proposed here.

The mathematical model presented earlier is in a form suitable for pulse tracer studies. If a pulse of tracer is injected into the region directly above the gas distributor (cell 1), the concentration of tracer in the liquid overflow as a function of time can be normalized to yield the exit age density function. The tracer injected into cell 1 can be assumed to be well mixed throughout that cell, giving the initial condition necessary to solve the model equations. The concentration of the slug liquid leaving the column corresponds to the liquid overflow and the model predictions should be compared to experimental results to obtain values of the exchange coefficient.

Note the simple manner in which the species conservation equations can be solved numerically. For the case of a pulse tracer study, the initial concentration throughout the column is zero except in cell 1 where the tracer has been input. The first slug can be assumed to form at time zero and it will exit the system at a time of L/V_s where L is the column length and V_s is the slug rise velocity (discussed earlier). This first slug can be followed up the column and the cell concentration can be determined as the slug passes through each cell and exchanges mass with it. Since the cells are assumed to be noncommunicating except as a slug passes, these new cell concentrations are those encountered by the second slug that enters the column at a time of $1/f_s$ (f_s, slug frequency) and exits the column at a time of $L/V_s + 1/f_s$. This second slug sets up the cell concentrations encountered by the third slug, etc., and this solution method can be continued to determine the exit age density function which is the normalized time record of the liquid overflow (slug liquid leaving the column) tracer concentration.

The bubble column system to be employed in this study is described in Section 5.3. A few modifications must be made to conduct the proposed tracer studies. The first modification is the addition of a system for injecting a pulse of tracer into the liquid. The tracer should be introduced at a point very close to the column and in a manner so that it is well mixed with the inlet stream as it enters the column. The tracer injection should be as close as possible to an ideal pulse. However, since the liquid mean residence time is of the order of minutes, an injection time of about one second should be sufficiently short. Injection by a syringe through a septum in the liquid inlet line at the base of the column should meet the above specifications. If a step change tracer input is needed, a syringe pump can be used to accurately meter a steady flow of tracer solution to the column. The bubble column system will have to be modified so that the electrical conductivity probes can be mounted flush to the column walls so as not to modify the flow in the system. From a consideration of the means of injecting and detecting the tracer, it can be seen that the mixing characteristic of only the column is being measured. No corrections will have to be made for sample collection or other mixing effects that must be accounted for with some systems.

The proposed research program has been outlined in Figure 5.7. The first attempt at modeling the liquid-phase backmixing in churn-turbulent bubble columns was outlined previously and the model equations were summarized in Table 5.1. The preceding discussion was aimed at the approximation of a number of the model parameters. Some simple experiments that can add insights to the modeling process and can help characterize the model parameters have already been performed for an air-water system

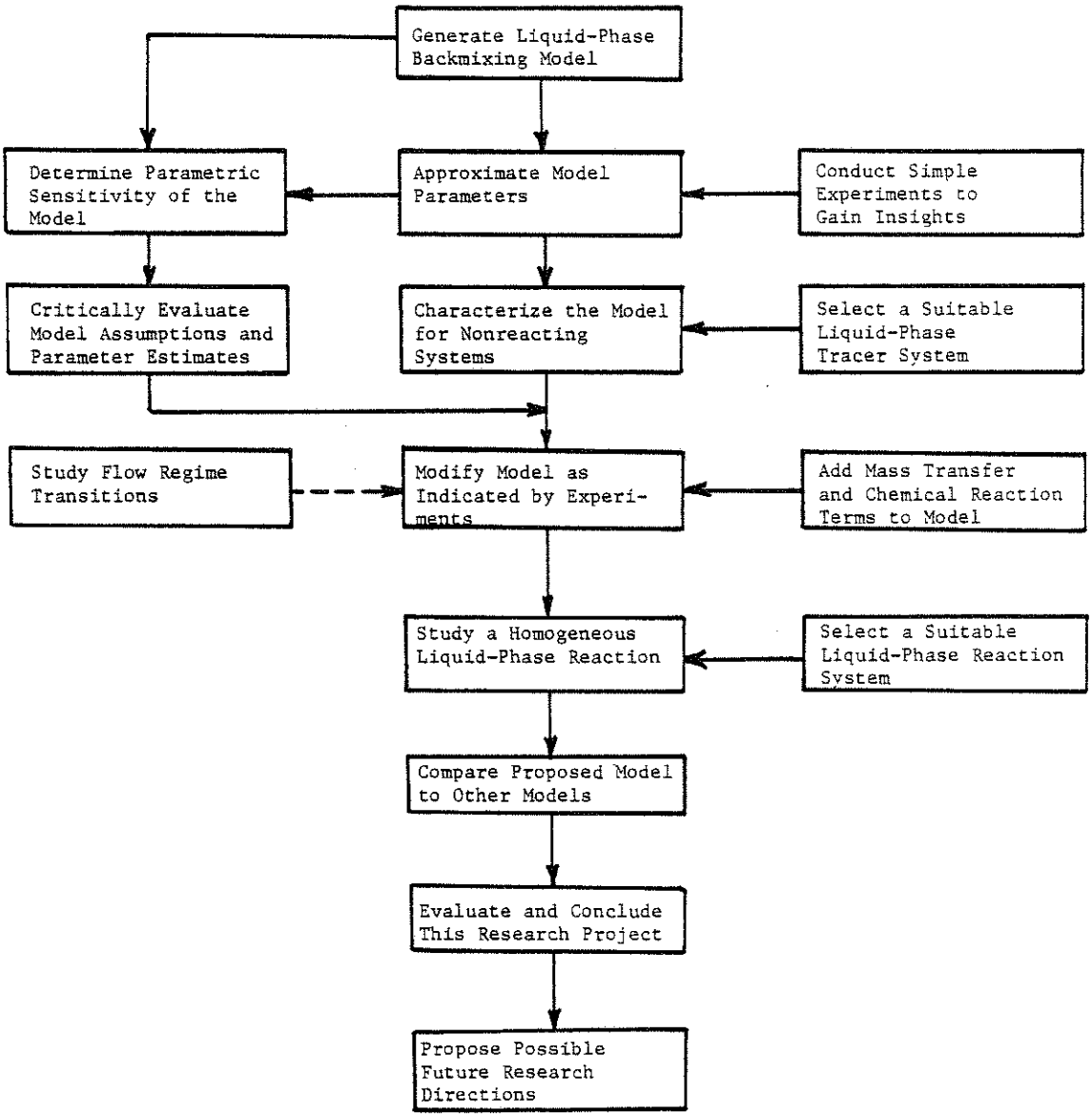

Figure 5.7 Flowsheet of the Proposed Research

(the experimental apparatus and preliminary results will be discussed later). The next step of the research program involves the characterization of the model for a nonreacting system. As was discussed, this is typically accomplished with tracer studies and matching the experimental system response with the response predicted by the model. At the same time that the tracer studies are being performed, the model assumptions and parameter estimations should be critically evaluated including the parametric sensitivity of the model. At this point in the research the model should be modified as indicated by the results of all the preceding studies. These modifications should include the addition of mass transfer and reaction terms so that the model can be applied to reacting systems. Any modifications as indicated by the ongoing consideration of flow regime transitions should also be included in the model analysis.

If the model can be successfully characterized for nonreacting systems and it appears promising, the model should be compared either experimentally or numerically with other models on a reacting system. As has been discussed, bubble columns are gas-liquid reactors and, in a typical system, the gas-phase reactant dissolves and diffuses into the liquid phase where it reacts with the liquid reactant. To model this behavior, the gas-phase RTD and interphase mass transfer must be considered. The main focus here is liquid-phase mixing which can be isolated by considering a homogeneous liquid-phase reaction. The effects of the gas phase would then be limited to agitation of the liquid phase. The proposed model can be modified for a reactive system by simply adding reaction terms for the cell and slug regions in the species conservation equations. A suitable liquid-phase reaction for

experimental study must undergo a conversion of about 25% to 75% at the concentrations and liquid mean residence time characteristic of the bubble column system. The reaction kinetics must also be well understood so that a new complicating factor is not introduced into the problem. A variety of models including plug flow, completely mixed, axial dispersion, tanks in series, and the proposed model can be compared on the basis of predicting the liquid-phase conversion when only the effects of liquid mixing and kinetics must be considered. No critical study of this nature has previously been reported in the literature.

5.3 EXPERIMENTAL APPRATUS

A lab-scale bubble column has been constructed and is illustrated in Figure 5.8. The material of construction is clear cast acrylic (plexiglass) which allows visual observation of the column contents. The column has an internal diameter of 19 cm (7.5 in) with a wall thickness of 0.64 cm (0.25 in). The total length (height) of the column is 244 cm (96 in) from the gas distributor to the liquid overflow. The column is composed of two sections of equal length that are joined by a flanged connection. A gasket is placed between the sections to prevent leaks. The liquid overflows into a 29.2 cm (11.5 in) inner diameter cylinder that is 33 cm (13 in) tall. The base of the overflow section is set below the top of the column so that overflowing liquid will not reenter the column. The base of the overflow section is also sloped to force the liquid to the liquid return line. The overflow cylinder was made rather tall to prevent liquid from splashing out of the system. The column is connected to support rods that extend from the floor to the ceiling to prevent vibrations that could crack the cast acrylic.

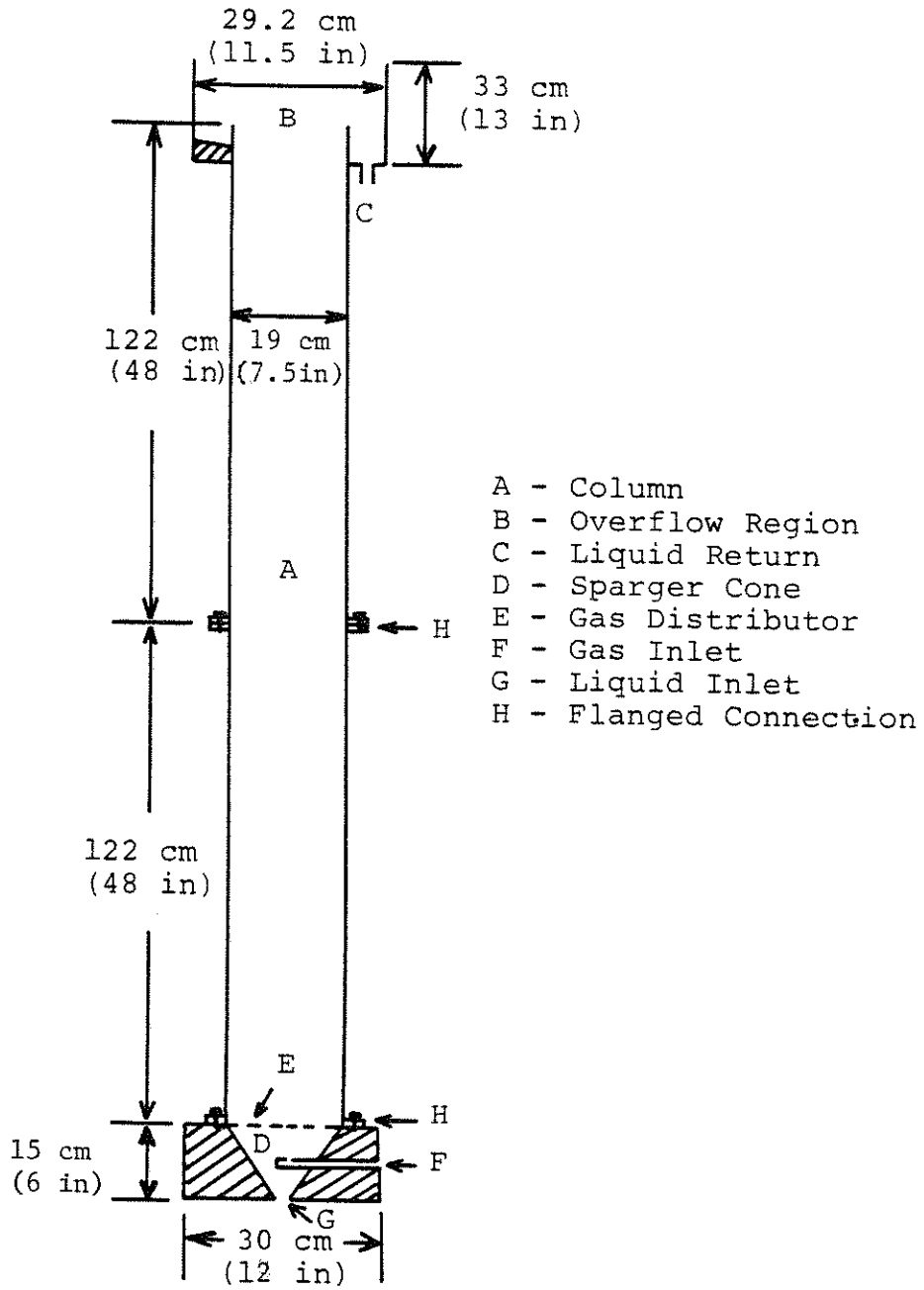

Figure 5.8 Lab-Scale Bubble Column

The support connections are made at the flange connection between the two sections of the column and just below the liquid overflow.

The gas and liquid are both introduced through 1/2 in nominal (Schedule 40) conduits into a conical sparger region that is placed at the base of the column. The conical sparger region was machined out of a 30 cm x 30 cm x 15 cm (12 in x 12 in x 6 in) block of cast acrylic which is placed on a small support stand. The liquid inlet is at the vertex (point) of the conical sparger region which lies on the axis of the column. The sparger region expands from the liquid inlet until it is 19 cm (7.5 in) in diameter at the point where it joins with the column which is of the same diameter. The gas inlet is through the side of the block of cast acrylic at a point between the liquid inlet and the column. A 1/2 in tube carries the gas to the center of the sparger cone where the gas is sparged through a 1/2 in hole that directs the gas upward along the column axis. The column is joined to the sparger region by a flanged connection which contains a gasket to prevent leaks. A stainless steel wire screen is placed across the column cross section at the top of the sparger region to disperse the gas. This gas distributor (the wire screen) is flexible and can fluctuate as the gas is sparged into the system.

A schematic of the entire apparatus is shown in Figure 5.9. The liquid can be stored in a 250 gal polypropylene tank. Connections to fill the tank with water from the building supply are available. This water is filtered through a 5 micron filter before it flows into the storage tank. The storage tank is placed upon a movable cart that is placed over a drainage trench into which the storage tank contents can be drained. The liquid is pumped through the system by a centrifugal

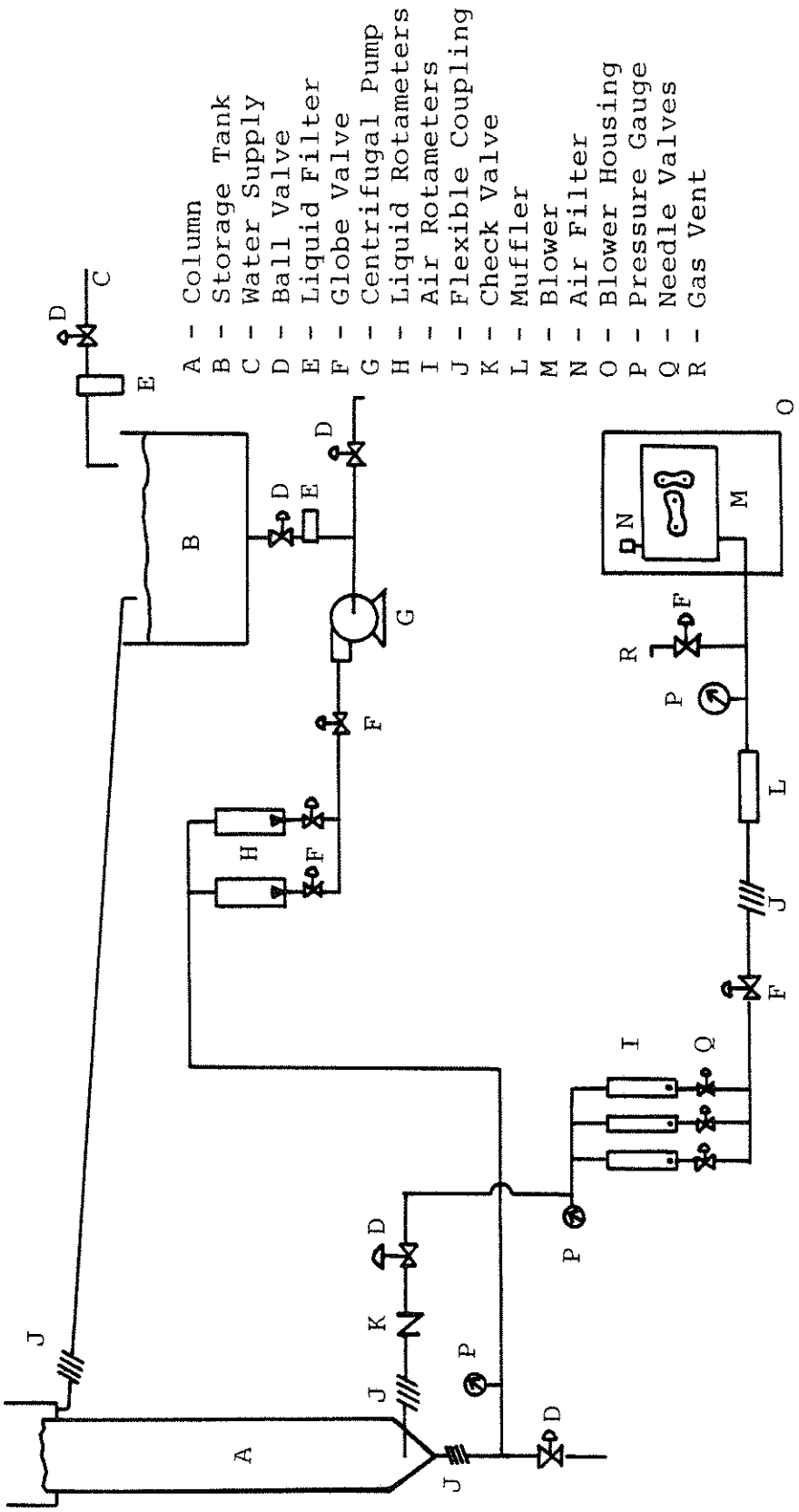

Figure 5.9 Schematic of Experimental Apparatus

pump (3/4 Hp, Worthington Model 520) that is capable of delivering approximately 15 gpm against the head provided by the column. This flowrate corresponds to a superficial liquid velocity of about 3 cm/s (1 in/s). The liquid flowrate is measured by two rotameters (Brooks) that can be used one at a time or in parallel. These rotameters were calibrated with water and the calibrations were linear and can be expressed as follows:

Small Rotameter: $\dot{Q}_L(\text{GPM}) = 0.0494 \times \text{Rotameter Scale}$ (5.40a)

$V_L(\text{cm/s}) = 0.0109 \times \text{Rotameter Scale}$ (5.40b)

Large Rotameter: $\dot{Q}_L(\text{GPM}) = 0.106 \times \text{Rotameter Scale}$ (5.41a)

$V_L(\text{cm/s}) = 0.0234 \times \text{Rotameter Scale}$ (5.41b)

The calibration for the small rotameter is valid within - 3.1% to +0.7% for rotameter scale readings from 30% to 90% of full scale and within -8.5% for rotameter readings down to 20% of full scale. This rotameter is inaccurate above 90% of full scale. The calibration for the large rotameter is valid within -0.9% to + 1.9% for readings between 20% and 100%. These rotameters as well as the gas rotameters, pressure gauges, and power supplies are mounted on a 120 cm x 240 cm (48 in x 96 in) plywood control panel. The liquid is filtered through a 5 micron filter as it is withdrawn from the storage tank and is delivered to the column through 1 in nominal (Schedule 40) polyvinyl chloride (PVC) pipe. PVC piping was used to avoid corrosion which would contaminate the system. A pressure gauge has been placed in the liquid line at the base of the column as well as a connection for draining the column liquid to the trench. Just before the liquid is delivered to the column, the

pipe is reduced to 1/2 in nominal (Schedule 40) and a flexible connection is placed between the column and the piping system to reduce the transmission of vibrations to the column. After the liquid passes through the column and into the overflow, it flows by gravity through a 1-1/2 in nominal (Schedule 40) PVC pipe back to the storage tank. This overflow line is connected to the column with a flexible coupling to isolate vibration.

Atmospheric air is used as the gas phase and it is delivered to the system by a positive displacement blower (Roots Series 22AF, 1-1/2 Hp). Gearing is available to operate the blower at speeds of 1750 rpm or 2600 rpm (the maximum blower speed). The lower speed corresponds to an air flowrate of 10 CFM (at conditions of 14.7 psia and 68°F) at an outlet pressure of 6 psig (the maximum operating pressure for the blower). This flowrate corresponds to a superficial gas velocity of about 15 cm/s (6 in/s). The higher speed corresponds to an air flowrate of 20 CFM at an outlet pressure of 6 psig which is equivalent to a superficial gas velocity of about 30 cm/s (12 in/s). The blower is housed in a plywood box that is lined with acoustic tile to reduce inlet noise. A muffler has also been placed on the blower outlet to reduce outlet noise. The inlet air is filtered to remove particulate matter. A vent has been installed on the blower outlet so that the excess capacity of the blower can be diverted to the atmosphere. The air conduit is 1 in nominal (Schedule 40) PVC pipe and a flexible connection separates the blower from the control panel so that the blower vibrations may be isolated. Three rotameter connections are available for monitoring the air flowrates. Five rotameters (Dwyer Model RMC) are available to cover

the entire range of operating conditions. The rotameter ranges are 10 to 100 SCFH, 20 to 200 SCFH, 40 to 400 SCFH, 60 to 600 SCFH, and 180 to 1800 SCFH (standard conditions are 14.7 psia and 32°F). The rotameters are factory calibrated and are accurate within $\pm$ 2% of full scale. Pressure gauges have been placed on the blower outlet and rotameter outlets to ensure operation within the pressure limits of the blower and to determine the pressure at which the air flowrates are measured, respectively. A check valve has been placed in the air line near the column to prevent liquid backflow. After this check valve, the air line is reduced to 1/2 in nominal (Schedule 40) and is connected to the column with a flexible coupling to isolate vibrations. Once the air passes through the column, it separates from the liquid in the overflow section and is released to the atmosphere. It should be noted that instruments for measuring the ambient temperature and pressure are in the lab. As was discussed previously (Section 5.2.5), no instrumentation has been set up but will be added shortly.

5.4 PRELIMINARY RESULTS

The preliminary results have been limited to visual observation and the determination of gas holdup in an air-water system. The following observations were made in the 19 cm (7.5 in) lab-scale column with an air-water system with a fixed superficial liquid velocity of 0.5 cm/s (0.2 in/s).

V_G = 0.5 cm/s - The bubble concentration is very low; a sheet (group) of bubbles is periodically released from the entire gas distributor area as the distributor fluctuates (1 to 2 times per second); even at this

low gas flow, some larger, spherical-cap bubbles rise up the column axis and the gas bubbles appear to be stagnant or moving downwards at the column wall; the average bubble diameter is about 1 cm (0.4 in).

V_G = 1.0 cm/s - The bubble concentration is much higher; some bubbles appear stagnant for short periods of time in the wall region; the distributor is similar to that discussed above except some gas jetting occurs in the center of the distributor above the point where the gas is sparged into the system.

V_G = 1.5 cm/s - The bubble concentration has increased; some larger bubbles are zig-zagging up the column axis which appears as a gas coring effect.

V_G = 2.0 cm/s - Some downward motion of the bubbles is now occurring at the column wall; more vigorous eddying in the wall region gives the small gas bubbles and the liquid an angular motion.

V_G = 2.5 cm/s - The gas release for the distributor is more uniform, but pulsing still occurs; the larger bubbles are causing vortices in their wakes.

V_G = 3.0 cm/s - The bubbles rising up the column axis are fairly large and rise rapidly; this could perhaps be the upper bound of pure bubble flow although the flow is not churn-turbulent.

V_G = 5.0 cm/s - The flow is fairly turbulent and the bubbles in the wall region appear to move in a random manner (left, right, up, or down) although there is little radial motion except at the cap and the rear of the large, fast-rising bubbles.

V_G = 6.0 cm/s - This could be seen as the onset of churn-turbulent flow because of the continuously churning nature of the small gas bubbles and liquid in the wall region caused by the large gas bubbles that are fairly prominent; the gas is coring (jetting) through the central portion of the gas distributor.

V_G = 8.0 cm/s - Gas jetting occurs to a point about one foot above the gas distributor where the large gas bubbles appear to gain their identity.

V_G = 10 cm/s - Flow is very turbulent; the liquid level at the top of the column is beginning to fluctuate; the gas jet at the distributor appears tornado-like and the distributor region is very chaotic.

V_G = 15 cm/s - Large gas slugs (which actually appear to be regions of high gas holdup with the highest holdup occurring in the core region) pass rapidly up the column at a frequency of one to two per second; the regions of high holdup are particularly visible because of the light that shines through them.

V_G = 20 cm/s - The gas-liquid dispersion is very frothy and the liquid level at the top of the column fluctuates markedly; it is not apparent whether the increased gas throughput is being transported by larger slugs, faster-rising slugs, or slugs at a greater frequency although the first two explanations would seem more likely.

No significant change in the hydrodynamic appearance of the column occurs as the superficial gas velocity is increased from 20 cm/s (8 in/s) to 30 cm/s (12 in/s) although the liquid level at the top of the column fluctuates a great deal at the highest gas velocities. Actually, the hydrodynamic appearance of the column does not change rapidly with the superficial gas velocity at superficial gas velocities greater than 10 cm/s (4 in/s).

Some of the observations noted here are similar to those of other researchers which were discussed earlier. One thing is apparent from these observations - there is no dramatic transition from bubble flow to churn-turbulent flow; rather, there is a slow transition from one flow regime to the other. Visual observation of the transition is difficult and the choice of a superficial gas velocity of 3.0 cm/s (1.2 in/s) as the upper limit of pure bubble flow and 6.0 cm/s (2.4 in/s) as the onset of churn-turbulent flow can only be taken as an approximation. Since visual observation cannot accurately indicate flow pattern transitions, research in this area should be focused on a parameter that varies significantly between regimes and affects the column behavior or upon the mechanism by which the large, fast-rising gas slugs characteristic of churn-turbulent flow are formed.

The gas holdup was determined as a function of the superficial gas velocity in the experimental column with a fixed superficial liquid velocity of 0.5 cm/s (0.2 in/s) employing the quick closing valve technique. In this method, the gas and liquid flows to the column are adjusted to the desired settings and the system is allowed to stabilize to steady state. The gas and liquid flows are then interrupted simultaneously and the gas escapes from the column while the liquid remains in the column. The gas holdup can then be calculated in the following manner.

$$\varepsilon = \frac{L - L'}{L} \tag{5.42}$$

where: L', the liquid level after gas disengagement

These data are presented in Figure 5.10. Each of these data points is the average of five runs and the maximum standard deviation in the data is less than 0.004.

The gas holdup can be seen to be a smooth function of the superficial gas velocity and nothing in the gas holdup behavior seems indicative of a change in flow regime. A number of gas holdup correlations are available in the literature. Three of these correlations and the range of parameters considered in their development are presented in Table 5.3. Note that these correlations have been reduced to the form applicable to an air-water system in the experimental bubble column. The only variable parameter is the superficial gas velocity which should be expressed in cm/s units for use with the correlations of Table 5.3. The experimental data of Figure 5.10 have been compared to the literature correlations in Figure 5.11. The

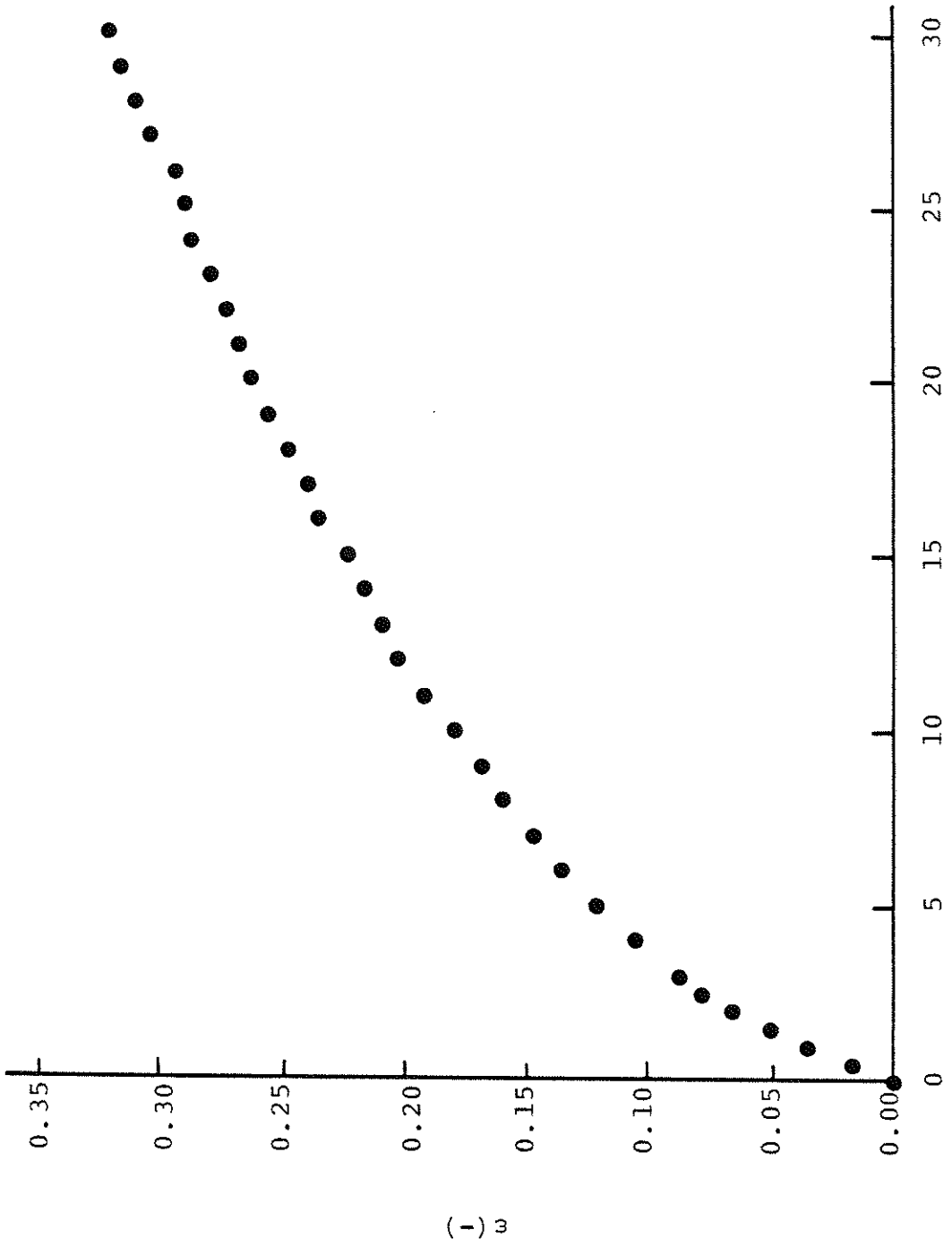

Figure 5.10 Gas Holdup Data for Air-Water System in 19 cm Diameter Column

Table 5.3 Literature Correlations for Gas Holdup as Applied to an Air-Water System in a 19 cm Diameter Column

Reference	Parameter Range	Proposed Correlation
Hughmark (99)	V_G = 0.4 - 45 cm/s D > 10 cm ρ_L = 0.78 - 1.7 g/cm^3 μ_L = 0.9 - 15.2 cp σ = 25 - 76 dyne/cm	$\varepsilon = \frac{1}{2 + 35/V_G}$
Hikita and Kikukawa (73)	V_G = 4.2 - 38 cm/s D = 10 - 19 cm L = 60 - 135 cm ρ_L = 0.91 - 1.2 g/cm^3 μ_L = 0.7-13.8 cp σ = 37.5 - 74.8 dyne/cm	$\varepsilon = 0.0580\ V_G^{0.47}$
Kumar et al. (100)	V_G = 0.14 - 14 cm/s D = 5 and 10 cm ρ_L = 0.8 - 1.1 g/cm^3 μ_L = 0.9 - 11.5 cp σ = 31.2 - 72 dyne/cm	$\varepsilon = 0.728\ U - 0.485\ U^2 + 0.0975\ U^3$ $U = 0.0614\ V_G$

Note - The superficial gas velocity should be expressed in cm/s units

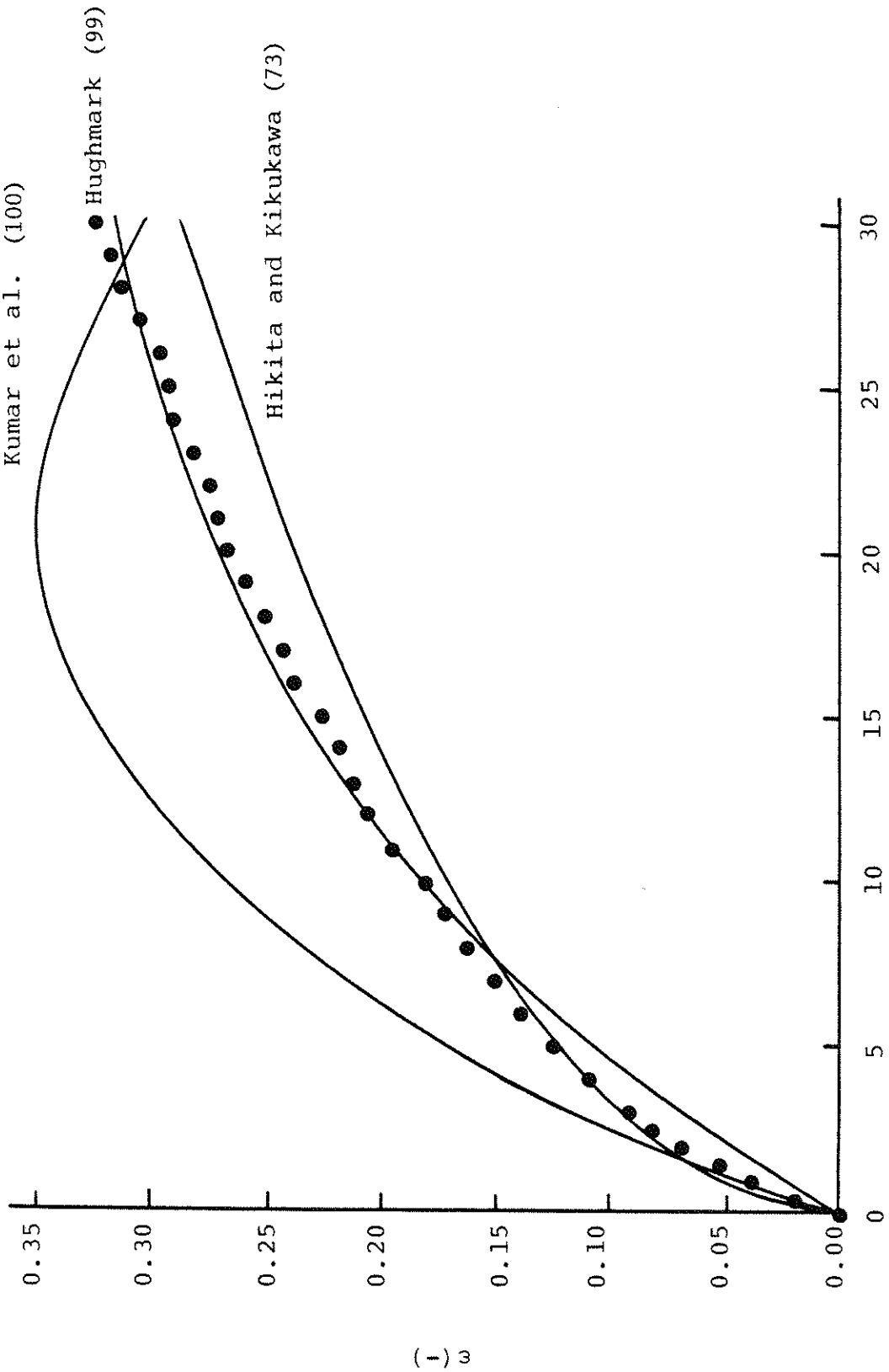

Figure 5.11 Comparison of Holdup Data with Literature Correlations

correlation of Kumar et al. (100) is inaccurate over the entire range because it has been extrapolated to a larger column and higher superficial gas velocities. None of the correlations are accurate at superficial gas velocities less than 4.0 to 6.0 cm/s (1.6 to 2.4 in/s) with most errors being about 20%. These deviations at lower superficial gas velocities may indicate an effect of gas distributor design. At superficial gas velocities greater than 4.0 cm/s (1.6 in/s), the correlation of Hikita and Kikukawa (73) is reasonably accurate with most errors being less than 10%. The correlation of Hughmark (99) is very accurate at superficial gas velocities greater than 6.0 cm/s (2.4 in/s) with a maximum error of 3%.

The holdup data presented in Figure 5.10 can be used to evaluate the methods of flow pattern delineation which were discussed previously. First, consider the flow map of Shah et al. (1) which was presented in Figure 3.1 . Since the diameter of the experimental column is 19 cm (7.5 in), all points above a superficial gas velocity of about 4.0 cm/s (1.6 in/s) fall into a transition range between slug flow and churn-turbulent flow. However, the behavior observed in the column is churn-turbulent and the flow map may be interpreted to predict bubble flow for superficial gas velocities below 4.0 cm/s (1.6 in/s) and churn-turbulent flow for superficial gas velocities above 7.0 cm/s (2.8 in/s). These predictions agree well with the observations of 3.0 cm/s (1.2 in/s) and 6.0 cm/s (2.4 in/s) observed visually in the experimental column.

The flow pattern delination criteria of Kawagoe et al. (23) were discussed in Section 3.2. These criteria focused on changes in the gas holdup-superficial gas velocity relations to delinate between flow regimes.

It was proposed that the gas holdup should be a linear function of the superficial gas velocity in the bubble flow regime. The holdup data obtained at low gas velocities in the 19 cm (7.5 in) column with an air-water system has been expanded in Figure 5.12. It is evident that the data deviates from linearity at a superficial gas velocity of about 2 cm/s (0.8 in/s). Recall that Kawagoe et al. (23) noted deviation at a superficial gas velocity of 3.5 cm/s (1.4 in/s) after analyzing numerous data.

Kawagoe et al. (23) also proposed that the inverse of the gas holdup should be a linear function of the inverse of the superficial gas velocity in churn-turbulent flow. The experimental data has been presented in this form in Figure 5.13. The transition to churn-turbulent flow occurs at a superficial gas velocity of about 9.0 cm/s (3.5 in/s). This is higher than the 6.0 cm/s (2.4 in/s) observed visually, but agrees well with the value of 10 cm/s (3.9 in/s) found by Kawagoe et al. (23). This difference may indicate the inability of visual observation to detect the hydrodynamic changes that occur during flow pattern transitions.

A plot such as that of Figure 5.10 indicates that the gas holdup is a smooth function of the superficial gas velocity and no change in behavior indicative of a flow pattern transition is evident. Figure 5.14 is a ln-ln plot of the experimental data which could reveal some behavior changes indicative of a flow regime transition. As has already been discussed, the gas holdup is a linear function of the superficial gas velocity for superficial gas velocities below about 2 cm/s (0.8 in/s). At superficial gas velocities above about 7 cm/s (3 in/s), the gas holdup is proportional to the square root of the superficial gas velocity. At

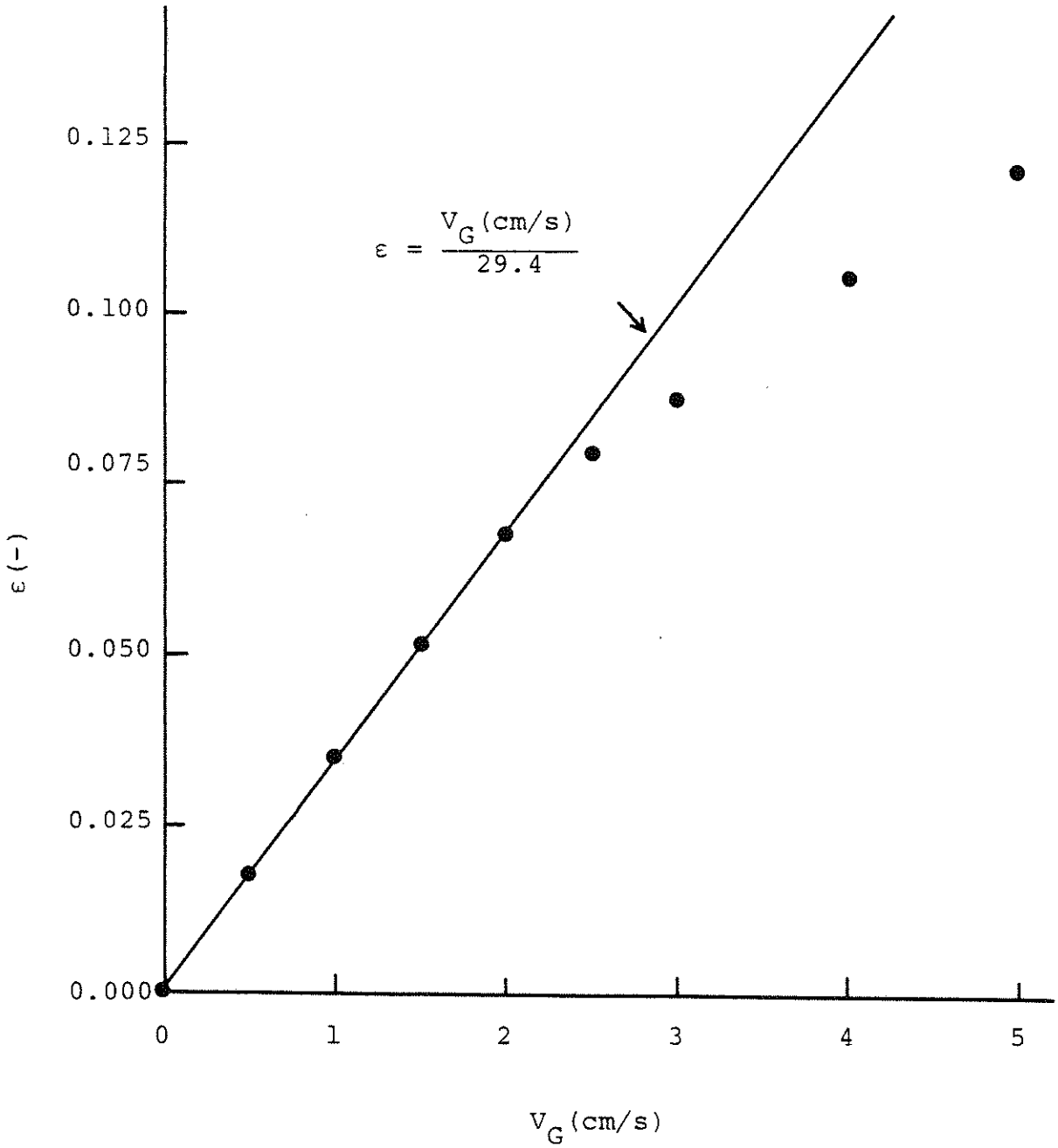

Figure 5.12 Holdup Data at Low Gas Flows

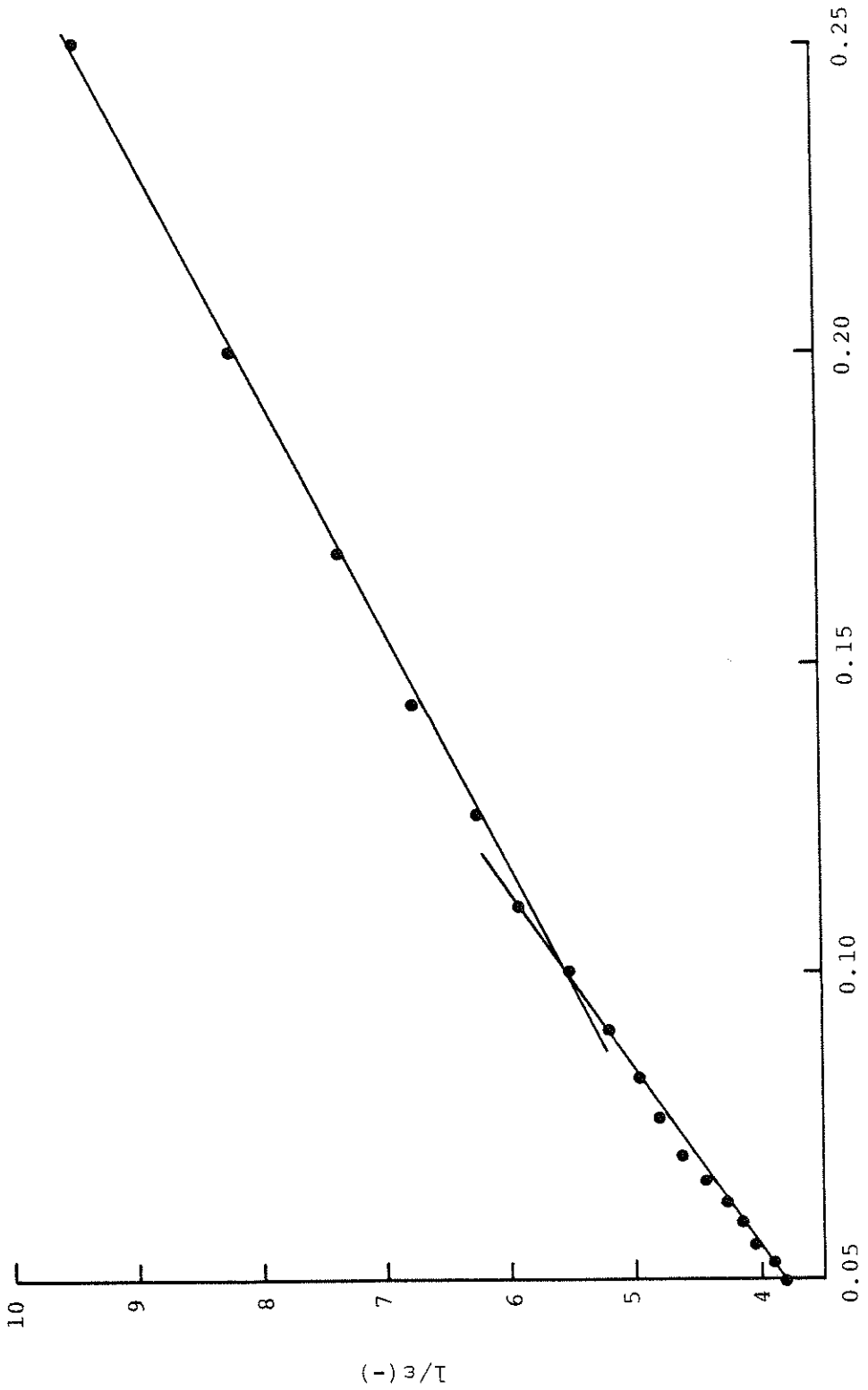

Figure 5.13 Holdup Data at High Gas Flows Treated with the Model of Kawagoe et al. (23)

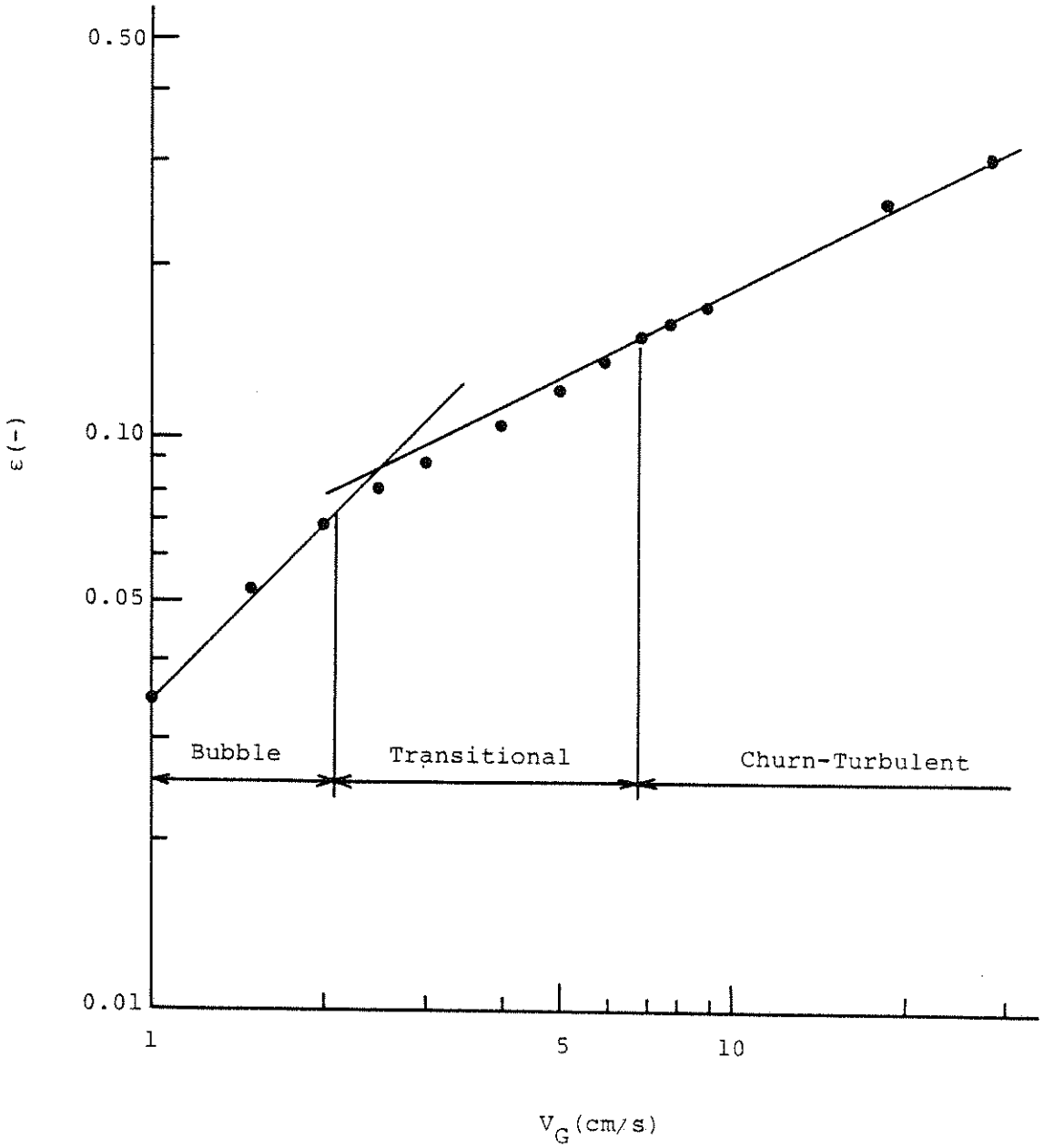

Figure 5.14 Ln-Ln Plot of Holdup Data

intermediate superficial gas velocities, a transitional relation is observed. This change in behavior is certainly due to the drastically different behavior of the gas bubbles of bubble flow and the gas bubbles of churn-turbulent flow.

The preceding comparison of the experimental data with the various methods of delinating flow regimes has given guidelines that may be followed to determine the prevailing flow regime of future experiments. Pure bubble flow occurs only at very low superficial gas velocities, less than about 3 cm/s (1 in/s). The onset of churn-turbulent flow occurs at a superficial gas velocity of about 6 or 7 cm/s (about 2.5 in/s) while the flow becomes fully churn-turbulent at superficial gas velocities of about 10 cm/s (4 in/s).

In Section 5.2.4 it was noted that the determination of the transport and entrained gas holdup by the dynamic gas disengagement technique of Vermeer and Krishna (32) could be useful for the characterization of the model parameters. The dynamic gas disengagement technique was used to characterize the gas holdup in this manner and the results are shown in Figure 5.15. Included in this plot are the total, the transport, and the entrained gas holdups. Again, the data points are the average of five runs and the maximum standard deviation in the transport holdup is 0.008. The data concerning the entrained and transport gas holdups at superficial gas velocities below 10 cm/s (4 in/s) may have no apparent physical interpretation since the flow may not be fully churn-turbulent. At the higher superficial gas velocities characteristic of churn-turbulent flow, the transport gas holdup is larger than the entrained gas holdup. This is opposite to

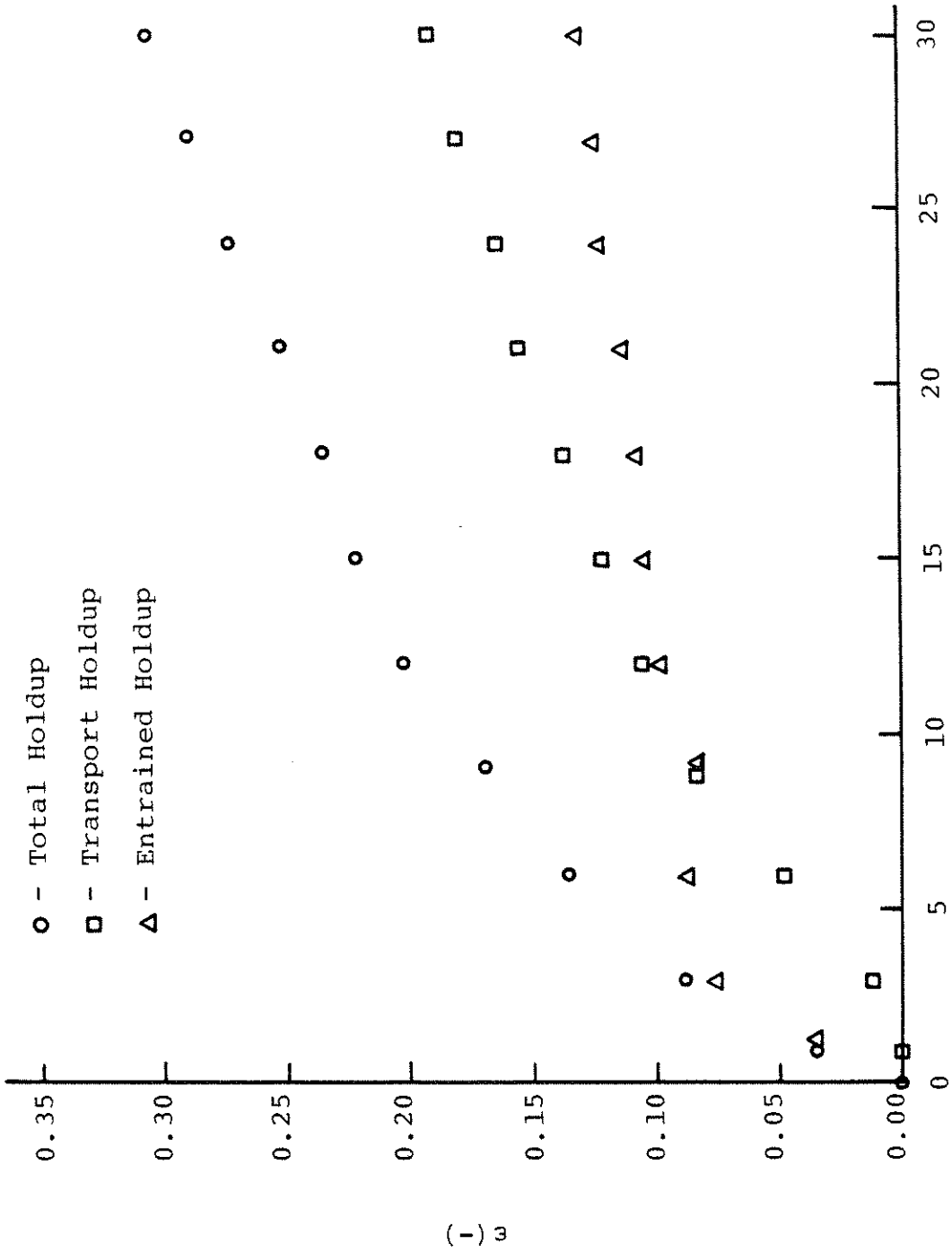

Figure 5.15 Total, Transport, and Entrained Gas Holdup for an Air-Water System in 19 cm Diameter Column

the behavior noted by Vermeer and Krishna (32); however, they employed a nitrogen-turpentine 5 system rather than the air-water system employed here (the column diameters were the same for both studies). In both the present study and that of Vermeer and Krishna (32), the transport gas holdup was found to increase at a faster rate than the entrained gas holdup with increasing superficial gas velocity.

In the proposed physical model it was assumed that all of the gas fed to the column is transported by the fast-rising gas slugs. If this assumption is taken as valid, the rise velocity of the gas slugs, V_s, can be calculated as the superficial gas velocity divided by the transport gas holdup. The slug velocity calculated on this basis is shown as a function of the superficial gas velocity in Figure 5.16. Although there is scatter in the data, the plot is fairly linear. Note that the slug velocities are in excess of 100 cm/s (40 in/s) for superficial gas velocities characteristic of churn-turbulent operation.

If the slug velocity is known from the preceding discussion and the slug frequency, f_s, and volume of liquid downflow during slug passage, $Q_{L,DF}$, can be approximated, the model equations can be solved to give some indication of the magnitudes of the model parameters. As has been discussed, the slug frequency appears to be fairly constant at about 2 s^{-1}. The volume of liquid downflow during slug passage can be approximated by integrating the empirical liquid velocity profiles across the region of downflow. The data of Hills (30) indicate that $Q_{L,DF}$ is equal to 1405 cm^3 at a superficial gas velocity of 16.9 cm/s. Using these approximations and the data obtained in the experimental column, the proposed model equations can be solved to yield the

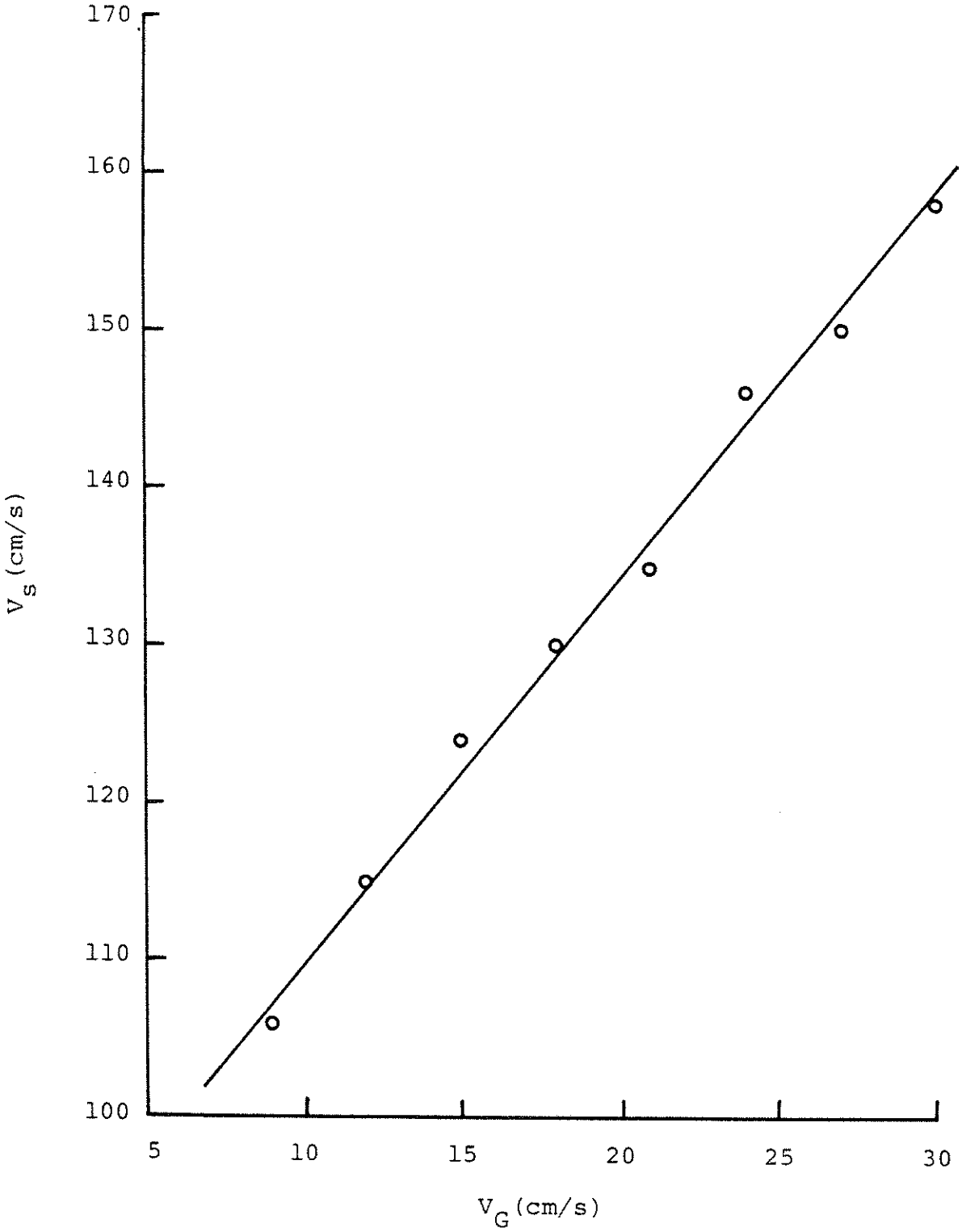

Figure 5.16 Slug Rise Velocity Data

information presented in Table 5.4. Some of the information listed in the table is not necessary for model solution, but is included because of its interesting nature. The large slug volume and the large volume of liquid downflow during slug passage are particularly notable among the model parameters. Knowing the model parameters of Table 5.4, the species conservation equations can be solved and compared with experimental residence time distribution data to obtain a value of the volumetric exchange coefficient, k_E, the last remaining model parameter, at these operating conditions.

5.5 COMPARISON WITH THE AXIAL DISPERSION MODEL

The mixing characteristics of the proposed model can qualitatively be compared to those of the axial dispersion model by considering a number of (nonvolatile, nonreactive) tracer studies. The first type of tracer test to be considered is that used by Argo and Cova (43) which is illustrated in Figure 5.17. For this test, tracer is continuously injected into the liquid phase at the top of the column (note that the tracer flowrate is small compared to the liquid feed flowrate) while the gas and liquid are fed cocurrently at the base of the column. The liquid feed generally does not contain any tracer and this is the case that will be considered here. The steady-state tracer concentration profile along the length of the column can be used to characterize the mixing of the liquid phase.

The conservation equation for the axial dispersion model was presented as Equation 4.2 and can be modified to consider the steady-state mixing of the liquid phase.

Table 5.4 Sample Case of Model Parameter Estimation

Parameter	Source	Value
D	System Parameter	19 cm
V_G	Operating Parameter	16.9 cm/s
V_L	Operating Parameter	0.5 cm/s
ε	Experiment	0.240
ε_T	Experiment	0.137
ε_E	Experiment	0.103
V_s	Figure 5.17	123 cm/s
f_s	Visual Observation	2 s^{-1}
$Q_{L,DF}$	Integration of Empirical Velocity Profile	1405 cm^3
t_c	Eqn. 5.35	0.15 s
ε_s	Eqn. 5.19	0.62
$(Vol)_s$	Eqn. 5.12	3860 cm^3
$(Vol)_c$	Eqn. 5.36	5390 cm^3
ε_c	Eqn. 5.39	0.13
$(Num)_s$	Eqn. 5.37	4

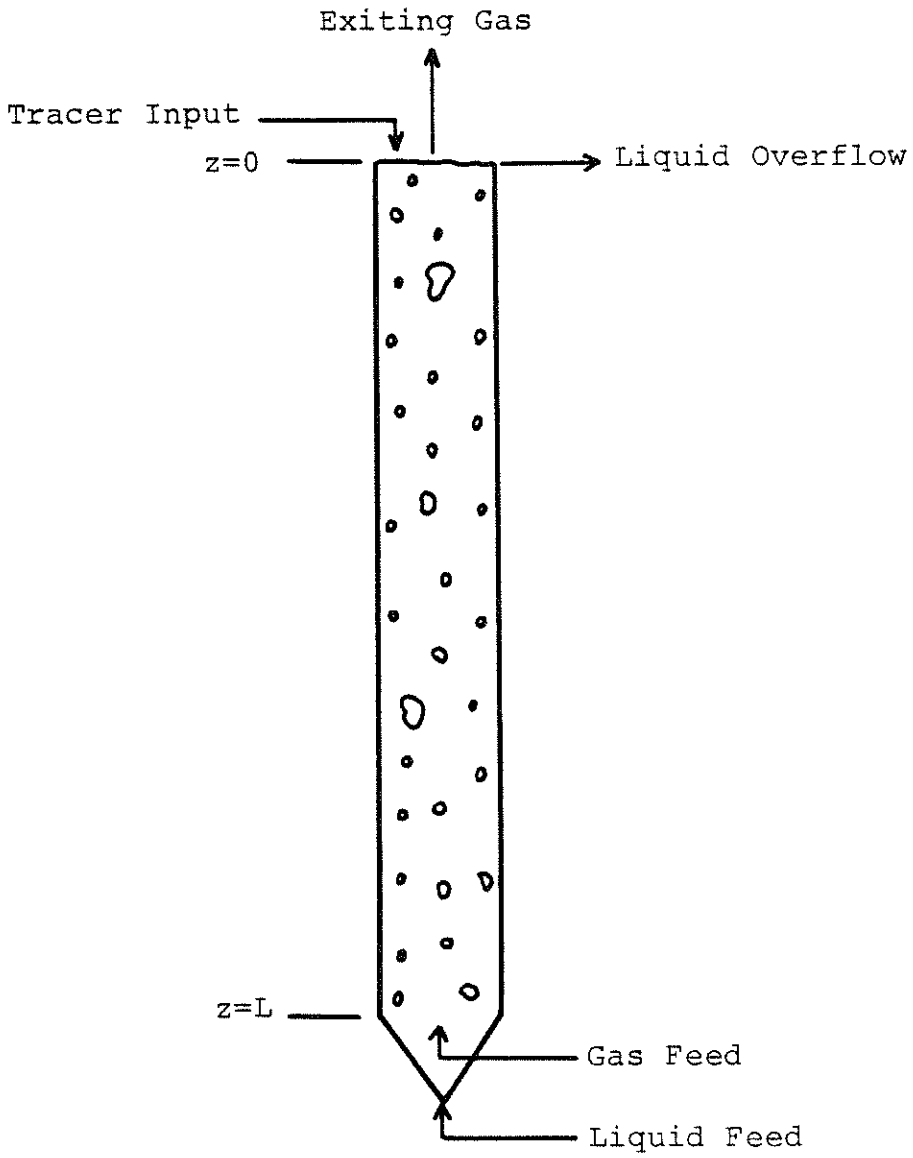

Figure 5.17 Tracer Test Employed by Argo and Cova (43)

$$\frac{\partial C}{\partial t} = 0 = E_L \frac{\partial^2 C}{\partial z^2} - V_L \frac{\partial C}{\partial z} \tag{5.43}$$

The Danckwerts boundary conditions should be used with this equation.

$$C = C_E \text{ at } z = 0 \tag{5.44}$$

$$\frac{E_L}{V_L} \frac{\partial C}{\partial z} + C = C_o \text{ at } z = L \tag{5.45}$$

C_E is the tracer concentration in the effluent from the reactor, C_o is the tracer concentration in the liquid feed, and z is the axial coordinate as shown in Figure 5.17. Note that the dispersion coefficient employed here is based on the entire column cross section. The solution to this model is as follows.

$$C = C_o + (C_E - C_o) \exp\left(-\frac{V_L}{E_L} \cdot z\right) \tag{5.46}$$

If C_o is zero the solution becomes

$$C = C_E \cdot \exp\left(-\frac{V_L}{E_L} \cdot z\right) \tag{5.47}$$

The species conservation equations of the proposed model (Table 5.1) can be modified to account for the tracer input at the top of the column and for steady-state operation. Determination of the tracer concentration profile becomes a problem of solving N (the number of cells in the column) linear algebraic equations in N

unknowns (the cell concentrations) which can easily be accomplished by matrix techniques. As a specific case, the system described in Table 5.4 may be considered. Examination of the model parameters in this table indicates that only the exchange coefficient, k_E, is unspecified. The steady-state tracer concentration profiles for values of the dimensionless parameter Y ranging from 0.01 to 0.30 are plotted in Figure 5.18 (note that varying Y is equivalent to varying k_E). The profiles have been smoothed for clarity except for one case which illustrates the stair-step profile predicted by the model which assumes that the cells are noncommunicating except during slug passage. The 'tailing' of the profiles that occurs at low values of Y is due to the direct relation between the tracer concentrations in cell 1 and cell 2 for this system ($C_{c1} = 0.96\ C_{c2}$ for all values of Y).

The axial dispersion model predicts that the tracer concentration should be linear on a semilog plot (Equation 5.47). The tracer profiles predicted by the proposed model have been plotted in a semilog manner in Figure 5.19. These plots can be seen to be linear and an 'equivalent' axial dispersion coefficient can be determined from the slope of these plots (equivalent meaning that value of the axial dispersion coefficient that yields the same tracer concentration profile as a particular value of the parameter Y). The equivalent values of Y and E_L are compared in Table 5.5. For this range of parameters, Y and E_L are simply related.

$$Y = \frac{72}{E_L} \quad (E_L\ [=]\ cm^2/s;\ 242 \leq E_L \leq 7143) \tag{5.48}$$

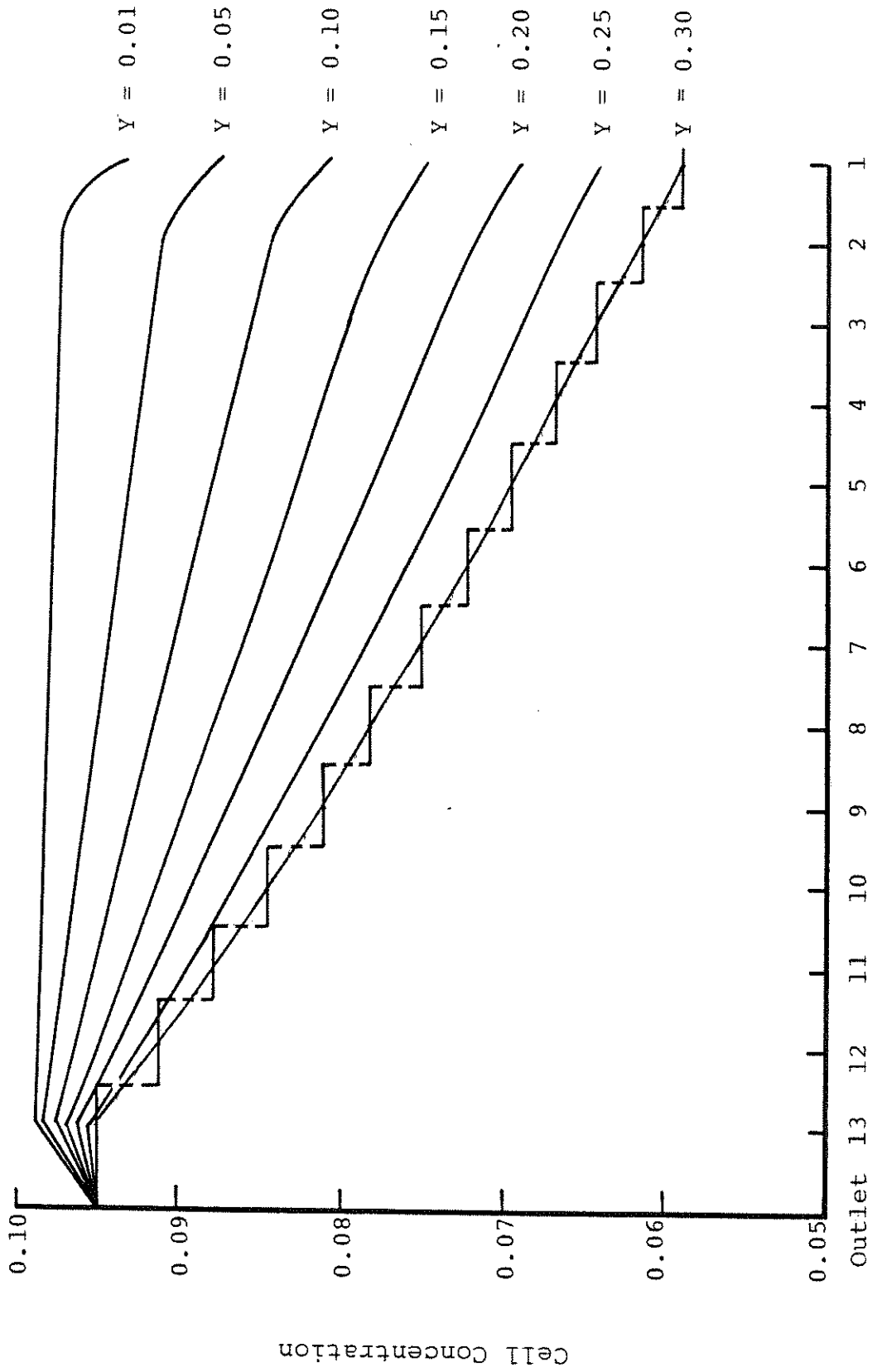

Figure 5.18 Steady-State Tracer Profiles Predicted by the Proposed Model

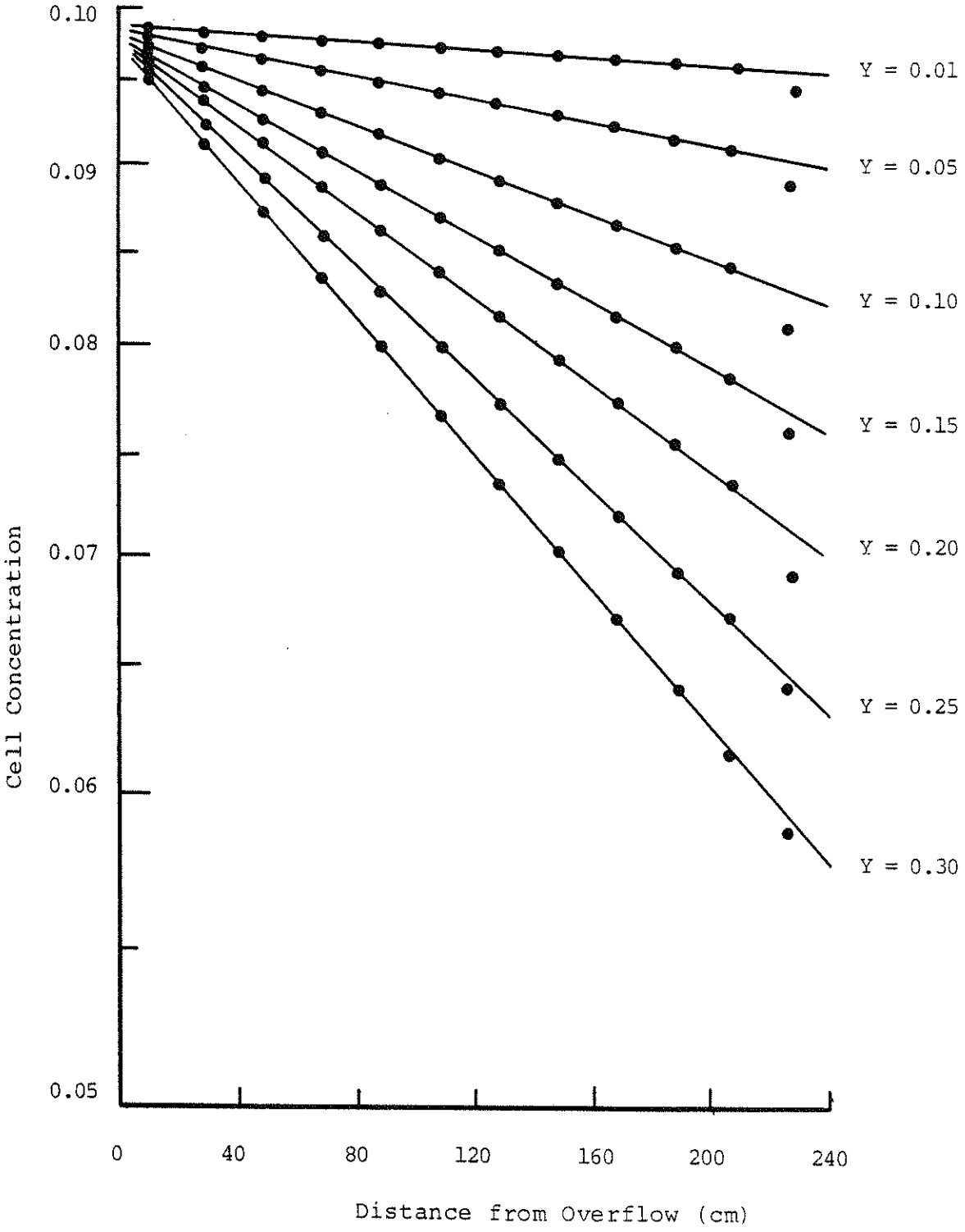

Figure 5.19 Semilog Plot of Tracer Profiles

Table 5.5 Comparison of Equivalent Values of Y and the Axial Dispersion Coefficient

Y (-)	E_L (cm^2/s)
0.01	7143
0.05	1433
0.10	719
0.15	484
0.20	362
0.25	288
0.30	242

Note that Y and E_L show opposite behavior when describing the degree of mixing. Small Y indicates more mixing while large Y indicates less mixing. On the other hand, small E_L indicates less mixing while large E_L indicates more mixing. The correlation of Baird and Rice (74) presented in Table 4.1 predicts an axial dispersion coefficient of 454 cm^2/s (70.4 in^2/s) for this system. Equation 5.48 can be used to determine that a Y value of 0.159 will yield the same steady-state tracer concentration profile.

The proposed models have been shown to be equivalent for the steady-state tracer test for the sample case when Y has a value of 0.159 and E_L has a value of 454 cm^2/s. It is interesting to compare the two model predictions for other types of tracer experiments. Figure 5.20 compares the model predictions of the exit age density function (RTD, normalized pulse response), $E(\theta)$, with those of a completely backmixed system. A similar comparison of the cumulative age distribution (unit step response), $F(\theta)$, is presented in Figure 5.21. The response of the axial dispersion model depends upon the choice of boundary conditions (45) in both cases discussed here. A closed-closed system was chosen to best represent bubble column operation. Figures 5.20 and 5.21 indicate differences between the proposed model and the axial dispersion model for these types of tracer tests even when the models were 'equivalent' for the steady-state tracer test discussed earlier. In both cases, the axial dispersion model more closely approximates a completely backmixed system. These differences might be capable of experimentally differentiating between the models.

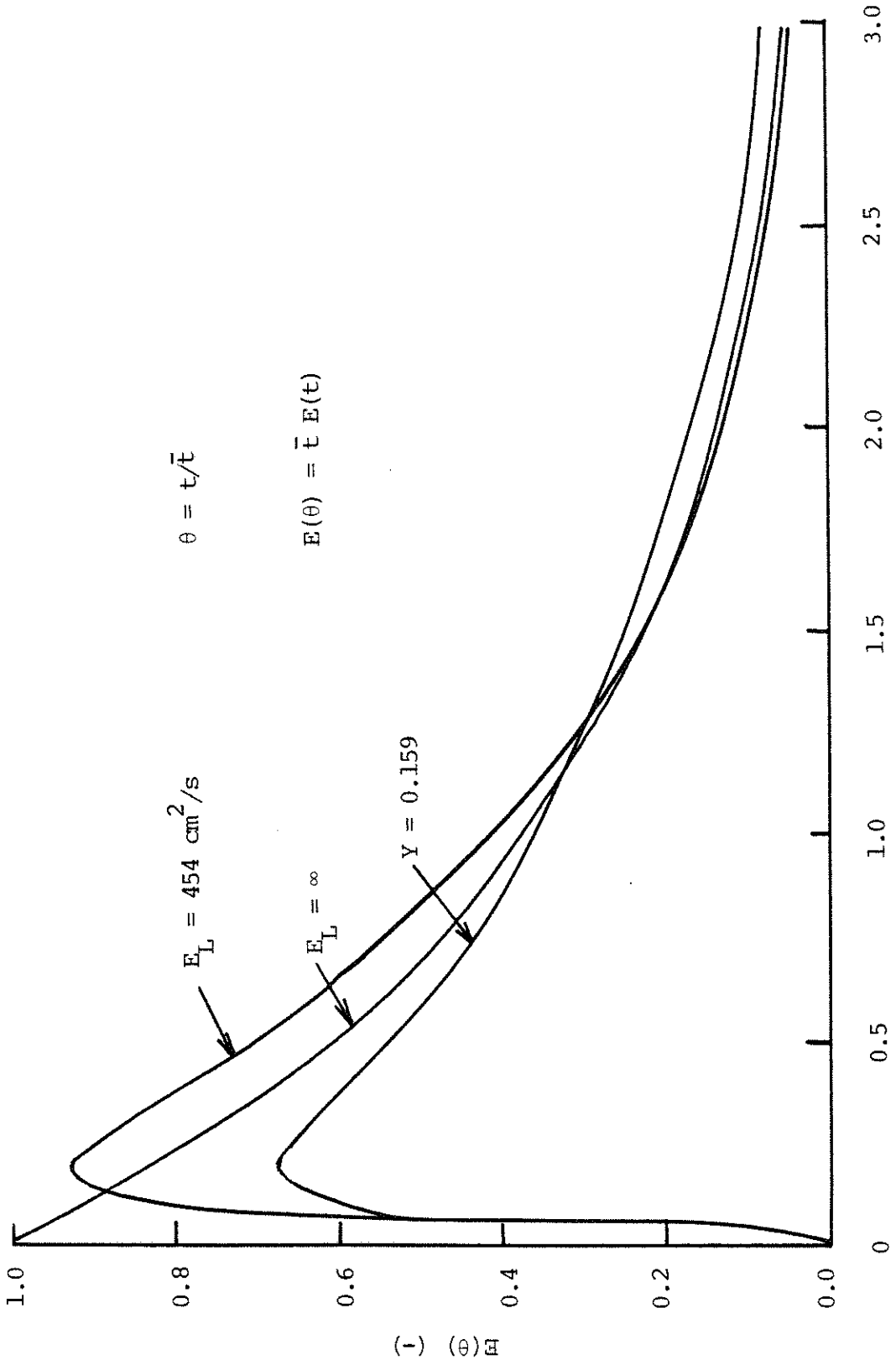

Figure 5.20 Comparison of Exit Age Density Functions

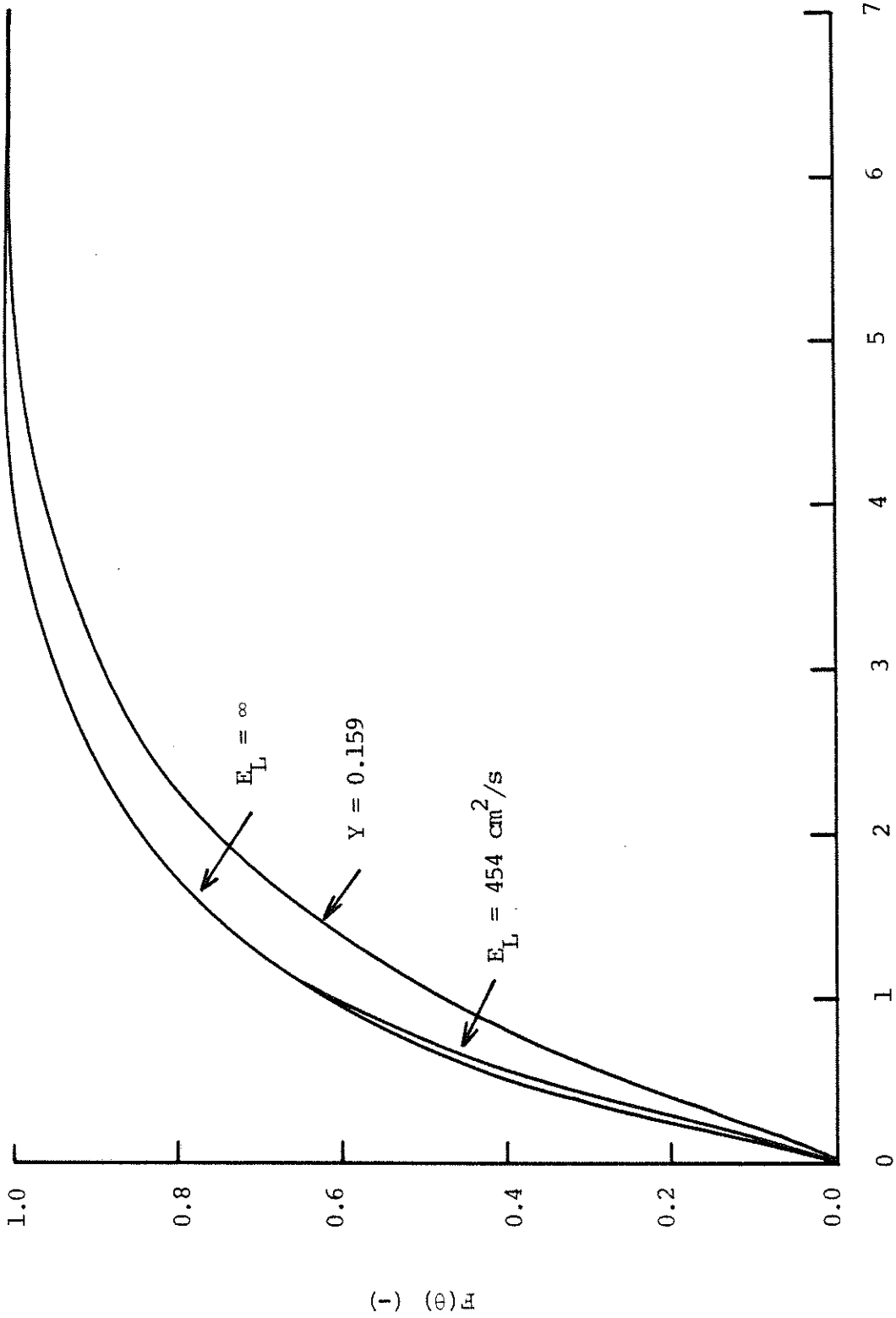

Figure 5.21 Comparison of Cumulative Exit Age Distribution Functions

6. ACKNOWLEDGMENTS

The author would like to express his gratitude to the Exxon Education Foundation for their support in the form of the Exxon Education Foundation Fellowship. Many thanks are also due to Lou Tolie for his assistance in equipment construction. The final thanks goes to the author's advisors, Dr. M. P. Dudukovic and Dr. P. A. Ramachandran, for their guidance and to the other members of CREL for their support and interest.

7. APPENDICES

APPENDIX 7.1

An Alternate Backmixing Model

Previously it was pointed out that liquid-phase backmixing in bubble columns was due to velocity profiles, wake effects, and turbulent eddies. All of these effects are lumped into a single parameter in the axial dispersion model. The dispersion model can be generalized to account for velocity profiles and radial effects in hopes of achieving a more accurate description of bubble column behavior. The liquid-phase species conservation equation then takes the following form in the absence of mass transfer and reaction.

$$(1-\varepsilon)\frac{\partial C}{\partial t} + u_z(r)\frac{\partial C}{\partial z} = E_z\frac{\partial^2 C}{\partial z^2} + E_r\frac{1}{r}\frac{\partial}{\partial r}\left(r\frac{\partial C}{\partial r}\right) \qquad (7.1)$$

The term $(1-\varepsilon)\frac{\partial C}{\partial t}$ accounts for accumulation in the system. $u_z(r)\frac{\partial C}{\partial z}$ accounts for the convection of liquid where $u_z(r)$ is the local liquid axial velocity which is a function of radial position and operating conditions. Previously it was noted that the liquid velocity has an upward sense in the central core of the column and a downward sense in the wall region (30). Miyauchi and coworkers (78, 79) have correlated the liquid axial velocity in terms of the turbulent kinematic viscosity, ν_t, which characterizes the intensity of turbulence in the column. The kinematic viscosity is not a fluid property; rather, it is a property of the system geometry and operating conditions. Miyauchi et al. (79) found the turbulent kinematic viscosity to be a strong function of column diameter and a weak function of the superficial gas velocity.

The species conservation equation contains two Fickian dispersion terms. $E_z\frac{\partial^2 C}{\partial z^2}$ represents axial dispersion about the front defined by the

liquid velocity profile. Axial dispersion is a result of wake effects and turbulent eddies. It can be proposed that the wake effects are a function of gas velocity and that the eddy effects are proportional to the turbulent kinematic viscosity since this characterizes the turbulence level in the column. The axial dispersion coefficient could then be taken to be of the following functional form.

$$E_z = \alpha \nu_t + f(V_G) \tag{7.2}$$

α is a constant of proportionality. $E_r \frac{1}{r} \frac{\partial}{\partial r} \left(r \frac{\partial C}{\partial r} \right)$ represents radial dispersion which is mainly due to turbulent eddies in the column. The radial dispersion coefficient could then be proposed to be proportional to the turbulent kinematic viscosity.

$$E_r = \beta \nu_t \tag{7.3}$$

Radial dispersion is usually assumed to be complete in bubble columns because of the intense turbulence and large length to diameter ratios typical of bubble column operations. However, radial dispersion is very important because it characterizes communication between the upward and downward flowing regions of the liquid. Reith et al. (65) qualitatively determined the magnitude of the radial dispersion coefficient in a bubble column and the radial dispersion coefficient was found to be about an order of magnitude smaller than the axial dispersion coefficient at the conditions studied.

This model could be characterized by tracer tests in much the same manner as the model proposed earlier. However, in this case multi-parameter optimization would be required to determine both model parameters from one tracer test. Point injections of tracer might be helpful to characterize this model, particularly the radial mixing. Like the previous

model, this model can be seen to be more complex than the axial dispersion model. However, this added complexity may be necessary to describe liquid-phase backmixing in bubble columns in a physically accurate manner.

APPENDIX 7.2

Nomenclature

Symbol	Meaning
C	Concentration
C_o	Reference concentration; inlet concentration
C'	Dimensionless concentration (C/C_o)
$C(x)$	Concentration at point x
C_{ci}	Concentration in cell i
C'_{ci}	Concentration in cell i after slug passage
C_{si}	Concentration in slug exiting cell i
D	Conduit diameter
d_o	Orifice diameter
E	Dispersion coefficient
E_B	Dispersion coefficient due to rising gas bubbles (used by Ohki and Inoue (29))
E_e	Eddy diffusivity (used by Baird and Rice (74))
E_L^*	Modified dispersion coefficient in churn-turbulent flow (used by Ohki and Inoue (29))
E_m	Molecular diffusion coefficient
$E(t)$	Exit age density function; $E(\theta)$, in dimensionless form
F	Net inward flux into a fluid element (used by Barkelew (60))
$F(t)$	Cumulative exit age distribution; $F(\theta)$, in dimensionless form
$F(z)$	Net inward flux into a fluid element at point z

f_s	Slug appearance frequency
g	Acceleration of gravity
K	A constant
$K(z,x)$	Dispersion kernel describing mass exchange between points z and x (used by Barkelew (60))
k	A constant
k_E	Exchange coefficient between slugs and cells
L	Reactor length; column height
ℓ	Characteristic length parameter (used by Baird and Rice (74))
N	Dispersive flux; number of cells in column
$(Num)_s$	Average number of slugs existing in column at a time
$\bar{n}$	Normal vector
Pe	Peclet number ($\frac{V_C D}{E_L}$ based on a circulation velocity)
P_m	Specific rate of energy dissipation in the liquid phase (used by Baird and Rice (74))
Q	A volume of liquid that flows during a specified time span
$Q_{L,DF}$	Volume of downflowing liquid during slug passage
$\dot{Q}$	Volumetric flowrate
R	Column radius
Re	Reynolds number ($\frac{DV_C\rho_L}{\mu_L}$ based on a circulation velocity)
r	Radial coordinate
S	Surface area

$S(c)$	A general volumetric source term (used by Barkelew (60))
t	Time
t'	Dimensionless time $(\frac{tu}{L})$
t_c	Contact time between slugs and cells
$\bar{t}$	Mean residence time
u	Mean fluid velocity
u_L	Characteristic liquid velocity (used by Ohki and Inoue (29)); local liquid velocity (used by Miyauchi and coworkers (78,79))
$\lvert u_w \rvert$	Absolute value of the liquid velocity at the column wall (used by Miyauchi and coworkers (78,79))
V	Superficial velocity; volume
$V_{b\infty}$	Terminal rise velocity of an isolated bubble in an infinite medium
V_C	Circulation velocity
V_s	Slug rise velocity
(Vol)	Volume (of a slug or cell)
X	Dimensionless parameter $(\frac{k_E t_c}{(1-\varepsilon_s)(Vol)_s})$
x	Position in column
Y	Dimensionless parameter $(\frac{k_E t_c}{(1-\varepsilon_c)(Vol)_c})$
Z	Dimensionless parameter $(\frac{Q_{L,DF}}{(1-\varepsilon_c)(Vol)_c})$
z	Axial coordinate; position in column
z'	Dimensionless axial coordinate (z/L)

GREEK LETTERS

Letter	Meaning
α	Parameter employed by Mashelkar and Ramachandran (75) $\left(\frac{V_G \rho_L g D^2}{8\mu_L V_{b\infty} V_L}\right)$
ϵ	Fractional gas holdup
θ	Dimensionless time ($t/\bar{t}$)
λ	Diffusion coefficient (used by Barkelew (60))
μ	Viscosity
ν	Kinematic viscosity
ν_t	Turbulent kinematic viscosity (used by Miyauchi and coworkers (78,79))
ρ	Density
σ	Surface tension

SUBSCRIPTS

Symbol	Meaning
$b\infty$	Refers to an isolated bubble in an infinite medium (as in $V_{b\infty}$)
C	Refers to circulation (as in V_C)
c	Refers to cell properties (as in ϵ_c); refers to contact between slugs and cells (as in t_c)
ci	Refers to properties of cell i (as in C_{ci})
E	Refers to exchange between slugs and cells (as in k_E); refers to entrained holdup (ϵ_E)

e	Refers to eddy parameters (as in E_e)
G	Refers to gas (as in V_G); G,In refers to gas entering column; G,Out refers to gas leaving column
i	Refers to cell i (as in C_{ci}) or the slug leaving cell i (as in C_{si})
L	Refers to liquid (as in V_L); L,In refers to liquid entering column; L,Out refers to liquid exiting column; L,DF refers to liquid downflowing during slug passage
m	Refers to a specific (as in P_m) or molecular (as in E_m) property
o	Refers to inlet or feed conditions (as in C_o); refers to orifice (as in d_o)
s	Refers to slug properties (as in ε_s)
si	Refers to properties of slug leaving cell i (as in C_{si})
T	Refers to transport holdup (ε_T)
t	Refers to turbulent kinematic viscosity (ν_t)
w	Refers to wall conditions (as in $\lvert u_w \rvert$)

SUPERSCRIPTS

Symbol	Meaning
-	Refers to a vector (as in $\bar{n}$)
'	Refers to conditions after slug passage (as in C'_{ci}); refers to dimensionless properties (as in C'); refers to conditions after gas disengagement (as in L')
*	Refers to modified parameters (as in E_L^*)

OTHER SYMBOLS

Symbol	Meaning
$\frac{\partial C}{\partial t}$	Partial derivative (specifically, of concentration with respect to time)
$\frac{DC}{Dt}$	Substantial time derivative (specifically, of concentration)
$\vec{\nabla}$	Vector differential operator
$\vec{\nabla}^2$	Laplacian operator $(\vec{\nabla}\cdot\vec{\nabla})$
$\int$	Integral
$\sum_x$	Summation over x
$\lvert\ \rvert$	Absolute value (as in $\lvert u_w \rvert$)

8. BIBLIOGRAPHY

1. Shah, Y. T., B. G. Kelkar, S. P. Godbole, and W.-D. Deckwer, "Design Parameters Estimations for Bubble Column Reactors", AIChE J., Vol. 28, No. 3, pp. 353-379 (1982).

2. Joshi, J.B., and M. M. Sharma, "Some Design Features of Radial Baffles in Sectionalised Bubble Columns", Can. J. Chem. Eng., Vol. 57, No. 3, pp. 375-377 (1979).

3. Miller, D. N., "Interfacial Area, Bubble Coalescence and Mass Transfer in Bubble Column Reactors", AIChE J., Vol. 29, No. 2, pp. 312-319 (1983).

4. Taitel, Y., D. Bornea, and A. E. Dukler, "Modelling Flow Pattern Transitions for Steady Upward Gas-Liquid Flow in Vertical Tubes", AIChE J., Vol. 26, No. 3, pp. 345-354 (1980).

5. Oshinowo, T., and M. E. Charles, "Vertical Two-Phase Flow Part I. Flow Pattern Correlations", Can. J. Chem. Eng., Vol. 52, No. 1, pp. 25-35 (1974).

6. Wallis, G. B., One-Dimensional Two-Phase Flow, McGraw-Hill, New York (1969).

7. Hills, J. H., "The Operation of a Bubble Column at High Throughputs I. Gas Holdup Measurements", Chem. Eng. J., Vol. 12, No. 2, pp. 89-99 (1976).

8. Hewitt, G. F., "Flow Regimes", Chapter 2 in Two-Phase Flow and Heat Transfer, D. Butterworth and G. F. Hewitt, eds., Oxford University Press, Oxford (1977).

9. Hewitt, G. F., Measurement of Two Phase Flow Parameters, Academic Press, New York (1978).

10. Jones, O. C., Jr., "Two-Phase Flow Measurement Techniques in Gas-Liquid Systems", Chapter 10 in Fluid Mechanics Measurements, R. J. Goldstein, ed., Hemisphere, Washington, D. C. (1983).

11. Govier, G. W., B. A. Radford, and J. S. C. Dunn, "The Upwards Vertical Flow of Air-Water Mixtures I. Effect of Air and Water-Rates on Flow Pattern, Holdup and Pressure Drop", Can. J. Chem. Eng., Vol. 35, No. 2, pp. 58-70 (1957).

12. Cichy, P. T., J. S. Ultman, and T. W. F. Russell, "Two-Phase Reactor Design Tubular Reactors-Reactor Model Development", Ind. Eng. Chem., Vol. 61, No. 8, pp. 6-26 (1969).

13. Griffith, P., and G. B. Wallis, "Two-Phase Slug Flow", Trans. ASME Ser. C (J. Heat Transfer), Vol. 83, No. 3, pp. 307-320 (1961).

14. Quandt, E., "Analysis of Gas-Liquid Flow Patterns", Preprint No. 47, Sixth National Heat Transfer Conf., AIChE-ASME, Boston (1963).

15. Zuber, N., and J. A. Findlay, "Average Volumetric Concentration in Two-Phase Flow Systems", Trans. ASME Ser. C (J. Heat Transfer), Vol. 87, No. 4, pp. 453-468 (1965).

16. Kunugita, E., M. Ikura, and T. Otake, "Liquid Behavior in Bubble Column", J. Chem. Eng. Jap., Vol. 3, No. 1, pp. 24-29 (1970).

17. Miller, D. N., "Gas Holdup and Pressure Drop in Bubble Column Reactor", Ind. Eng. Chem. Process Des. Dev., Vol. 19, No. 3, pp. 371-377 (1980).

18. Kirkpatrick, J. P., private communication (1981).

19. Shulman, H. L., and M. C. Molstad, "Gas-Bubble Columns for Gas-Liquid Contacting", Ind. Eng. Chem., Vol. 42, No. 6, pp. 1058-1070 (1950).

20. Braulick, W. J., J. R. Fair, and B. J. Lerner, "Mass Transfer in a Sparged Contactor: Part I. Physical Mechanisms and Controlling Parameters", AIChE J., Vol. 11, No. 1, pp. 73-79 (1965).

21. Fair, J. R., "Designing Gas-Sparged Reactors", Chem. Eng., Vol. 74, No. 14, pp. 67-74 (1967).

22. Yoshitome, H., and T. Shirai, "The Intensity of Bulk Flow in a Bubble Bed", J. Chem. Eng. Jap., Vol. 3, No. 1, pp. 29-33 (1970).

23. Kawagoe, K. T., T. Inoue, K. Nakao, and T. Otake, "Flow-Pattern and Gas-Holdup Conditions in Gas-Sparged Contactors", Int. Chem. Eng., Vol. 16, No. 1, pp. 176-183 (1976).

24. Lockett, M. J., and R. D. Kirkpatrick, "Ideal Bubbly Flow and Actual Flow in Bubble Columns", Trans. Instn. Chem. Engrs., Vol. 53, No. 4, pp. 267-273 (1975).

25. Rice, R. G., J. M. I. Tupperainen, and R. M. Hedge, "Dispersion and Hold-Up in Bubble Columns-Comparison of Rigid and Flexible Spargers", Can. J. Chem. Eng., Vol. 59, No. 6, pp. 677-687 (1981).

26. Richardson, J. F., and W. N. Zaki, "Sedimentation and Fluidisation: Part I", Trans. Instn. Chem. Engrs., Vol. 32, pp. 35-53 (1954).

27. Lapidus, L., and J. C. Elgin, "Mechanics of Vertical-Moving Fluidized Systems", AIChE J., Vol. 3, No. 1, pp. 63-68 (1957).

28. Deckwer, W.-D., Y. Louisi, A. Zaidi, and M. Ralek, "Hydrodynamic Properties of the Fischer-Tropsch Slurry Process", Ind. Eng. Chem. Process Des. Dev., Vol. 19, No. 4, pp. 699-708 (1980).

29. Ohki, Y., and H. Inoue, "Longitudinal Mixing of the Liquid Phase in Bubble Columns", Chem. Eng. Sci., Vol. 25, No. 1, pp. 1-16 (1970).

30. Hills, J. H., "Radial Non-Uniformity of Velocity and Voidage in a Bubble Column", Trans. Instn. Chem. Engrs., Vol. 52, No. 1, pp. 1-9 (1974).

31. Towell, G. D., C. P. Strand, and G. H. Ackerman, "Mixing and Mass Transfer in Large Diameter Bubble Columns", AIChE-IChemE Symp. Ser. No. 10, pp. 97-105 (1965).

32. Vermeer, D. J., and R. Krishna, "Hydrodynamics and Mass Transfer in Bubble Columns Operating in the Churn-Turbulent Regime", Ind. Eng. Chem. Process Des. Dev., Vol. 20, No. 3, pp. 475-482 (1981).

33. Hills, J. H., and R. C. Darton, "The Rising Velocity of a Large Bubble in a Bubble Swarm", Trans. Instn. Chem. Engrs., Vol. 54, No. 4, pp. 258-264 (1976).

34. Schumpe, A., Y. Serpemen, W.-D. Deckwer, "Effective Use of Bubble Column Reactors", Ger. Chem. Eng., Vol. 2, p. 234 (1979).

35. Joseph, S., and Y. T. Shah, "A Two-Bubble Class Model for Churn Turbulent Bubble Column Slurry Reactor", Chemical and Catalytic Reactor Modeling (ACS Symp. Ser. 237), M. P. Dudukovic and P. L. Mills, eds., pp. 149-167, American Chemical Society, Washington, D. C. (1984).

36. Mashelkar, R. A., "Bubble Columns", Brit. Chem. Eng., Vol. 15, No. 10, pp. 1297-1304 (1970).

37. Pavlica, R. T., and J. H. Olson, "Unified Design Method for Continuous-Contact Mass Transfer Operations", Ind. Eng. Chem., Vol. 62, No. 12, pp. 45-58 (1970).

38. Mecklenburgh, J. C., "Backmixing and Design: A Review", Trans. Instn. Chem. Engrs., Vol. 52, No. 2, pp. 180-192 (1974).

39. Shah, Y. T., G. J. Stiegel, and M. M. Sharma, "Backmixing in Gas-Liquid Reactors", AIChE J., Vol. 24, No. 3, pp. 369-400 (1978).

40. Joshi, J. B., and Y. T. Shah, "Hydrodynamic and Mixing Models for Bubble Column Reactors", Chem. Eng. Commun., Vol. 11, No. 1-3, pp. 165-199 (1981).

41. Shah, Y. T., and W.-D. Deckwer, "Hydrodynamics of Bubble Columns", Chapter 22 in Handbook of Fluids in Motion, N. P. Cheremisinoff and R. Gupta, eds., Ann Arbor Science, Ann Arbor, Mi. (1983).

42. Hartland, S., and J. C. Mecklenburgh, "The Concept of Backmixing", Chem. Eng. Sci., Vol. 23, No. 2, pp. 186-187 (1968).

43. Argo, W. B., and D. R. Cova, "Longitudinal Mixing in Gas-Sparged Tubular Vessels", Ind. Eng. Chem. Process Des. Dev., Vol. 4, No. 4, pp. 352-359 (1965).

44. Levenspiel, O., Chemical Reaction Engineering, 2nd ed., J. Wiley and Sons, New York (1972).

45. Levenspiel, O., The Chemical Reactor Omnibook, Oregon State Univ., Corvallis, Or. (1979).

46. Taylor, G. I., "Dispersion of Soluble Matter in Solvent Flowing Slowly through a Tube", Proc. Roy. Soc. Lond., Vol. A219, No. 1137, pp. 186-203 (1953).

47. Taylor, G. I., "The Dispersion of Matter in Turbulent Flow through a Pipe", Proc. Roy. Soc. Lond., Vol. A223, No. 1155, pp. 446-468 (1954).

48. Taylor, G. I., "Conditions under Which Dispersion of a Solute in a Stream of Solvent Can Be Used to Measure Molecular Diffusion", Proc. Roy. Soc. Lond., Vol. A225, No. 1163, pp. 473-477 (1954).

49. Aris, R., "On the Dispersion of a Solute in a Fluid Flowing through a Tube", Proc. Roy. Soc. Lond., Vol. A235, No. 1200, pp. 67-77 (1956).

50. Levenspiel, O., and W. K. Smith, "Notes on the Diffusion-Type Model for the Longitudinal Mixing of Fluids in Flow", Chem. Eng. Sci., Vol. 6, No. 4/5, pp. 227-233 (1957).

51. van der Laan, E. Th., "Notes on the Diffusion-Type Model for the Longitudinal Mixing in Flow", Chem. Eng. Sci., Vol. 7, No. 3, pp. 187-191 (1958).

52. Aris, R., "Notes on the Diffusion-Type Model for Longitudinal Mixing in Flow", Chem. Eng. Sci., Vol. 9, No. 4, pp. 266-267 (1959).

53. Bischoff, K. B., "Accuracy of the Axial Dispersion Model for Chemical Reactors", AIChE J., Vol. 14, No. 5, pp. 820-821 (1968).

54. Gill, W. N., "Axial Dispersion with Time Variable Flow in Multiphase Systems", AIChE J., Vol. 15, No. 5, pp. 745-749 (1969).

55. Gill, W. N., and R. Sankarasubramanian , "Exact Analysis of Unsteady Convective Diffusion", Proc. Roy. Soc. Lond., Vol. A316, No. 1526, pp. 341-350 (1970).

56. Wehner, J. F., and R.H. Wilhelm, "Boundary Conditions of Flow Reactor", Chem. Eng. Sci., Vol. 6, No. 2, pp. 89-93 (1956).

57. Wen, C. Y., and L. T. Fan, Models for Flow Systems and Chemical Reactors, Marcel Dekker, New York (1975).

58. Corrsin, S., "Limitations of Gradient Transport Models in Random Walks and in Turbulence", Advances in Geophysics, Vol. 18A, pp. 25-60, Academic Press, San Francisco (1974).

59. Sreenivasan, K. R., S. Tavoularis, and S. Corrsin, "A Test of Gradient Transport and Its Generalizations", Third Int. Symp. on Turbulent Shear Flows, L. J. S. Bradbury, F. Durst, B. E. Launder, F. W. Schmidt, J. H. Whitelaw, eds., pp. 96-112, Springer-Verlag, Berlin (1982).

60. Barkelew, C. H., private communication (1981).

61. Danckwerts, P. V., "Continuous Flow Systems. Distribution of Residence Times", Chem. Eng. Sci., Vol. 2, No. 1, pp. 1-13 (1953).

62. Carbonell, R. G., "Flow Nonuniformities in Packed Beds: Effect on Dispersion", Chem. Eng. Sci., Vol. 35, No. 6, pp. 1347-1356 (1980).

63. Sundaresan, S., N. R. Amundson, and R. Aris, "Observations on Fixed-Bed Dispersion Models: The Role of the Interstitial Fluid, AIChE J., Vol. 26, No. 4, pp. 529-536 (1980).

64. Levenspiel, O., and T. J. Fitzgerald, "A Warning on the Misuse of the Dispersion Model", Chem. Eng. Sci., Vol. 38, No. 3, pp. 489-491 (1983).

65. Reith, T., S. Renken, and B. A. Israel, "Gas Hold-up and Axial Mixing in the Fluid Phase of Bubble Columns", Chem. Eng. Sci., Vol. 23, No. 6, pp. 619-628 (1968).

66. Hanratty, T. J., G. Latinen, and R. H. Wilhelm, "Turbulent Diffusion in Particulately Fluidized Beds of Particles", AIChE J., Vol. 2, No. 3, pp. 372-380 (1956).

67. Hatton, T. A., and E. N. Lightfoot, "Dispersion, Mass Transfer and Chemical Reaction in Multiphase Contactors Part I. Theoretical Developments", AIChE J., Vol. 30, No. 2, pp. 235-243 (1984).

68. Linek, V., P. Beněs, J. Sinkule, and Z. Křivský, "Simultaneous Determination of Mass Transfer Coefficient and of Gas and Liquid Axial Dispersions and Holdups in a Packed Absorption Column by Dynamic Response Method", Ind. Eng. Chem. Fund., Vol. 17, No. 4, pp. 298-305 (1978).

69. Bischoff, K. B., and J. B. Phillips, "Longitudinal Mixing in Orifice Plate Gas-Liquid Reactors", Ind. Eng. Chem. Process Des. Dev., Vol. 5, No. 4, pp. 416-421 (1966).

70. Deckwer, W.-D., R. Burckhart, and G. Zoll, "Mixing and Mass Transfer in Tall Bubble Columns", Chem. Eng. Sci., Vol. 29, No. 11, pp. 2177-2188 (1974).

71. Chen, B.-H., "Effects of Liquid Flow on Axial Mixing of Liquid in a Bubble Column", Can. J. Chem. Eng., Vol. 50, No. 3, pp. 436-438, (1972).

72. Aoyama, Y., K. Ogushi, K. Koide, and H. Kubota, "Liquid Mixing in Concurrent Bubble Columns", J. Chem. Eng. Jap., Vol. 1, No. 2, pp. 158-163 (1968).

73. Hikita, H., and H. Kikukawa, "Liquid-Phase Mixing in Bubble Columns: Effect of Liquid Properties", Chem. Eng. J., Vol. 8, No. 3, pp. 191-197 (1974).

74. Baird, M. H. I., and R. G. Rice, "Axial Dispersion in Large Unbaffled Columns", Chem. Eng. J., Vol. 9, No. 2, pp. 171-174 (1975).

75. Mashelkar, R. A., and P. A. Ramachandran, "Longitudinal Dispersion in Circulation Dominated Bubble Columns", Trans. Instn. Chem. Engrs., Vol. 53, No. 4, pp. 274-277 (1975).

76. Crabtree, J. R., and J. Bridgwater, "Chain Bubbling in Viscous Liquids", Chem. Eng. Sci., Vol. 24, No. 12, pp. 1755-1768 (1969).

77. de Nevers, N., "Bubble Driven Fluid Circulations", AIChE J., Vol. 14, No. 2, pp. 222-226 (1968).

78. Ueyama, K., and T. Miyauchi, "Properties of Recirculating Turbulent Two Phase Flow in Gas Bubble Columns", AIChE J., Vol. 25, No. 2, pp. 258-266 (1979).

79. Miyauchi, T., S. Furusaki, S. Morooka, and Y. Akida, "Transport Phenomena and Reaction in Fluidized Catalyst Beds", Advances in Chemical Engineering, Vol. 11, pp. 275-448, Academic Press, New York (1981).

80. Walter, J. F., and H. W. Blanch, "Liquid Circulation Patterns and Their Effect on Gas Hold-Up and Axial Mixing in Bubble Columns", Chem. Eng. Commun., Vol. 19, No. 4-6, pp. 243-262 (1983).

81. Whalley, P. B., and J. F. Davidson, "Liquid Circulation in Bubble Columns", Proc. Symp. Two-Phase Flow Systems (Instn. Chem. Engrs. Symp. Ser. No. 38), paper J5 (1974).

82. Joshi, J. B., and M. M. Sharma, "A Circulation Cell Model for Bubble Columns", Trans. Instn. Chem. Engrs., Vol. 57, No. 4, pp. 244-251 (1979).

83. van den Akker, H. E. A., and K. Rietema, Correspondence to Trans. Instn. Chem. Engrs., Vol. 60, No. 4, pp. 255-256 (1982).

84. Joshi, J. B., Correspondence to Trans. Instn. Chem. Engrs., Vol. 60, No. 4, p. 256 (1982).

85. Lehrer, I. H., Correspondence to Trans. Instn. Chem. Engrs., Vol. 60, No. 2, p. 126 (1982).

86. Joshi, J. B., Correspondence to Trans. Instn. Chem. Engrs., Vol. 60, No. 2, pp. 126-127 (1982).

87. Field, R. W., and J. F. Davidson, Correspondence to Trans. Instn. Chem. Engrs., Vol. 60, No. 2, pp. 127-128 (1982).

88. Joshi, J. B., "Axial Mixing in Multiphase Contactors - A Unified Correlation", Trans. Instn. Chem. Engrs., Vol. 58, No. 3, pp. 155-165 (1980).

89. Viswanathan, K., and D. Subba Rao, "Circulation in Bubble Columns", Chem. Eng. Sci., Vol. 38, No. 3, pp. 474-478 (1983).

90. Viswanathan, K., and D. Subba Rao, "Inviscid Liquid Circulation in Bubble Columns", Chem. Eng. Commun., Vol. 25, No. 1-6, pp. 133-155 (1984).

91. Freedman, W., and J. F. Davidson, "Holdup and Liquid Circulation in Bubble Columns", Trans. Instn. Chem. Engrs., Vol. 47, No. 8, pp. T251-T262 (1969).

92. Rietema, K., "Science and Technology of Dispersed Two-Phase Systems-I and II", Chem. Eng. Sci., Vol. 37, No. 8, pp. 1125-1150 (1982).

93. Bouré, J. A., and J. M. Delhaye, "General Equations and Two-Phase Flow Modeling", Chapter 1.2 in Handbook of Multiphase Systems, G. Hetsroni, ed., Hemisphere (McGraw-Hill), New York (1982).

94. Bird, R. B., W. E. Stewart, and E. N. Lightfoot, Transport Phenomena, J. Wiley and Sons, New York (1960).

95. Gray, W. P., and P. C. Y. Lee, "On the Theorems for Local Volume Averaging of Multiphase Systems", Int. J. Multiphase Flow, Vol. 3, No. 4, pp. 333-340 (1977).

96. Nigmatulin, R. I., "Spatial Averaging in the Mechanics of Heterogeneous and Dispersed Systems", Int. J. Multiphase Flow, Vol. 5, No. 5, pp. 353-385 (1979).

97. Lin, C. C., and L. A. Segel, Mathematics Applied to Deterministic Problems in the Natural Sciences, Macmillan, New York (1974).

98. Blok, J. R., and A. A. H. Drinkenburg, "Hydrodynamic Properties of Pulses in Two-Phase Downflow Operated Packed Columns", Chem. Eng. J., Vol. 25, No. 1, pp. 89-99 (1982).

99. Hughmark, G. A., "Holdup and Mass Transfer in Bubble Columns", Ind. Eng. Chem. Process Des. Dev., Vol. 6, No. 2, pp. 218-220 (1967).

100. Kumar, A., T. E. Degaleesan, G. S. Laddha, and H. E. Hoelscher, "Bubble Swarm Characteristics in Bubble Columns", Can. J. Chem. Eng., Vol. 54, No. 6, pp. 503-508 (1976).